UAB
Universitat Autònoma de Barcelona

Immunological characterization of myelodysplastic syndromes and their association with clonal hematopoiesis and disease progression

A translational study of the immune microenvironment and clonal dynamics in myelodysplastic syndromes

Antonieta G. Molero Yordi

ADVERTIMENT. L'accés als continguts d'aquesta tesi queda condicionat a l'acceptació de les condicions d'ús establertes per la següent llicència Creative Commons: https://creativecommons.org/licenses/?lang=ca

ADVERTENCIA. El acceso a los contenidos de esta tesis queda condicionado a la aceptación de las condiciones de uso establecidas por la siguiente licencia Creative Commons: https://creativecommons.org/licenses/?lang=es

WARNING. The access to the contents of this doctoral thesis it is limited to the acceptance of the use conditions set by the following Creative Commons license: https://creativecommons.org/licenses/?lang=en

Doctoral thesis

Immunological characterization of myelodysplastic syndromes and their association with clonal hematopoiesis and disease progression

A translational study of the immune microenvironment and clonal dynamics in myelodysplastic syndromes

Author:

Antonieta G. Molero Yordi

Supervisor:

David Valcárcel Ferreiras, MD PhD

Tutor:

Francesc Bosch Albareda, MD PhD

Doctoral Program in Medicine

Department of Medicine

Universitat Autònoma de Barcelona

Barcelona, 2026

ACKNOWLEDGEMENTS

I would like to express my deepest gratitude to my PhD supervisor, Dr. David Valcárcel, for his guidance, support, and trust throughout this work. Beyond his invaluable help with this thesis, I am especially grateful for his continued support in the development of my professional career, and I truly appreciate the opportunities and encouragement he has given me along the way.

I also thank Dr. Francesc Bosch, Head of the Department, for fostering the academic and clinical environment that made this research and my professional growth possible.

My sincere thanks go to the Hematology Department of Vall d'Hebron University Hospital and to the laboratories involved in this project, as well as to all my colleagues, whom I now consider friends. I am particularly grateful to the technical team, especially Lidia, Isa, and Sara, for their invaluable help. I would also like to give a special thank you to Laura and Bárbara for their expertise, which was essential for the completion of this work.

I am also grateful to the myeloid pathology research team, past, present, and new members, for the continuous learning, collaboration, and support that have made this journey both intellectually enriching and personally meaningful.

My deepest gratitude goes to my family for giving me everything. To my father, for being an example of professionalism, perseverance, and resilience; to my mother, for her unconditional love and support; and to my sisters, for paving the way and making things easier along the journey. I would not be who I am today without you.

To Javi, that tireless person who inspires me every day to become a better version of myself. Achieving this milestone would not have been possible without you. Thank you for walking this path with me, now alongside our daughter Noa, who arrived in our lives only a few months ago and has already given us so much to be grateful for. Because of her, my motivation to grow, to learn, and to become a better person has only become stronger.

Completing this thesis marks the end of an important chapter, and I carry forward everything I have learned during this journey with deep gratitude.

"When we are no longer able to change a situation, we are challenged to change ourselves."

— Viktor E. Frankl

LIST OF ABBREVIATIONS

Abbreviation	Definition
AML	Acute Myeloid Leukemia
ANC	Absolute Neutrophil Count
BM	Bone Marrow
BMA	Bone Marrow Aspiration
BMB	Bone Marrow Biopsy
CCL	C-C Motif Chemokine Ligand
CI	Confidence Interval
CXCL	C-X-C Motif Chemokine Ligand
EGF	Epidermal Growth Factor
FGF-2	Fibroblast Growth Factor 2
G-CSF	Granulocyte Colony-Stimulating Factor
GM-CSF	Granulocyte-Macrophage Colony-Stimulating Factor
HD	Healthy Donors
HGF	Hepatocyte Growth Factor
HLA	Human Leukocyte Antigen
HR-MDS	High-Risk Myelodysplastic Syndromes
ICUS	Idiopathic Cytopenia of Undetermined Significance
IFN	Interferon
IL	Interleukin
IP-10	Interferon-γ–Induced Protein 10
IPSS-R	Revised International Prognostic Scoring System
IPSS-M	Molecular International Prognostic Scoring System
IQR	Interquartile Range
KIR	Killer-Cell Immunoglobulin-Like Receptor
LR-MDS	Low-Risk Myelodysplastic Syndromes
MCP-1	Monocyte Chemoattractant Protein 1

MDS	Myelodysplastic Syndromes / Myelodysplastic Neoplasms
MDSCs	Myeloid-Derived Suppressor Cells
MIG	Monokine Induced by Gamma Interferon
MIP-1α	Macrophage Inflammatory Protein 1 Alpha
MIP-1β	Macrophage Inflammatory Protein 1 Beta
Mo-MDSCs	Monocytic Myeloid-Derived Suppressor Cells
Gr-MDSCs	Granulocytic Myeloid-Derived Suppressor Cells
NGS	Next-Generation Sequencing
NK	Natural Killer
OS	Overall Survival
PCR	Polymerase Chain Reaction
PCR-SSO	Polymerase Chain Reaction – Sequence-Specific Oligonucleotide
RS	Ring Sideroblast
TNF-α	Tumor Necrosis Factor Alpha
VEGF-A	Vascular Endothelial Growth Factor A
WHO	World Health Organization

LIST OF FIGURES

Figure 1. Age distribution of participants diagnosed with AML and MDS in Spain. 14
Figure 2. BM hematopoietic stem cell (HSC) niche under physiological conditions. 15
Figure 3. Schematic representation of the effects of aging on innate and adaptive immunity. 17
Figure 4. Immune microenvironmental differences between low- and HR-MDS. 21
Figure 5. Low-risk MDS treatment algorithm. 41
Figure 6. Proposed High-risk MDS treatment algorithm. 42
Figure 7. Distribution of NK cell subpopulations across study groups. 55
Figure 8. Differential expression of NK-cell ligands. 58
Figure 9. KIR Gene Repertoire and Haplotype Distribution. 62
Figure 10. Integrative Immunogenetic Analysis of KIR-HLA-C Profiles and Clinical Outcomes. 63
Figure 11. NK receptor expression according to IPSS-R 3.5 risk cut-off. 65
Figure 12. Peripheral T-cell subsets according to IPSS-R 3.5 risk cut-off. 69
Figure 13. MDSCs according to IPSS-R risk category. 70
Figure 14. Cytokine expression profiles across study groups. 76
Figure 15. Cytokine concentrations according to risk groups. 77
Figure 16. MDS and ICUS genomic landscape. 78
Figure 17. Mutational profile of CCUS patients. 79
Figure 18. Immune Parameters with Observed Differences Between Mutated MDS and CCUS. 81
Figure 19. VEGF-A Levels in Mutated MDS versus CCUS. 82
Figure 20. Immune Subpopulation Distribution According to MDS Mutational Category. 83
Figure 21. KIR2DL1 Expression According to IPSS-M Risk in MDS. 84
Figure 22. Longitudinal Changes in NK Receptor Expression from Diagnosis to One-Year Follow-Up. 86

LIST OF TABLES

Table 1. Commonly mutated genes in MDS and their prognostic impact. 23
Table 2. Peripheral Blood, BM, and Cytogenetic Findings in MDS (WHO 2017)..... 30
Table 3. Classification and Defining Features of MDS (WHO 2022). 31
Table 4. ICC 2022 MDS Classification..... 32
Table 5. Comparison Between WHO 2022 and ICC 2022. 33
Table 6. IPSS-R for MDS. 35
Table 7. Risk Stratification by IPSS-M Categories..... 38
Table 8. Demographics and baseline laboratory characteristics at diagnosis. 52
Table 9. Stratification of MDS patients..... 53
Table 10. Expression of activating NK cell receptors across study groups..... 56
Table 11. Expression of inhibitory NK cell receptors and cytotoxic markers. 57
Table 12. Activating KIR receptors in MDS and HD. 59
Table 13. KIR receptors expression. 60
Table 14. NK cells frequency according to Risk stratification..... 64
Table 15. Peripheral lymphocyte and T-cell subset distribution in MDS, ICUS, and HD. 67
Table 16. Cytokine and Chemokines concentrations in BM supernatant samples. 73
Table 17. Immune cell subsets showing significant differences according to mutational status in MDS patients..... 80
Table 18. Summary of the immune subpopulations over time. 85

LIST OF SUPPLEMENTARY TABLES AND FIGURES

Supplementary Table 1. Lymphocyte subpopulations. 125
Supplementary Table 2. Multiparametric flow cytometry panels used for immune cell profiling. 126
Supplementary Table 3. Detailed cytogenetic and molecular risk stratification of MDS patients. 128
Supplementary Table 4. Expression of NK cell ligands on hematopoietic precursors and myeloid cells in ICUS, MDS, and healthy donors. 129
Supplementary Table 5. Distribution of KIR genotypes in the study cohort. 130
Supplementary Table 6. NK receptor expression according to IPSS-R 3.5 risk. 131
Supplementary Table 7. Cytokine concentrations in LR-MDS and HR-MDS BM samples. 133
Supplementary Table 8. Immune cell subsets and soluble mediators according to mutational status in MDS patients. 135
Supplementary Table 9. Immune cell subsets, NK receptors, and circulating cytokines in MDS^{Mut} versus CCUS. 137
Supplementary Table 10. Hematologic parameters and immune cell populations at diagnosis and 1-year follow-up in MDS patients. 141

Supplementary Figure 1. NK receptor expression according to IPSS-R risk stratification. 142

TABLE OF CONTENTS

ABSTRACT 11

RESUMEN 12

1. INTRODUCTION 13

1.1. Myelodysplastic syndromes (MDS) 13

1.1.1 Definition and historical background 13

1.1.2 Epidemiology 13

1.1.3 Pathogenesis 14

1.1.3.1 Role of inflammation in MDS 16

1.1.3.2 Immune dysregulation in MDS 17

1.1.3.3 Somatic gene mutations 22

1.1.4 Clonal hematopoiesis and pre-MDS conditions 26

1.1.4.1 Clonal hematopoiesis of indeterminate potential (CHIP) 26

1.1.4.2 ICUS and clonal cytopenia of undetermined significance (CCUS) 27

1.1.5 Clinical presentation and diagnosis 28

1.1.6 Genetic abnormalities in diagnosis 29

1.1.7 Classification of MDS 29

1.1.7.1 2022 classifications 30

1.1.8 Prognostic assessment in MDS 34

1.1.9 Treatment of MDS 38

1.1.9.1 Management of lower-risk MDS 39

1.1.9.2 Management of higher-risk MDS 41

2. HYPOTHESIS 44

3. OBJECTIVES 44

3.1 Main objective 44

3.2 Secondary objectives 44

4. MATERIALS AND METHODS 45

4.1 Study design 45

4.2 Study population and sample collection 45

4.2.1 Study population 45

4.2.2 Sample collection and processing 45

4.2.3 Clinical data collection 46

4.2.4 Diagnostic classification and risk stratification 46

4.2.5 Follow-up definitions 46

4.3 Laboratory assessments and analyses 46
4.3.1 Characterization of immune cell populations 46
4.3.2 Analysis of cytokines and chemokines 48
4.3.3 KIR and HLA genotyping and haplotype determination 48
4.3.4 Molecular analyses 49
4.4 Statistical analysis 50
4.5 Ethical considerations 50
5. RESULTS 52
5.1 Subjects baseline characteristics 52
5.2 Main Findings 54
5.2.1 Immune cells subpopulation 54
5.2.1.1 NK cells 54
5.2.1.1.1 Phenotypic expression of NK cell receptors in BM 54
5.2.1.1.2 KIR phenotype and genotyping analysis in MDS patients 58
5.2.1.1.3 NK cell phenotypic and functional differences according to risk stratification in MDS 64
5.2.1.2 T cells 65
5.2.1.2.1 Differential expression of T cell receptors in peripheral blood 65
5.2.1.3 MDSCs 69
5.2.2 Cytokines and chemokines 71
5.2.3 Mutational landscape in MDS and ICUS 78
5.2.3.1 Association with disease risk and immune profile 78
5.3 Follow-up of MDS patients 85
5.3.1 Immune phenotypic and functional differences 85
6. DISCUSSION 87
7. CONCLUSIONS 102
8. FUTURE DIRECTIONS 103
9. REFERENCES 104
10. APPENDICES 124
10.1 Funding 124
10.2 Supplementary Tables 125

ABSTRACT

Myelodysplastic neoplasms (MDS) are clonal and heterogeneous disorders of hematopoietic stem cells characterized by dysplasia, ineffective hematopoiesis, and variable risk of progression. Although disease biology is primarily driven by intrinsic myeloid abnormalities, accumulating evidence confirms a contributory role of immune dysregulation within the bone marrow (BM) microenvironment. We hypothesized that alterations in natural killer (NK) cell frequency and phenotype, expansion of myeloid-derived suppressor cells (MDSCs), and dysregulated cytokine signaling may contribute to disease biology and progression. We therefore conducted an integrative analysis of BM immune populations and cytokine concentrations in 71 subjects, including 50 patients with MDS, 11 with idiopathic cytopenia of undetermined significance (ICUS), and 10 healthy donors (HD). Cytokines were quantified in BM supernatants, and immune populations were characterized in BM and peripheral blood by multiparametric flow cytometry. Associations with clinical variables, mutational status assessed by next-generation sequencing, and risk categories were explored.

Marked inter-individual variability was observed, and most comparisons did not reach statistical significance. ICUS cases displayed the most distinctive immune features, with a relatively cytotoxic NK cell profile characterized by enrichment of mature $CD56^{dim}CD16^{bright}$ NK cells. In contrast, MDS cases showed substantial heterogeneity in NK cell composition without a consistent receptor-level signature. Reduced expression of the activating receptor DNAM-1 was observed in ICUS compared with MDS, and several activating Killer-cell immunoglobulin-like receptor (KIR) were decreased in both relative to HD. Risk-stratified analyses did not identify a uniform immune pattern across IPSS-R categories. However, high-risk MDS exhibited features suggestive of immune exhaustion, including increased granulocytic MDSCs and a trend toward higher TIGIT expression. Despite the predominance of activating KIR haplotype B genotypes, corresponding phenotypic expression was not consistently observed. Cytokine and chemokine concentrations in BM were largely comparable across groups, although exploratory analyses suggested increased IL-10 levels in high-risk MDS.

In summary, the BM immune microenvironment is highly heterogeneous and context dependent. Rather than identifying a single predictive biomarker, this study underscores the complexity of immune remodeling in MDS and supports further prospective and mechanistic investigations.

RESUMEN

Las neoplasias mielodisplásicas (SMD) son trastornos clonales y heterogéneos de las células madre hematopoyéticas, caracterizados por displasia, hematopoyesis ineficaz y un riesgo variable de progresión. Aunque la biología de la enfermedad está caracterizada por alteraciones mieloides intrínsecas, la evidencia acumulada apoya el papel de la desregulación inmunitaria en el microambiente de la médula ósea (MO). Se planteó la hipótesis de que las alteraciones en la frecuencia y el fenotipo de las células natural killer (NK), la expansión de las células supresoras derivadas de mieloides (MDSCs) y la señalización desregulada de citocinas contribuyen a la biología y progresión de la enfermedad. Con este objetivo, realizamos un análisis en las poblaciones inmunitarias en MO y de las concentraciones de citocinas en 71 sujetos: 50 pacientes con SMD, 11 con citopenia idiopática de significado incierto (ICUS) y 10 donantes sanos (HD). Las citocinas se cuantificaron en sobrenadante de MO, y las poblaciones inmunitarias se caracterizaron en MO y sangre periférica mediante citometría de flujo multiparamétrica. Se exploraron asociaciones con variables clínicas, estado mutacional y categorías de riesgo.

Se observó una marcada variabilidad interindividual y la mayoría de las comparaciones no alcanzaron significación estadística. ICUS mostró las características inmunitarias más distintivas, con un perfil de células NK relativamente citotóxico, caracterizado por el enriquecimiento de células NK maduras $CD56^{dim}CD16^{bright}$. En contraste, los casos de SMD presentaron una heterogeneidad sustancial en la composición de las células NK, sin consistencia a nivel de expresión de receptores. La expresión de DNAM-1 fue menor en ICUS en comparación con SMD, y varios receptores tipo inmunoglobulina de las células NK (KIR) activadores estuvieron disminuidos en ambos grupos respecto a HD. El análisis estratificado por riesgo no identificó un patrón inmunitario uniforme entre categorías IPSS-R. No obstante, los SMD de alto riesgo mostraron características sugestivas de agotamiento inmunitario, incluyendo aumento de MDSCs granulocíticas y tendencia a mayor expresión de TIGIT. Las concentraciones de citocinas y quimiocinas en MO fueron globalmente comparables entre grupos, aunque los análisis exploratorios sugirieron niveles aumentados de IL-10 en MDS de alto riesgo.

En conjunto, el microambiente inmunitario en la médula ósea es altamente heterogéneo y dependiente del contexto, lo que manifiesta la complejidad del sistema inmunitario en SMD y respalda la necesidad de estudios prospectivos y mecanismos adicionales.

1. INTRODUCTION

1.1. Myelodysplastic syndromes (MDS)

1.1.1 Definition and historical background

Myelodysplastic syndromes, also known as myelodysplastic neoplasms (MDS), are a heterogeneous group of clonal hematopoietic stem cell disorders characterized by morphological dysplasia, ineffective hematopoiesis in the bone marrow (BM), peripheral cytopenias, and a variable risk of progression to acute myeloid leukemia (AML) [1-3]

Although individual cases of what are now recognized as MDS were described in the early 20th century, the formalization of the term and its classification as a distinct group of hematologic neoplasms only emerged in the mid-1970s. The disease was formally defined and classified for the first time in 1982 by the morphological French-American-British (FAB) classification, evolving from the earlier concepts of refractory anemia and preleukemia described in the 1940s–1950s.

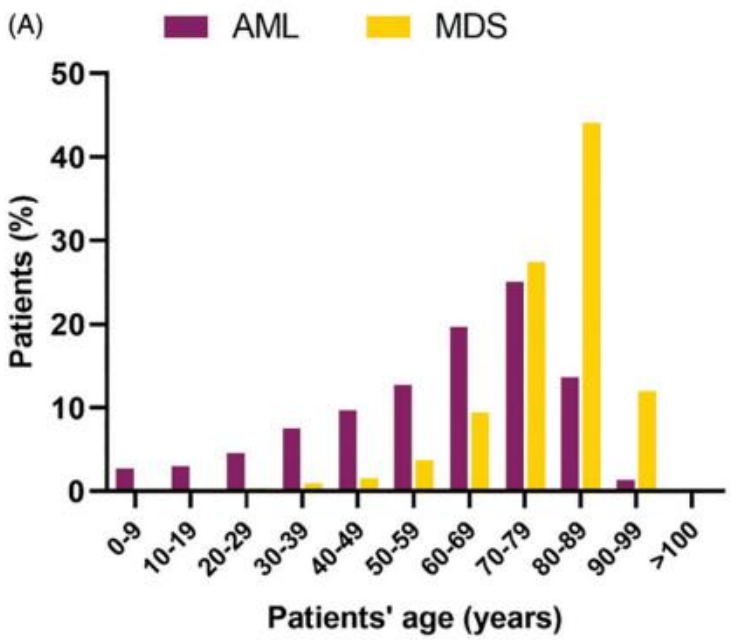
Over the past two decades, MDS has evolved from a purely morphologic diagnosis and classification toward a deeper understanding of the role of somatic mutations, reflected in successive updates of the World Health organization (WHO) classifications from 2001 to 2016. In recent years, major efforts have focused on improving disease stratification, incorporating next-generation sequencing (NGS) into clinical practice for more precise prognostic assessment and personalized treatment, as reflected in the molecular international prognostic scoring systems (IPSS-M) [4].

Furthermore, increasing evidence indicates that, beyond somatic mutations, immune dysregulation and chronic inflammation also play key roles in the pathogenesis and progression of MDS [5].

1.1.2 Epidemiology

MDS is mainly an elderly disease with a median age at diagnosis older than 70 years. Its prevalence is around 3–4 individuals per 10^5, but it increases with age reaching 7–35 per 10^5 in people older than 60 years [5-6]. It affects more commonly male than females **(Figure 1)** [7-8]. Given the continuous aging of the population and the improvement in the diagnostic approaches, the number of MDS participants has grown.

Figure 1. Age distribution of participants diagnosed with AML and MDS in Spain.

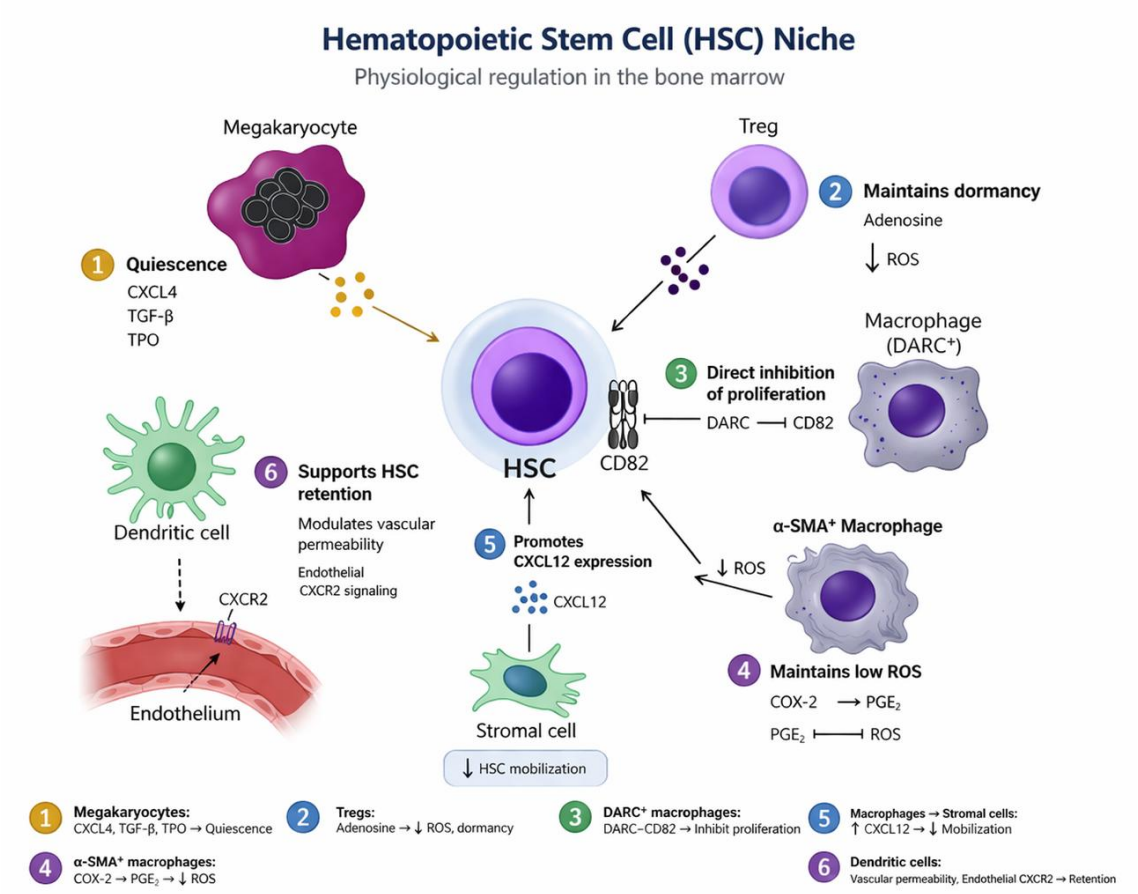


The incidence of MDS increases sharply with advancing age, peaking between 80 and 89 years *(*Marsà A. *et al*. Journal of Medical Economics. 2020).

1.1.3 Pathogenesis

Under physiological conditions, the BM microenvironment tightly regulates Hematopoietic Stem Cell (HSC) function through complex interactions among stromal, endothelial, mesenchymal, immune, and hematopoietic cells. Within this niche, signals from megakaryocytes, regulatory T cells (Tregs), and macrophages maintain HSC quiescence, self-renewal, and retention in the marrow by modulating cytokines, chemokines, and metabolic stress **(Figure 2).**

Figure 2. BM hematopoietic stem cell (HSC) niche under physiological conditions.



(1) Megakaryocyte-derived signals support HSC quiescence. (2) Regulatory T cells promote dormancy through adenosine-mediated protection from oxidative stress. (3) DARC$^+$ macrophages restrain HSC proliferation via CD82-dependent interactions. (4) α-SMA$^+$ macrophages maintain low ROS levels through COX-2–dependent PGE_2 production. (5) Macrophage–stromal crosstalk enhances CXCL12 expression, contributing to HSC retention. (6) Dendritic cells regulate vascular permeability and endothelial CXCR2 signaling, supporting niche retention.

*(*Adapted and modified from Kouroukli *et al.*, Cancers (Basel), 2022*.)*

HSC, hematopoietic stem cell; DARC, Duffy antigen receptor for chemokines; α-SMA, alpha smooth muscle actin; ROS, reactive oxygen species; COX-2, cyclooxygenase-2; PGE_2, prostaglandin E_2; CXCL12, C–X–C motif chemokine ligand 12; CXCR2, C–X–C chemokine receptor 2.

This finely balanced environment preserves hematopoietic homeostasis throughout life. However, with aging or chronic inflammatory stress, these regulatory networks become

disrupted, leading to HSC dysfunction, loss of quiescence, and clonal advantage of mutated progenitors [9].

The pathogenesis of MDS originates from the clonal expansion of HSCs harboring somatic mutations. These initiating genetic events confer a selective growth advantage, leading to the emergence and dominance of mutant clones [10-12]. BM microenvironment plays a pivotal role in this process, as inflammatory signaling and immune dysregulation promote clonal expansion and contribute to disease progression. Overall, age is recognized as a major risk factor contributing to the development and establishment of MDS [13-14].

1.1.3.1 Role of inflammation in MDS

Chronic inflammation has been increasingly recognized as a key component of the pathophysiology of MDS and other age-related hematologic disorders. In this context, inflammaging refers to the chronic, sterile, low-grade systemic inflammation that develops with advancing age and is characterized by persistently elevated circulating levels of proinflammatory mediators, including cytokines (e.g., IL-6, TNF-α), chemokines, and acute-phase proteins, in the absence of overt infection [15-18]. This phenomenon is distinct from acute inflammation and is now recognized as a hallmark of biological aging, contributing to multiple age-related diseases. [15-16, 19].

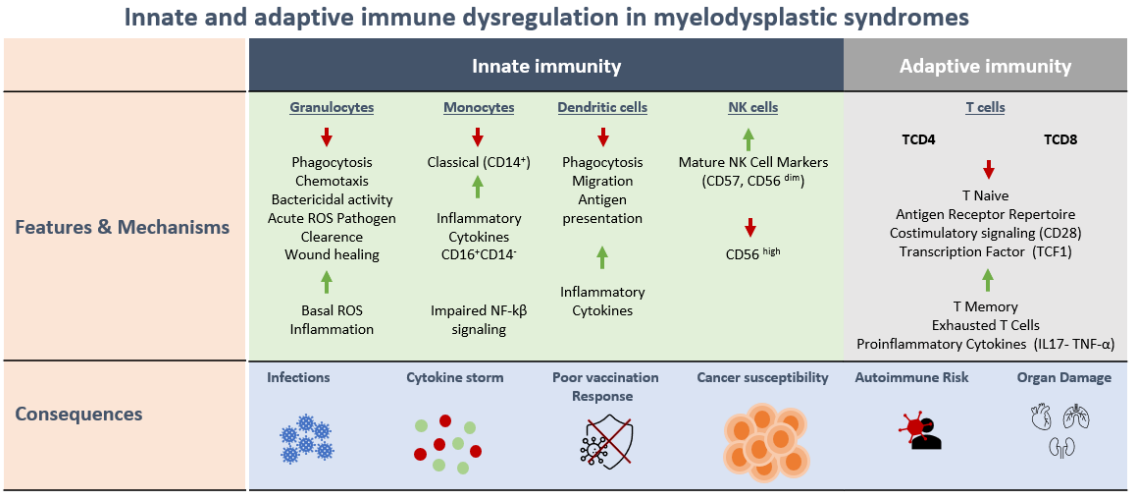
Mechanistically, inflammaging results from a convergence of factors, including lifelong antigenic stimulation, accumulation of senescent cells and their associated secretory phenotype, mitochondrial dysfunction, metabolic alterations, immune dysregulation (immunosenescence), and changes in the gut microbiota [15-16, 20-22]. The process involves both innate and adaptive immune compartments, with enhanced activation of pattern-recognition receptors and persistent interferon signaling playing central roles [23] **(Figure 3).**

Clinically, inflammaging is recognized as a major risk factor for morbidity and mortality in older adults, correlating with multimorbidity and decline in physical and cognitive performance [18, 24-25].

These age-related changes alter the BM microenvironment, leading to HSC dysfunction and providing a selective advantage to clones harboring somatic mutations commonly observed in MDS, such as *TET2, DNMT3A,* and *ASXL1* [26-29]. Several cytokines and chemokines are upregulated in both older individuals and participants with MDS, inducing intrinsic and extrinsic alterations in normal hematopoiesis that facilitate clonal expansion [27, 30-33].

Activation of innate immune signaling pathways, particularly the NLRP3 inflammasome and non-canonical NF-κB signaling, plays a central role in the pathogenesis of MDS in the context of inflammaging. These pathways promote pyroptotic cell death, expansion of myeloid-derived suppressor cells (MDSCs), and the propagation of malignant clones (32) (34-36).

Figure 3. Schematic representation of the effects of aging on innate and adaptive immunity.



Innate immune cells exhibit reduced phagocytic and chemotactic capacity, altered ROS production, and impaired NF-κB signaling, contributing to chronic inflammation. In parallel, adaptive immunity shows a loss of naïve lymphocytes, expansion of memory and exhausted T and B cells, and reduced receptor diversity. These alterations collectively lower immune competence, promote a pro-inflammatory milieu. (Adapted from Singh A, *et al*., Cold *Spring Harb Perspect Med.* 2024) (25).

ROS, reactive oxygen species; NF-κB, nuclear factor kappa B.

1.1.3.2 Immune dysregulation in MDS

The pathogenesis of MDS reflects the convergence of intrinsic genetic lesions and alterations in the BM immune microenvironment, that contributes to hematopoietic failure and clonal selection, shifting from an early pro-inflammatory, pro-apoptotic state to an immunosuppressive niche that enables malignant clone persistence and disease progression in High-risk MDS (HR-MDS) **(Figure 4)** (9).

- **Alteration of BM microenvironment in MDS:**

Cytokine milieu: Low-risk MDS (LR-MDS) is dominated by elevated pro-inflammatory cytokines such as TNF-α, IL-1β, IL-6, IL-8, and IFN-γ, promoting apoptosis and ineffective hematopoiesis. In contrast, HR-MDS shows upregulation of inhibitory cytokines such as IL-10, TGF-β, and soluble IL-2 receptors, contributing to immune tolerance, reduced apoptosis, and clonal expansion. Expression of TNF receptor 1 (TNFR1) predominates in low-risk disease, mediating apoptotic signaling, whereas TNFR2, associated with anti-apoptotic pathways, is increased in HR-MDS. Elevated levels of IL-6, GM-CSF, and CXCL10 correlate with advanced disease and adverse prognosis [(9) (37-40)].

Lymphocytes: Early-stage MDS is characterized by clonal and functionally altered T-cell populations, including $CD8^+$ cytotoxic T cells that mediate hematopoietic suppression through antigen-driven or autoreactive mechanisms. Over time, increased expression of immune checkpoint molecules, PD-1, PD-L1, and CTLA-4, leads to T-cell exhaustion and loss of antitumor activity. $CD4^+$ T cells and Tregs are reduced in LR-MDS but expanded and suppressive in HR-MDS, reflecting the immune shift from activation to tolerance [(35) (41)]. Accordingly, increased proportions of Tregs are frequently correlated with more advanced disease features, including higher blast counts, lower hemoglobin levels, and reduced overall survival (OS) [(42)].

Macrophages: exhibit reduced differentiation and phagocytic capacity in MDS. In low-risk disease, they promote apoptosis of progenitor cells via calreticulin-mediated recognition, whereas in advanced MDS, overexpression of the anti-phagocytic molecule CD47 on progenitors inhibits macrophage clearance. HR-MDS is also associated with skewing toward an M2-like (tumor-associated) phenotype, which supports angiogenesis and clonal expansion [(9)(42).]

Natural killer (NK) and dendritic cells (DCs): NK cells display quantitative and functional defects, including decreased expression of activating receptors and cytotoxic mediators impairing immune surveillance. Dendritic cells derived from MDS progenitors are numerically and functionally deficient, with reduced antigen presentation, impaired cytokine secretion, and limited ability to activate T cells, contributing to immune evasion [(9)(42)(43).]

Participants with MDS exhibit profound alterations in NK cell differentiation and function, characterized by a shift toward immature phenotypes, reduced cytotoxic granule content,

and limited receptor repertoire diversity [43–46]. These immunologic defects contribute to impaired immune surveillance and are closely associated with disease progression.

Killer immunoglobulin-like receptors (KIRs) are critical regulators of NK cell activation and tolerance, and their genetic and phenotypic alterations have been implicated in the pathogenesis and clinical course of MDS [43–46]. KIR haplotypes are broadly categorized into A haplotypes, which are predominantly inhibitory, and B haplotypes, which contain a greater number of activating KIR genes. MDS participants typically harbor fewer activating KIR genes than healthy controls, and the predominance of haplotype A has been identified as an independent predictor of adverse prognosis, including higher risk of transformation to AML and shorter OS [48].

At the phenotypic level, MDS BM displays a reduction in mature, functionally competent NK cells and a restricted KIR expression profile, indicating decreased receptor diversity and defective NK cell licensing. These abnormalities are particularly evident in HR-MDS subgroups and correlate with unfavorable clinical outcomes, including increased risk of leukemic transformation and reduced OS [44–45, 50].

Immunogenetic studies further suggest that specific KIR–HLA ligand combinations and KIR/HLA mismatches, as well as cytokine gene polymorphisms, influence disease susceptibility and immune regulation in MDS [48–49, 51–52]. In particular, variants in TNF-α, TGF-β, and IL-10 genes have been linked to ineffective hematopoiesis, immune-mediated BM failure, and increased risk of disease progression [48, 51–52].

Collectively, these findings support a model in which KIR-mediated NK cell dysfunction represents a central feature of MDS pathophysiology, shaping both disease evolution and response to immunotherapeutic strategies [43–47].

MDSCs: are a group of heterogeneous myeloid cells that can be primarily categorized into two distinct subsets: granulocytic MDSCs (Gr-MDSCs) and monocytic MDSCs (Mo-MDSCs). The PMN-MDSCs are identified as the expression of CD11b+/CD14−/CD15+ (or CD66b+), whereas Mo-MDSCs express CD11b+/CD14+/CD15−/HLA-DR-/low [41]**.** MDSCs are markedly increased in high-risk MDS and contribute to immune suppression by secreting IL-10, TGF-β, nitric oxide, and arginase. Their expansion is driven by inflammatory signals such as S100A9, IL-6, and CCL2, acting through STAT3 activation. MDSCs promote T cell exhaustion via PD-1/PD-L1 and TIM-3/Gal-9 signaling pathways and inhibit normal hematopoiesis, reinforcing the immunosuppressive microenvironment [9][35]. Moreover, MDS participants exhibit increased CD33 expression on MDSCs compared with healthy controls. The binding of S100A9 to CD33 promotes MDSC

expansion within the BM, establishing a self-reinforcing inflammatory loop that amplifies innate immune activation and contributes to disease progression [41].

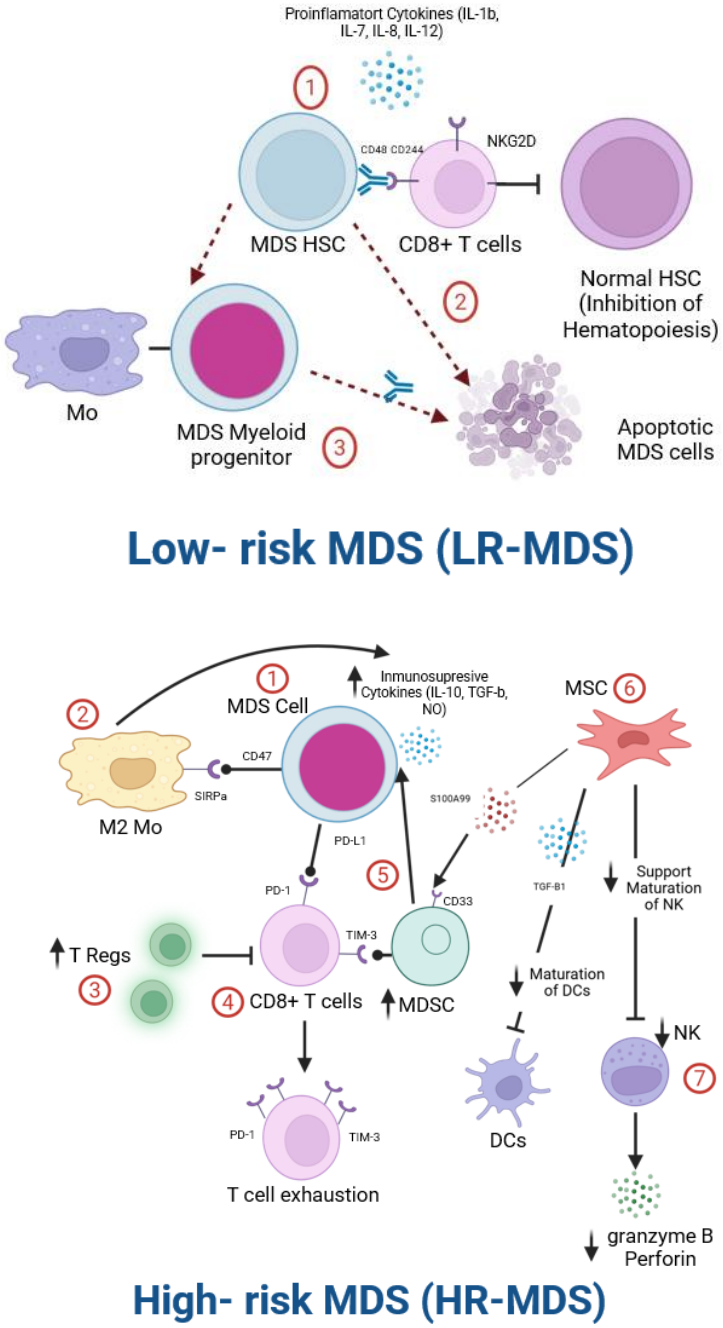
Mesenchymal stromal cells (MSCs): MSCs from MDS participants show independent genetic and epigenetic abnormalities, secrete S100A8/9 that induces genotoxic stress in HSCs, and contributes to disease progression through activation of p53 and Toll-like receptor (TLR) signaling. In advanced MDS, MSCs become highly immunosuppressive, inhibiting DCs maturation and NK and T-cell function through TGF-β1 secretion [9][35][41].

Aberrant activation of innate immune signaling in HSCs plays a pivotal role in the development of MDS. Elevated pro-inflammatory cytokines such as interleukin-1β (IL-1β) within the BM microenvironment reflect a chronic inflammatory state that promotes hematopoietic dysfunction. Overexpression of TLR4)on $CD34^+$ progenitor cells enhance responsiveness to damage- and pathogen-associated molecular patterns (DAMPs/PAMPs), initiating the MyD88–IRAK–TRAF6 signaling cascade and subsequent NF-κB activation. This pathway drives the transcription of inflammatory mediators, perpetuating inflammation and clonal stress in the BM niche.

Among the major DAMPs implicated in MDS, the calcium-binding proteins S100A8 and S100A9 are key amplifiers of innate immune signaling. Their expression increases with age and MDS progression, acting through the TLR4/MyD88/NF-κB axis and NADPH oxidase (NOX) activation. NOX-derived reactive oxygen species (ROS) promote assembly of the NLRP3 inflammasome, leading to caspase-1 activation, cleavage of gasdermin D (GSDMD), and release of IL-1 β and IL-18 that culminate in HSC pyroptosis and ineffective hematopoiesis. In parallel, ROS stabilizes β-catenin signaling, enhancing proliferation, and malignant transformation of HSCs**.**

Collectively, sustained innate immune activation through S100A8/A9-driven inflammasome signaling disrupts hematopoietic homeostasis, fostering cytopenia and clonal evolution characteristics of MDS [41].

Figure 4. Immune microenvironmental differences between low- and HR-MDS.



Low-risk MDS shows a pro-inflammatory, pro-apoptotic milieu with elevated cytokines, increased Fas/TNFR1 signaling, and enhanced $CD8^+$ T-cell cytotoxicity via NKG2D/CD244, which also suppresses normal hematopoiesis. Myeloid progenitors expressing calreticulin (CRT) promote phagocytic clearance. *High-risk MDS*, by contrast, develops an immunosuppressive, anti-apoptotic environment characterized by TNFR2/CD47 expression, M2 macrophage polarization, Treg expansion, $CD8^+$ T-cell exhaustion (PD-1/PD-L1, TIM-3), accumulation of MDSCs, and MSC-derived TGF-β/S100A9, leading to impaired NK-cell function and immune evasion.

CRT, calreticulin; IL, interleukin; MDSC, myeloid-derived suppressor cell; MSC, mesenchymal stromal cell; NK, natural killer cell; PD-1, programmed cell-death protein 1; PD-L1, programmed death-ligand 1; TGF-β, transforming growth factor-β; TIM-3, T-cell immunoglobulin and mucin-domain-containing 3; TNFR, tumor necrosis factor receptor. *(Adapted from: Kouroukli O et al. Cancers (Basel). 2022.* [9].

1.1.3.3 Somatic gene mutations

Somatic gene mutations play a central role in the pathogenesis, clinical heterogeneity, and prognosis of MDS. NGS and new techniques, improved our understanding of molecular pathogenesis. More than 90% of participants with MDS carry mutations. High-throughput sequencing studies have shown that only a limited number of these mutations occur in more than 10% of cases, while most participants exhibit between two and four distinct genetic alterations [43].The most frequently mutated genes in MDS are involved in RNA splicing (e.g., *SF3β1, SRSF2, U2AF1, ZRSR2*), DNA methylation (e.g., *TET2, DNMT3A, IDH1/2*), histone modification (e.g., *ASXL1, EZH2*), transcription regulation (e.g., *RUNX1*), DNA repair (e.g., *TP53*), signal transduction (e.g., *NRAS, JAK2*), and the cohesin complex **(Table 1)** [10, 54-59].

Table 1. Commonly mutated genes in MDS and their prognostic impact.

Category	Gene	Frequency (%)	Location	Prognostic Impact
RNA splicing (40–50%)	*SF3β1*	25–30	2q33	Favorable; unfavorable if combined with del(5q)
	SRSF2	15	17q25	Unfavorable OS; high risk of AML transformation
	U2AF1	10–15	21q22	Unfavorable OS; high risk of AML transformation
	ZRSR2	5–10	Xp22	Unclear
	U2AF2	Rare	19q13	Unfavorable; associated with high-risk MDS and AML
DNA methylation (30–40%)	*TET2*	20–30	4q24	Unclear
	DNMT3A	15	2q23	Unfavorable; associated with AML transformation
	IDH2	5	2q33	Unclear; studies suggest unfavorable prognosis
	IDH1	2	15q26	Unfavorable
Chromatin modification (≈20%)	*ASXL1*	15–20	20q11	Unfavorable
	EZH2	5–10	7q36	Unfavorable

Transcription factors (10–15%)	*RUNX1*	10	21q22	Unfavorable
	BCOR	5	Xp11	Unfavorable
	ETV6	<5	12p13	Unfavorable
	GATA2	<5	3q21	Unfavorable
Cohesin complex (≈10%)	*STAG2*	5	Xq25	Unfavorable
Signal transduction (5–10%)	*JAK2*	<5	9p24	Unclear
	CBL	5	11q23	Unfavorable
	NRAS	<5	1q13	Unfavorable
	KRAS	<5	12p12	Unfavorable
	FLT3-ITD	<5	13q12	Unfavorable
	KIT	<5	4q11–12	Unclear
	PTPN11	<5	12q24	Unclear

Tumor suppressors (5–10%)	*TP53*	10*	17p13	Unfavorable
	WT1	5	11p13	Unfavorable; associated with AML progression
	PHF6	5	Xq26–27	Unfavorable

Summary of the most frequently mutated genes in myelodysplastic syndromes (MDS), grouped according to their biological function. The table includes mutation frequency, chromosomal location, and reported prognostic impact based on current literature. Frequencies represent approximate prevalence among patients with MDS. Prognostic associations refer mainly to overall survival and risk of progression to acute myeloid leukemia. *Adapted from* Hoff FW *et al*. published in Cells (2023) [(43)].

*Up to 50 in complex karyotype

MDS, myelodysplastic syndromes; AML, acute myeloid leukemia; OS, overall survival; del(5q), deletion of the long arm of chromosome 5; ITD, internal tandem

The IPSS-M **(See section MDS prognostic assessment)**, represents a major advancement in risk stratification. This model established a new prognostic framework by integrating molecular mutation data, specifically 31 genes incorporated as independent prognostic variables, together with conventional cytogenetic and clinical parameters, significantly enhances predictive accuracy across all major clinical outcomes, enabling more precise risk-adapted therapeutic decision-making. These mutations are assessed using targeted NGS panels and are encoded as binary variables (mutated vs. wild-type), with selected genes modeled according to allelic status or co-mutational patterns (e.g., *TP53* multihit status and *SF3β1* subgroups), within a multivariable Cox regression framework to derive an individualized risk score [43, 60].

Mutations in *TP53, RUNX1, ASXL1, EZH2, ETV6, U2AF1, DNMT3A, SRSF2*, and *RAS* pathway genes are consistently associated with adverse clinical outcomes, including reduced OS and increased risk of transformation to AML, irrespective of traditional prognostic models [60, 11]. Among these, *TP53* mutations, particularly biallelic alterations, which refer to the inactivation of both *TP53* alleles, most commonly resulting from multiple mutations or from a mutation in combination with loss of heterozygosity (including copy-neutral LOH) or deletion of the wild-type allele, define a biologically distinct subgroup characterized by extremely poor prognosis and high relapse rates, independent of other clinical variables [43, 64, 65].

In contrast, *SF3β1* mutations are linked to a more favorable prognosis and distinct clinicopathologic features, most notably the presence of ring sideroblasts (RS) [43, 60,66]. However, this effect can be modulated by co-mutations in adverse genes such as *RUNX1, STAG2, BCOR, BCORL1, SRSF2, NRAS, and IDH2*. Notably, the co-existence of *SF3β1* mutation with del(5q) or other high-risk lesions identifies distinct biological subsets *(SF3β1^{5q}*) with less favorable clinical behavior [43, 66, 67]. Incorporating molecular mutation profiles into established clinical scoring systems enhances prognostic precision and supports a more personalized, risk-adapted therapeutic approach in MDS [67].

1.1.4 Clonal hematopoiesis and pre-MDS conditions

1.1.4.1 Clonal hematopoiesis of indeterminate potential (CHIP)

In recent years, multiple studies have demonstrated that somatic mutations can be detected in hematopoietic cells of otherwise healthy individuals, usually of advanced age, a condition known as CHIP. CHIP is defined by the presence of somatic mutations in leukemia-associated driver genes with a variant allele frequency (VAF) ≤2%, occurring in individuals without cytopenias, BM dysplasia, or other evidence of hematologic

malignancy. This age-related phenomenon represents a premalignant state that increases the risk of developing myeloid neoplasms and other age-associated disorders.

The most frequently affected genes include *DNMT3A, TET2*, and *ASXL1*. The presence of CHIP confers an estimated 0.5–1% annual risk of progression to MDS or AML, with risk influenced by the specific mutation, number of mutated genes, and clone size. Additional somatic mutations and clonal expansion are typically required for progression from CHIP to overt MDS [68–70].

Beyond its hematologic implications, CHIP is recognized as an early, asymptomatic clonal state driven by somatic mutations that not only predisposes to hematologic malignancies, but also to cardiovascular disease and other adverse age-related outcomes, independent of leukemic transformation [68, 70–74].

1.1.4.2 ICUS and clonal cytopenia of undetermined significance (CCUS)

The diagnostic hallmark of MDS is BM cell dysplasia. Classification of MDS subtypes follows the criteria established by the WHO **(See section MDS classification)**. In many patients, cytopenias are mild, and dysplastic changes are minimal or absent, with or without cytogenetic abnormalities or detectable somatic mutations, making it challenging to confirm or exclude an overt diagnosis of MDS. Such cases present a diagnostic challenge, as they may represent early or borderline forms of clonal hematopoiesis, including ICUS and CCUS, rather than overt MDS [10, 75].

ICUS is defined as persistent unexplained cytopenia(s) in one or more peripheral blood lineages, with no evidence of dysplasia, no MDS-defining cytogenetic abnormalities, and no detectable somatic mutations in genes recurrently mutated in myeloid neoplasms. ICUS is a diagnosis of exclusion and carries a variable risk of progression; some cases may represent early or preclinical myeloid neoplasms, but most do not progress rapidly [76-78].

CCUS is characterized by unexplained cytopenia(s) in one or more lineages, with the presence of a somatic mutation (VAF ≥2–20%) in a gene recurrently mutated in myeloid neoplasms, but without sufficient morphologic dysplasia, excess blasts, or MDS-defining cytogenetic abnormalities to meet criteria for MDS. CCUS is associated with a significantly increased risk of progression to myeloid neoplasms, especially when high-risk mutations (e.g., spliceosome genes, multiple co-occurring mutations, or higher VAF) are present. Of the pre-MDS conditions CCUS implies the highest-risk precursors for MDS, depending on mutation type, number of mutations, and VAF [79-84].

1.1.5 Clinical presentation and diagnosis

As previously discussed, the diagnosis of MDS can be challenging. In recent years, significant progress has been made toward establishing standardized diagnostic criteria that are applicable worldwide. MDS represents a heterogeneous group with no single pathognomonic feature, and clinical presentation can vary widely. The presence of cytopenia affecting at least one hematopoietic lineage, together with morphologic evidence of dysplasia, remains fundamental for diagnosis.

Despite major advances in molecular and cytogenetic testing, which now refine and support diagnostic assessment, morphologic evaluation continues to serve as the cornerstone of MDS diagnosis. The conventional diagnostic workup includes peripheral blood counts and smear examination, Bone Marrow Aspiration (BMA) to evaluate dysplastic changes and quantify blast percentage, and cytogenetic and molecular analyses to identify chromosomal abnormalities and driver gene mutations relevant for both diagnosis and prognostic classification [10]. A BMB is also recommended to assess cellularity and the presence of fibrosis. Additionally, a comprehensive clinical evaluation is essential to exclude secondary causes of dysplasia and cytopenia. The main clinical manifestations of MDS are related to cytopenia-associated complications, such as anemia, infection, and bleeding [85].

In the WHO 2022 classification, the term MDS was replaced by myelodysplastic neoplasms (although the acronym was maintained for historical reasons) to emphasize their neoplastic nature. Definitions of cytopenia were harmonized as follows: hemoglobin <13 g/dL in males and <12 g/dL in females, absolute neutrophil count (ANC) <1.8 × 10^9/L, and platelet count <150 × 10^9/L. In both the WHO 2022 and International Consensus Classification (ICC) 2022 systems, the threshold for morphologic dysplasia remains ≥10% of cells in any hematopoietic lineage. Certain dysplastic features, such as micromegakaryocytes, are considered relatively specific for MDS and show high interobserver reproducibility.

The distinction between MDS and AML has been conceptually refined in the past years, while blast quantification remains central to diagnostic assessment, its inherent variability, arising from sampling differences, subjective interpretation, and the absence of a universal reference standard, is recognized. The WHO 2022 classification retained the 20% cutoff to preserve diagnostic consistency and prevent overtreatment, whereas the ICC introduced the category MDS/AML for cases with 10–19% blasts. Both frameworks consider these entities within the MDS spectrum rather than overt AML **(See section MDS classification)** [2,3].

1.1.6 Genetic abnormalities in diagnosis

Genetic abnormalities play a crucial role in the diagnosis, prognosis, and classification of MDS in both the WHO and ICC frameworks. Such abnormalities are detected in 40-50% of de novo MDS patients and up to 80% of therapy related MDS. The most frequent recurrent cytogenetic abnormalities include del(5q), monosomy 7/del(7q), trisomy 8 (+8) and del(20q). The Revised International Prognostic Scoring System (IPSS-R) stratifies the cytogenetic complexity into five subgroups derived from Schanz *et al*. and distinguish complex Karyotype (≥ 3 independent cytogenetic abnormalities, except -Y) and very complex karyotype (≥5 independent cytogenetic abnormalities) **(See section MDS prognostic assessment)** [83, 84].

Among the subtypes with defining genetic lesions, MDS with isolated del(5q) (MDS-5q) retains its diagnostic definition. The presence of *SF3β1* or single-hit *TP53* mutations does not supersede this classification. In addition, MDS with *SF3β1* mutation (MDS-*SF3β1*) has been recognized as a distinct entity, encompassing over 90% of cases with ≥5% RS. Cases lacking *SF3β1* mutation but showing ≥15% RS may still be classified as MDS with low blasts and RS. Importantly, the ICC introduced MDS with mutated *TP53* (MDS-bi*TP53*) as a new entity characterized by biallelic (multi-hit) *TP53* alterations, which confer adverse prognosis and high risk of leukemic transformation [84].

1.1.7 Classification of MDS

The history of MDS classification has progressively evolved from morphology-based criteria toward integrated morphologic-genetic systems, encompassing almost five decades from the pre-leukemic era before FAB and 2022 classifications driven by genomics. Early classifications primarily relied on peripheral blood and BM blast percentages and introduced foundational entities such as refractory anemia (RA) and refractory anemia with excess blasts (RAEB). The WHO 2001 classification, was the first WHO classification of MDS, revised the FAB system and represented a major step forward by incorporating dysplasia across lineages, recognizing cytogenetic abnormalities such as isolated del(5q), and lowering the AML threshold to 20% blasts. The subsequent WHO 2008 revision refined the classification concepts by standardizing diagnostic criteria, emphasizing the distinction between unilineage and multilineage dysplasia, consolidating overlapping subtypes, and integrating RS more formally into disease definitions [88-90]. These developments laid the groundwork for modern classifications, which further incorporate molecular genetics and refine disease boundaries.

The major modifications published in 2016 were based on the integration of genetic and molecular features refinement on morphologic criteria and disease boundaries **(Table 2)** [86].

Table 2. Peripheral Blood, BM, and cytogenetic findings in MDS (WHO 2017).

Subtype	Dysplasia	Cytopenia	RS%	Blast % (BM / PB)	Cytogenetic Findings
MDS-SLD	1	1–2	<15% / <5%	BM <5%, PB <1%, no Auer rods	Any, unless isolated del(5q)
MDS-MLD	2–3	1–3	<15% / <5%	BM <5%, PB <1%, no Auer rods	Any, unless isolated del(5q)
MDS-RS	1–3	1–3	≥15% (or ≥5% if *SF3β1*-mutated)	BM <5%, PB <1%, no Auer rods	Any, unless isolated del(5q)
MDS with isolated del(5q)	1–3	1–2	None or any	BM <5%, PB <1%, no Auer rods	del(5q) +/-one add.abnormality except −7 or del(7q)
MDS-EB1	0–3	1–3	None or any	BM 5–9%, PB 2–4%, no Auer rods	Any
MDS-EB2	0–3	1–3	None or any	BM 10–19%, PB 5–19%, or Auer rods	Any
MDS-U	1–3	1–3	None or <15%	BM <5%, PB ≤1%, no Auer rods	Any, or defining cytogenetic abnormality

MDS, Myelodysplastic syndrome; BM, Bone marrow; PB, Peripheral blood; del(5q), Deletion of long arm of chromosome 5; *SF3β1,* Splicing factor 3B subunit 1; Hb, Hemoglobin; ANC, Absolute neutrophil count.

1.1.7.1 2022 classifications

The 2022 WHO and ICC classifications **(Table 3 and Table 4)** both reflect the evolving biological understanding of MDS, incorporating molecular and cytogenetic findings into diagnostic criteria. However, diverge in key aspects: the WHO system retains the traditional 20% blast threshold to define AML from MDS, whereas the ICC introduces the MDS/AML for cases with 10–19% blasts, considered within the MDS categories. The ICC also gives greater prominence to mutationally defined entities, such as multi-hit

TP53 disease, while the WHO maintains distinct genetic subtypes like MDS-bi*TP53* and MDS-*SF3β1*. These refinements enhance diagnostic uniformity, improve risk stratification, and have direct therapeutic implications, particularly in guiding treatment **(Table 5)** [2,3] [87].

Table 3. Classification and defining features of MDS (WHO 2022).

Subtype	Blast Percentage (BM / PB)	Cytogenetic Features	Defining Mutations
MDS-5q	<5% BM, <2% PB	del(5q) alone, or with one add abnormality other than −7 or del(7q)	—
MDS-*SF3β1*[a]	<5% BM, <2% PB	No del(5q), monosomy 7, or complex karyotype	*SF3b1*
MDS-bi*TP53*	<20% BM, <2% PB	Usually, complex karyotype	≥2 *TP53* mutations, or one mutation with loss of heterozygosity (cnLOH)
MDS-LB	<5% BM, <2% PB	Variable	—
MDS-h[b]	<5% BM, <2% PB	Variable	—
MDS-IB1	5–9% BM, 2–4% PB	—	—
MDS-IB2	10–19% BM, 5–19% PB, or Auer rods present	—	—
MDS-f	5–19% BM, <2% PB	Fibrotic marrow	—

[a]Detection of ≥15% ring sideroblasts may substitute for *SF3β1* mutation. Acceptable related terminology: “MDS with low blasts and ring sideroblasts.”

[b]Defined by ≤25% bone marrow cellularity, age adjusted.

MDS, Myelodysplastic syndrome; BM, Bone marrow; PB, Peripheral blood; *SF3β1,* Splicing factor 3B subunit 1; *TP53,* Tumor protein p53; cnLOH, Copy-neutral loss of heterozygosity.

Table 4. ICC 2022 MDS classification.

Subtype	Dysplasia	Cytopenia	Cytoses*	BM / PB Blasts	Cytogenetics†	Key Mutations
MDS-*SF3b1*	Typically, ≥1‡	≥1	None	BM <5%, PB <2%	Any, except isolated del(5q), −7/del(7q), abn(3q26.2), or complex	*SF3b1* (VAF ≥10%), without multi-hit *TP53* or *RUNX1*
MDS with isolated del(5q)	Typically ≥1‡	≥1	Thrombocytosis allowed	BM <5%, PB <2%	del(5q) with ≤1 additional abnormality (except −7 or del(7q))	Any, except multi-hit *TP53*
MDS, NOS without dysplasia	0	≥1	None	BM <5%, PB <2%	−7/del(7q) or complex	Any, except multi-hit *TP53* or *SF3b1* (≥10% VAF)
MDS, NOS with single-lineage dysplasia	1	≥1	None	BM <5%, PB <2%	Any, except meeting criteria for MDS-del(5q)	Any, except multi-hit *TP53* or *SF3b1*
MDS, NOS with multilineage dysplasia	≥2	≥1	None	BM <5%, PB <2%	Any, except meeting criteria for MDS-del(5q)	Any, except multi-hit *TP53* or *SF3b1*
MDS-EB	Typically, ≥1‡	≥1	None	BM 5–9% or PB 2–9%	Any	Any, except multi-hit *TP53*
MDS/AML	Typically, ≥1‡	≥1	None	BM 10–19% or PB ≥2%§	Any, except AML-defining cytogenetics¶	Any, except *NPM1*, *bZIP CEBPA*, or *TP53*

*Cytoses: Sustained WBC ≥13×10⁹/L, monocytes ≥0.5×10⁹/L, or platelets ≥450×10⁹/L. Thrombocytosis may occur in MDS-del(5q).

†BCR::ABL1 rearrangement or other fusions defining myeloid/lymphoid neoplasms exclude MDS.

‡Dysplasia is usually present but not required.

§2% PB blasts on two occasions qualifies as MDS-EB.

AML-defining cytogenetics are listed in the WHO/ICC AML section.

MDS, Myelodysplastic syndrome; AML, Acute myeloid leukemia; BM, Bone marrow; PB, Peripheral blood; NOS, Not otherwise specified; del(5q), Deletion of the long arm of chromosome 5; VAF, Variant allele frequency; *SF3b1,* Splicing factor 3B subunit 1; *TP53,* Tumor protein p53; RUNX1, Runt-related transcription factor 1; *CEBPA,* CCAAT/enhancer-binding protein alpha; WBC, White blood cells.

Table 5. Comparison between WHO 2022 and ICC 2022.

Feature	WHO 2022	ICC 2022
Terminology	Use "Myelodysplastic Neoplasms (MDS)" to emphasize the neoplastic nature of the disease.	Retains "Myelodysplastic Syndromes (MDS)" but groups them under the broader category of "MDS and MDS/AML."
Subtypes with defining genetic abnormalities	Recognizes: • MDS with isolated del(5q) • MDS with *SF3β1* mutation • MDS with biallelic *TP53* inactivation (MDS-bi*TP53*)	Recognizes: • MDS with *SF3β1* mutation • MDS with del(5q) • MDS with multi-hit *TP53* mutation as a distinct high-risk entity
Blast count (MDS vs AML)	Retains 20% blast threshold to define AML; cases with 10–19% blasts are still classified as MDS (MDS-IB2).	Introduces a new MDS/AML overlap category for 10–19% blasts in BM or PB, recognizing biological and therapeutic overlap between MDS and AML.
Morphologic subtypes	Maintains morphological categories: • MDS with low blasts (LB) • MDS with increased blasts (IB1/IB2) • MDS with fibrosis (MDS-f) • MDS, hypoplastic	Combines similar morphology-based subtypes under broader genetic/molecular categories. Does not separately list MDS-h or MDS-f as distinct entities.
Definition of dysplasia	Remains ≥10% dysplastic cells in any lineage	Remains ≥10% dysplastic cells in any lineage
RS/*SF3β1*	Defines MDS with low blasts and *SF3β1* mutation (or ≥15% ring sideroblasts if *SF3β1* wild type).	Similar entity: MDS with *SF3β1* mutation (VAF ≥10%), excludes multi-hit *TP53* or *RUNX1* co-mutations.

Cytopenia definitions	Harmonized thresholds: Hb <13 g/dL (men), <12 g/dL (women); ANC <1.8 ×10⁹/L; platelets <150 ×10⁹/L.	Adopts same thresholds, aligned with WHO 2022.
Nomenclature changes	Introduces “MDS with low blasts (LB)” and “MDS with increased blasts (IB)” replacing RA, RCMD, etc.	Retains broader “MDS” terminology but integrates molecularly defined and blast-based groups under unified nomenclature.
Clinical integration	Recognizes MDS-bi*TP53* as AML-equivalent for therapeutic purposes, though not classified as AML.	Formally defines MDS/AML as an intermediate entity, acknowledging shared treatment pathways with AML.

WHO, World Health Organization; ICC, International Consensus Classification; MDS, myelodysplastic syndromes; AML, acute myeloid leukemia; MDS/AML, myelodysplastic syndrome/acute myeloid leukemia overlap category; MDS-IB1/IB2, myelodysplastic syndromes with increased blasts 1 or 2; MDS-LB, myelodysplastic syndromes with low blasts; MDS-f, myelodysplastic syndromes with fibrosis; MDS-h, hypoplastic myelodysplastic syndromes; MDS-bi*TP53*, myelodysplastic syndromes with biallelic *TP53* inactivation; BM, bone marrow; PB, peripheral blood; Hb, hemoglobin; ANC, absolute neutrophil count; RS, ring sideroblasts; VAF, variant allele frequency.

Recent efforts have aimed to harmonize the 2022 MDS classification systems (WHO 5th edition and ICC). Komrokji *et al*. proposed a data-driven framework based on nine genomic clusters with hierarchical organization, prioritizing genetically defined entities such as biallelic *TP53* inactivation, MDS with isolated del(5q), and *SF3β1*-mutated MDS. Cases not fitting these categories are classified morphologically as MDS with low blasts (MDS-LB) or increased blasts (MDS-IB), further stratified by a 10% blast threshold. RS retains diagnostic value when *SF3β1* status is unavailable or wild type. This model demonstrated high concordance with WHO 2022 (97.2%) and ICC 2022 (98.1%). [88,89,90].

1.1.8 Prognostic assessment in MDS

Risk stratification is a cornerstone in the management of MDS, guiding therapeutic decisions, and predicting clinical outcomes. Over time, multiple prognostic models have been developed to capture disease heterogeneity. The International Prognostic Scoring System (IPSS), introduced in 1997, represented the first standardized framework, integrating BM blasts, cytogenetics, and number of cytopenias into four risk categories. Despite its long-standing clinical utility, the IPSS was derived from a relatively limited cohort and placed predominant weight on blast percentage, with a simplified cytogenetic classification [57, 95].

The IPSS-R, introduced in 2012, refined the original IPSS by incorporating a more detailed assessment of cytogenetic abnormalities, the degree of cytopenias, and a lower BM blast percentage. The revision expanded cytogenetic categories from three to five, allowing for a more accurate stratification of genetic risk, and introduced graded evaluation of hemoglobin, platelet, and neutrophil counts rather than counting the number of cytopenias alone **(Table 6)**. This enhanced precision improved prognostic discrimination across all outcome measures, including overall survival and progression to acute myeloid leukemia, establishing the IPSS-R as the standard prognostic tool for clinical decision-making and risk-adapted therapy in MDS [92-96].

Table 6. IPSS-R for MDS.

Prognostic Variable	Score 0	Score 0.5	Score 1	Score 1.5	Score 2	Score 3	Score 4
Cytogenetics*	Very good	-	Good	-	Intermediate	Poor	Very poor
BM Blasts (%)	≤2	-	>2–<5	-	5–10	>10	-
Hemoglobin (g/dL)	≥10	-	8–<10	-	<8	-	-
Platelets (×10⁹/L)	≥100	50–<100	<50	-	-	-	-
ANC (×10⁹/L)	≥0.8	<0.8	-	-	-	-	-
Risk Group	**Total Score Range**	**Median OS (Years)**		**Median Time to 25% AML Evolution (Years)**			
Very Low	≤1.5	8.8		Not reached			
Low	>1.5–3	5.3		10.8			
Intermediate	>3–4.5	3.0		3.2			

High	>4.5–6	1.6	1.4
Very High	>6	0.8	0.7

* Cytogenetic Risk Categories: Very Good: -Y, del(11q). Good: Normal, del(5q), del(12p), del(20q), double including del(5q). Intermediate: del(7q), +8, +19, i(17q), or any other single or double abnormality not included in other groups. Poor: -7, inv(3)/t(3q)/del(3q), or double including -7/del(7q). Very Poor: Complex karyotype (≥3 abnormalities).

BM, Bone marrow; OS, Overall survival; AML, Acute myeloid leukemia; ANC, Absolute neutrophil count.

In addition to IPSS-based models, other prognostic systems have contributed to refining risk stratification in MDS. The WHO-based Prognostic Scoring System (WPSS) introduced a dynamic approach, allowing risk assessment at different time points during disease evolution by incorporating WHO classification, cytogenetics, and transfusion-dependent anemia, and defining five risk categories [(90)]. Complementarily, the Spanish MDS Group (GESMD) proposed a model focused on identifying higher-risk features within clinically lower-risk patients, demonstrating that factors such as adverse cytogenetics, severe cytopenias, or BM fibrosis can uncover subgroups with poorer outcomes who may benefit from more intensive therapeutic strategies. Together, these approaches highlighted the clinical heterogeneity of MDS and contributed to the evolution toward more refined and personalized prognostic models [(92)].

Other prognostic approaches have been developed to refine clinical risk stratification. A key refinement of the IPSS-R, to better guide therapeutic decisions and monitor disease progression, is the application of a threshold of 3.5, which distinguishes lower-risk (≤3.5) from higher-risk (>3.5) disease. This cutoff has been validated across different cohorts as a clinically meaningful discriminator, effectively separating participants with longer median survival and lower rates of progression to acute myeloid leukemia. Participants with scores ≤3.5 are typically managed with supportive measures or lower-intensity therapies, whereas those with scores >3.5 are candidates for disease-modifying treatments. [(97 - 99)]. Although molecular profiling and dynamic scoring models continue to enhance precision, the 3.5 cutoff remains a cornerstone in contemporary MDS risk assessment [(10, 12)].

In 2022, The IPSS-M was introduced, representing a major advance in risk stratification for MDS by integrating molecular genetics with established clinical and cytogenetic

parameters. It incorporates mutations in 31 genes, including key drivers such as *TP53, SF3β1, ASXL1, SRSF2, RUNX1, DNMT3A, TET2, U2AF1 and STAG2*, together with BM blast percentage, cytopenias, and cytogenetic abnormalities, to classify participants into six categories: Very Low, Low, Moderate-Low, Moderate-High, High, and Very High **(Table 7)** [(99)]**.** Notably, the IPSS-M models bone marrow blast percentage as a continuous variable integrated within a multivariable regression framework, rather than using discrete cutoffs as in previous scores. In contrast to earlier systems that categorized cytopenias individually, the IPSS-M incorporates hematologic parameters quantitatively, with hemoglobin and platelet count included as continuous predictors of risk, while absolute neutrophil count does not retain independent prognostic significance. Cytogenetic risk categories are derived from the IPSS-R framework and are integrated alongside mutational data, with 31 genes evaluated, of which a subset carries independent prognostic weight and the remainder contribute as residual genetic risk. The key feature of the IPSS-M is the incorporation of the somatic mutations (31 genes), these molecular alterations are incorporated through a hierarchical structure comprising 16 main-effect genes (*TP53*$^{\text{multi-hit}}$*, MLL*$^{\text{PTD}}$*, FLT3, SF3B1, NPM1, RUNX1, NRAS, ETV6, IDH2, CBL, EZH2, U2AF1, SRSF2, DNMT3A, ASXL1, KRAS*) with independent prognostic impact and an additional residual mutation category of 15 genes (*BCOR, BCORL1, CEBPA, ETNK1, GATA2, GNB1, IDH1, NF1, PHF6, PPM1D, PRPF8, PTPN11, SETBP1, STAG2, WT1)* capturing the cumulative contribution of other recurrently mutated genes. Among molecular variables, *TP53* alterations, particularly multihit status, carry the greatest prognostic weight, and the model accounts for gene-gene interactions [(99)].

Compared with the IPSS-R, the IPSS-M provides improved prognostic accuracy for overall survival, leukemia-free survival, and risk of transformation to AML, reclassifying nearly half of participants and thereby influencing therapeutic decisions such as treatment escalation or eligibility for hematopoietic stem cell transplantation [(99-101)]. Its performance remains robust across diverse subtypes, including therapy-related and hypoplastic MDS, with a core set of 16 genes recommended for optimal predictive value [(99, 102-103)].

The model has been validated mainly for baseline assessment, with uncertain utility for dynamic monitoring during disease evolution. [(101-102)]. Real-world studies confirm the superior prognostic power of the IPSS-M and its ability to refine risk categorization and clinical management, though prospective evidence demonstrating improved patient outcomes through IPSS-M–guided therapy is still emerging. Ongoing research aims to

integrate this molecularly informed model into broader treatment algorithms for personalized MDS management [103, 104-109].

Table 7. Risk Stratification by IPSS-M Categories.

IPSS-M Category	Participants, % (n=2701)	Risk Score	HR* (95% CI)	Median LFS, yrs (25–75%)	Median OS, yrs (25–75%)	AML at 1 / 2 / 4 yrs, %	Death w/o AML at 1 / 2 / 4 yrs, %
Very Low	14% (381)	≤ 1.5	0.51 (0.3–0.6)	9.7 (5.0–17.4)	10.6 (5.1–17.4)	0.0 / 1.2 / 2.8	2.2 / 7.0 / 15.9
Low	33% (889)	> 1.5 to 0.5	Reference	5.9 (2.6–12.0)	6.0 (3.0–12.8)	1.7 / 3.4 / 6.4	8.5 / 16.2 / 29.5
Moderate-Low	11% (302)	> 0.5 to 0	1.5 (1.2–1.8)	4.5 (2.0–6.9)	4.6 (2.0–7.4)	4.9 / 8.1 / 11.4	12.0 / 18.9 / 33.6
Moderate-High	11% (281)	> 0 to 0.5	2.5 (2.1–3.1)	2.3 (0.9–4.7)	2.8 (1.2–5.5)	9.5 / 14.0 / 18.9	18.0 / 31.1 / 51.1
High	14% (379)	> 0.5 to 1.5	3.7 (3.1–4.4)	1.5 (0.8–2.8)	1.7 (1.0–3.4)	14.3 / 21.2 / 29.2	19.3 / 33.8 / 54.2
Very High	17% (469)	> 1.5	7.1 (6.0–8.3)	0.76 (0.33–1.5)	1.0 (0.5–1.8)	28.2 / 38.6 / 42.8	30.6 / 45.6 / 51.3

*Hazard ratio for the risk of AML or death; the Low category is used as the reference level.

AML, acute myeloid leukemia; CI, Confidence interval; LFS, leukemia-free survival; OS, overall survival; yrs, years.

(Adapted from Bernard E, *et al*. NEJM Evid. 2022.)

Beyond established prognostic models such as the IPSS-M, increasing evidence highlights the importance of *TP53* mutational characteristics for risk stratification in MDS-del(5q). A large multicenter study by Montoro *et al*. demonstrated that in MDS-del(5q) the prognostic impact of *TP53* mutations depends on allelic state and VAF, with monoallelic mutations ≥20% VAF behaving similarly to multihit TP53 alterations, whereas VAF <20% resembles TP53-wild-type disease [110].

1.1.9 Treatment of MDS

The management of MDS is risk-adapted and guided by disease severity, cytopenia profile, cytogenetic, molecular characteristics, comorbidities, and patient preferences.

These parameters are critical determinants of OS and the probability of progression to AML, as discussed in the risk stratification section [10].

Although substantial advances have been made in elucidating the pathobiology of MDS and improving prognostic classification systems, therapeutic options remain limited. Allogeneic hematopoietic stem cell transplantation is currently the only potentially curative modality; however, it is applicable to a minority of participants, given that MDS predominantly affects elderly individuals who are frequently ineligible for intensive treatment at the time of diagnosis [111].

Over the past decade, several novel agents have been approved, primarily for lower-risk MDS, with the main objective of ameliorating cytopenias such as anemia. These therapies have reduced the dependence on supportive interventions, including red blood cell transfusions, and have contributed to an improvement in quality of life among lower-risk participants [5] [112].

Despite these advances, there have been no recent approvals for the treatment of HR-MDS, and effective disease-modifying strategies for this population remain an unmet medical need. Consequently, the enrollment of MDS participants in clinical trials is essential to facilitate therapeutic innovation and improve long-term outcomes.

1.1.9.1 Management of lower-risk MDS

Historically, the primary therapeutic goals in LR-MDS focused on symptom control, reduction of transfusion dependence, improvement of quality of life, rather than modification of disease course. However, emerging therapies are beginning to shift this paradigm by demonstrating hematologic responses that may reflect improvement of OS, although definitive confirmation remains pending. In particular, imetelstat has shown the ability to reduce clonal burden in LR-MDS, suggesting potential disease-modifying activity [116]. Management is highly individualized and should consider patient preferences, comorbidities, and disease biology, emphasizing shared decision-making throughout the treatment continuum [111].

Standard treatment approaches for LR-MDS include supportive care measures, erythropoiesis-stimulating agents (ESAs), lenalidomide for participants with del(5q), luspatercept for MDS with ring sideroblasts (MDS-RS) or following ESA failure, or imetelstat in patients failing ESA. Other not approved options that may have a role in certain situations are immunosuppressive therapy and thrombopoietin receptor agonists for thrombocytopenia, or lower doses of hypomethylating agents for refractory cytopenias. Allogeneic hematopoietic stem cell transplantation is reserved for rare young

cases with high transfusion burden and refractory to previous therapies **(Figure 5).** [113–114].

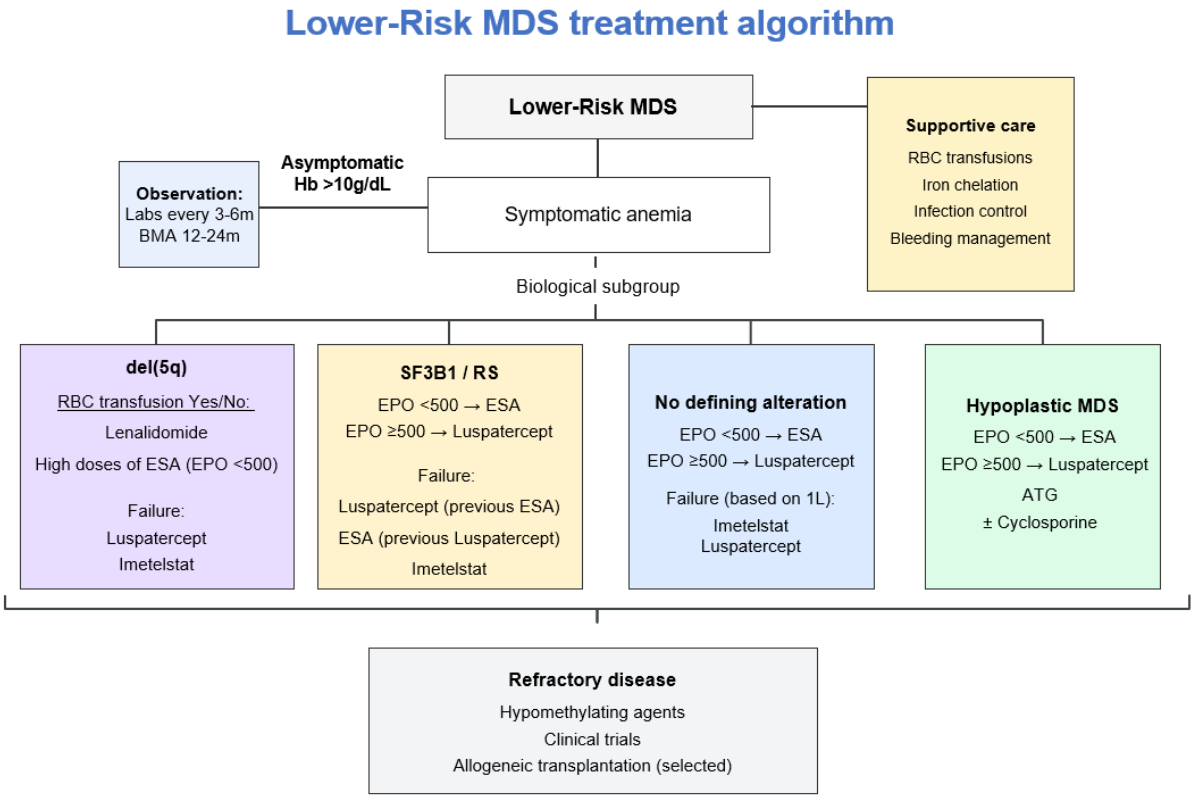
Luspatercept and imetelstat are the most recent FDA-approved agents for participants with LR-MDS and transfusion-dependent anemia refractory to or ineligible for ESAs.

Luspatercept is a recombinant fusion protein that functions as a ligand trap for members of the transforming growth factor-β (TGF-β) superfamily, thereby promoting late-stage erythroid maturation. It is indicated for adults with very low-, low-, or intermediate-risk MDS who require regular RBC transfusions, including those with RS or *SF3β1* mutations, and after ESA failure. Clinical trials have demonstrated superior efficacy compared with placebo in the post-ESA setting and superiority over ESA in the frontline setting, with higher and more durable rates of transfusion independence, particularly in participants with ring sideroblasts or *SF3β1* mutations, but also in non-ring sideroblast subgroups when used as first-line therapy [115–122].

Imetelstat is a first-in-class telomerase inhibitor approved for adults with low- to intermediate-1-risk MDS and transfusion-dependent anemia (≥4 units/8 weeks) who have failed or are not candidates for ESA therapy. In the phase 3 IMerge trial, imetelstat achieved significantly higher transfusion independence rates (40% for ≥8 weeks; 28% for ≥24 weeks) compared with placebo, with responses observed across clinical subgroups, including participants without RS [120–122]. The most frequent adverse events were grade 3–4 neutropenia and thrombocytopenia, typically reversible and manageable with appropriate dose modifications [122].

Together, luspatercept and imetelstat represent significant advances in the treatment of LR-MDS with transfusion-dependent anemia, addressing a longstanding unmet need for effective second-line options following ESA failure [115–122].

Figure 5. **Low-risk MDS treatment algorithm**.



Simplified therapeutic algorithm for lower-risk myelodysplastic syndromes (LR-MDS) based on the 2026 recommendations of the Spanish Myelodysplastic Syndromes Group (GESMD) [117]. Treatment selection is guided by the presence of symptomatic anemia and biological subgroups defined by cytogenetic or molecular features.

ESA, erythropoiesis-stimulating agents; HMA, hypomethylating agents.

1.1.9.2 Management of higher-risk MDS

In contrast to LR-MDS, the primary therapeutic goal in HR-MDS is to modify disease course, prevent leukemic transformation, and prolong survival, as these patients typically have a poor prognosis with a median survival of approximately 1–2 years. Treatment decisions remain individualized, taking into account age, performance status, comorbidities, genetic features, donor availability, and patient preferences [124-128]. However, aside from allogeneic hematopoietic stem cell transplantation (Allo-HSCT), the only potentially curative approach, available therapies provide only modest survival benefit. First-line therapy for HR- MDS are the hypomethylating agents (HMAs) azacitidine and decitabine, which remain to be the unique therapy for most of these participants. Azacitidine is supported by randomized phase 3 data (AZA-001) showing improved OS compared to conventional care regimens (median survival 24.5 vs 15 months) [129]. Decitabine has similar efficacy, though survival benefits over best

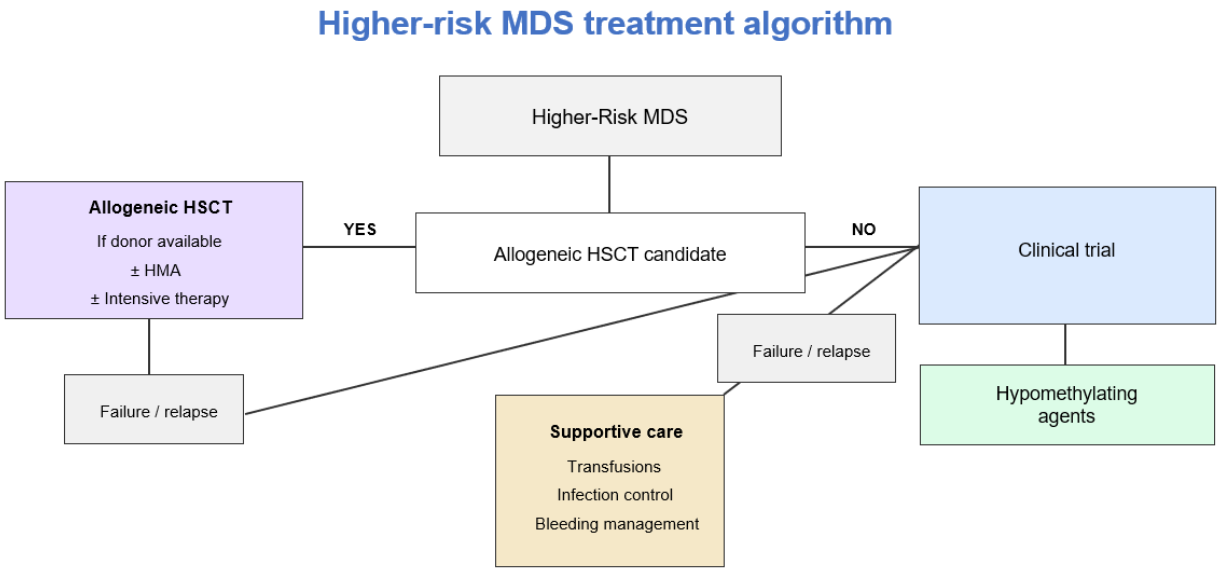
supportive care are less robust [12]. HMA-based combinations with at least 10 different drugs have failed to demonstrate any survival benefit over monotherapy in randomized trials [130-134].

Allo- HSCT should be considered for all eligible participants at diagnosis [125-128]. Early referral and transplant after optimal donor identification is associated with improved outcomes [12]. Pre-transplant cytoreduction with HMAs or intensive chemotherapy may be considered, especially in participants with excess blasts (>10%) [129]. However, most participants are ineligible due to age and comorbidity **(Figure 6)**.

Management after HMA failure is challenging, as median survival drops below 6 months, and no standard therapies exist [12] [135]. Options include cytotoxic chemotherapy (e.g., low dose cytarabine, sometimes combined with venetoclax), clinical trial enrollment, and investigational targeted agents (e.g., IDH1/2 inhibitors for participants with relevant mutations) [130-134]. The expanding landscape of combination and targeted therapies, particularly those addressing *TP53*-mutated and relapsed/refractory disease, represents a major step toward improving survival outcomes in this high-risk population.

Supportive care is essential throughout the disease course and includes transfusions for cytopenias, prophylactic antibiotics for infection risk, and iron chelation for transfusion-dependent participants [135]. These measures improve quality of life and reduce complications.

Figure 6. Proposed high-risk MDS treatment algorithm.



Therapeutic algorithm for higher-risk myelodysplastic syndromes (HR-MDS). Allogeneic hematopoietic stem cell transplantation (Allo-HSCT) remains the only potentially curative therapy and is recommended for eligible patients. Hypomethylating agents or clinical trials are the main options for non-transplant candidates or for patients awaiting transplantation.

HSCT, hematopoietic stem cell transplantation; HMA, hypomethylating agents.

2. HYPOTHESIS

Immune system dysregulation, particularly impaired NK cell function, expansion of MDSCs, and altered cytokine signaling, contributes to the pathogenesis and clinical progression of MDS.

3. OBJECTIVES

In order to test our hypothesis, we carried out a comprehensive set of analyses aimed at achieving the following objectives:

3.1 Main objective

To characterize the immune landscape of participants with MDS, focusing on innate and adaptive immune cell populations, their phenotypic and molecular profiles, and their association with disease progression.

3.2 Secondary objectives

- To characterize immune cell populations in the BM of MDS participants, including lymphocyte subsets, NK cells, and MDSCs, and analyze their KIR genotypes.
- To evaluate the interaction between BM NK cells and MDSCs cells in MDS participants.
- To analyze BM cytokine and chemokine concentrations in MDS participants and assess their relationship with clonal populations and major immune subsets.

4. MATERIALS AND METHODS

4.1 Study design

This was a prospective, observational, longitudinal, and comparative cohort study across three Spanish hematology centers: Vall d'Hebron University Hospital (Barcelona), IBSAL–Salamanca University Hospital (Salamanca), and the Centro de Investigación Médica Aplicada (CIMA), University of Navarra–IDISNA (Pamplona), between January 2018 and December 2024.

Three predefined cohorts were included: participants with MDS diagnosed according to the WHO 2017 criteria, individuals with ICUS, and healthy donors (HD) who served as controls.

4.2 Study population and sample collection

4.2.1 Study population

This study prospectively enrolled a total of seventy-one subjects between January 2018 and December 2021. BMA and peripheral blood samples were collected prospectively from three predefined cohorts: fifty participants with MDS without RS or isolated del(5q), eleven individuals with ICUS, and ten HD. Cases with RS or isolated del(5q) were excluded because these represent distinct biological entities with well- characterized behavior that could confound the analysis. The ICUS group included subjects presenting with persistent cytopenia and a clinical suspicion of MDS but with inconclusive BM findings that did not meet the diagnostic criteria for MDS according to the WHO 2017 classification. HD were BM donors whose samples were obtained during the harvest procedure.

4.2.2 Sample collection and processing

BMA was performed at the time of diagnosis in all MDS and ICUS participants. In nineteen participants, a second BMA and Peripheral blood sample was obtained at the one-year follow-up. The limited number of follow-up samples reflect both logistical constraints related to sample collection and referral between participating centers, as well as clinical factors. In some patients, follow-up samples were not indicated due to stable disease without evidence of progression, compounded by pandemic-related constraints. When clinically indicated, a repeat analysis was also performed prior to treatment initiation. Therefore, longitudinal analyses were performed on all available follow-up samples.

All samples were processed and shipped within 24 hours of collection following standardized institutional procedures to ensure specimen integrity and reproducibility. Due to sample availability and occasional quality limitations, not all patients had

evaluable material for every experimental analysis. Because BM sampling is invasive, procedures were not repeated solely for research purposes when samples were missing or of insufficient quality. Consequently, the number of patients included varies across analyses. Only samples meeting predefined quality criteria were included, and analyses were performed on all available evaluable samples without imputation. The number of evaluable samples for each analysis is reported in the corresponding Results section.

4.2.3 Clinical data collection

Baseline clinical data, including comorbidities, history of autoimmune disease, and concomitant medications, together with baseline laboratory parameters and cytogenetic findings from BMA, were retrieved from the electronic medical records at the time of diagnosis and follow-ups. In addition, cytomegalovirus (CMV) serology was performed on peripheral blood serum collected concurrently with the diagnostic BM sample, given the known impact of prior CMV infection on NK cell differentiation and repertoire composition, including modulation of KIR expression and KIR–HLA interactions.

4.2.4 Diagnostic classification and risk stratification

The diagnosis of MDS was established according to the WHO 2017 classification [86]. Disease risk was assessed using the IPSS-R [96], with scores ≤3.5 defining lower-risk disease [97-98]. In addition, patients were stratified using the IPSS-M [94], calculated retrospectively in all patients based on available molecular data.

4.2.5 Follow-up definitions

Follow-up time was defined as the interval from the date of diagnosis to the date of death or last clinical assessment, whichever occurred first. Patients who were alive at last follow-up or had unknown vital status were censored at the date of their last available clinical contact. In cases where the last follow-up date coincided with or preceded the date of diagnosis, follow-up duration was recorded as zero months. Clinical follow-up analysis was performed exclusively on the MDS and ICUS cohorts. Healthy donors were utilized solely as a control group.

4.3 Laboratory assessments and analyses

4.3.1 Characterization of immune cell populations

Immune cell populations were analyzed by multiparametric flow cytometry following a standardized membrane staining protocol. Fresh BM and peripheral blood samples were processed within 24 hours of collection. Red blood cell lysis was performed using an ammonium chloride/based lysing solution (Pharm Lyse, BD Biosciences), followed by washing with phosphate-buffered saline containing 0.2% bovine serum albumin (PBS–BSA). Approximately 1-2x10^6 cells were used for staining each tube.

Cells were incubated with fluorochrome-conjugated monoclonal antibodies according to the predefined panels for 30 minutes at room temperature in the dark. After incubation, samples were washed with PBS–BSA, centrifuged, and resuspended in staining buffer prior to acquisition. Data acquisition was performed immediately after staining, collecting up to 500,000 nucleated events per tube.

Data acquisition was performed on a Navios EX flow cytometer (Beckman Coulter, Brea, CA, USA) equipped with 10 colors and 3 lasers. Data was analyzed and interpreted using Kaluza software (Beckman Coulter, Brea, CA, USA).

NK and T lymphocyte cells were expressed as a percentage of the total lymphocyte pool. NK subpopulations were analyzed in BM samples and were determined by $CD45^{+}CD3^{-}CD19^{-}$ cells in the lymphocyte gate and defined with the following monoclonal antibodies (moAbs): CD56 and CD16 differentiating mature NK cells ($CD56^{dim}CD16^{bright}$), immature NK cells ($CD56^{bright}CD16^{neg}$), and inhibitory NK cells ($CD56^{neg}CD16^{bright}$).

The expression of activating receptors (NKp46, NKp30, NKp44, NKG2C, NKG2D, and DNAM) and inhibitory receptors (TIGIT, NKG2A/CD94, IRp60, and PD-1), together with the cytotoxic effector molecules perforin and granzyme B, were evaluated within these subpopulations. In parallel, the expression of NK-cell ligands, including HLA-ABC, MICA/B, CD155, and PD-L1, was examined on disease precursor cells, monocytes, and granulocytes.

T-cell subpopulations were analyzed in peripheral blood samples using a preconfigured Duraclone® panel (Beckman Coulter), which includes markers for T-cell differentiation and activation, as well as CD16 and CD56 for NK cell identification. T-cell subsets were defined as $CD45^{+}CD3^{+}$ lymphocytes. Subsets included $CD4^{+}$ and $CD8^{+}$ T cells, naïve T cells ($CCR7^{+}CD45RA^{+}$), central memory ($CCR7^{+}CD45RA^{-}$), effector memory ($CCR7^{-}CD45RA^{-}$), and effector T cells ($CCR7^{-}CD45RA^{+}$), as well as Tregs ($CD4^{+}CD25^{+}CD127low$) and T helper subsets (Th1: $CXCR3^{+}CCR6^{-}$; Th2: $CCR4^{+}CCR6^{-}$; Th17: $CCR6^{+}CCR4^{+}$). PD-1 expression was evaluated in $CD4^{+}$ and $CD8^{+}$ T cells. The classification of T immune cell subsets according to the markers used is summarized in **Supplementary Table S1.**

Additionally, MDSCs were evaluated, distinguishing between granulocytic (Gr-MDSCs; $CD11b^{+}CD33^{+}HLA\text{-}DR^{-}CD15^{+}CD14^{-}$) and monocytic (Mo-MDSCs; $CD11b^{+}CD33^{+}$HLA-DR^low^$CD15^{+}CD14^{+}$) subsets.

All antibodies, fluorochromes, clones, and manufacturers used in the study are detailed in **Supplementary Table S2,** which summarizes the complete flow cytometry panels employed for immune phenotyping.

4.3.2 Analysis of cytokines and chemokines

Cytokine and chemokine concentrations were analyzed from BM supernatant samples collected at a single time point during the diagnosis. Samples were processed within 24 hours of collection by centrifugation at 1,300 × g for 10 minutes, after which the plasma supernatant was aliquoted and stored at −80 °C until analysis. Cytokine quantification was performed using a bead-based multiplex immunoassay (ProcartaPlex™ 32-plex panel, Thermo Fisher Scientific, Waltham, MA, USA) on the Luminex® MAGPIX platform, following the manufacturer's instructions. This technology uses fluorescently coded magnetic microspheres coated with capture antibodies to simultaneously quantify multiple soluble analytes in a single sample.

The assay quantified a wide range of soluble mediators, including pro- and anti-inflammatory cytokines (IL-1α, IL-1β, IL-1RA, IL-2, IL-3, IL-4, IL-5, IL-6, IL-7, IL-8, IL-9, IL-10, IL-12p70, IL-13, IL-15, IL-17A/CTLA-8, and IL-22), immunomodulatory cytokines (IFN-α, IFN-γ, TNF-α), chemokines (eotaxin/CCL11, IP-10/CXCL10, MCP-1/CCL2, MIG/CXCL9, MIP-1α/CCL3, and MIP-1β/CCL4), and growth factors (FGF-2, EGF, G-CSF, GM-CSF, HGF, and VEGF-A). Each sample was analyzed in duplicate to ensure technical accuracy. Data acquisition and quantification were performed using the Invitrogen ProcartaPlex Analysis App, applying a five-parameter logistic (5-PL) standard curve fitting for concentration determination. The sensitivity of the assay varied according to the specific analyte measured.

4.3.3 KIR and HLA genotyping and haplotype determination

KIR genotyping was performed using PCR-SSO (polymerase chain reaction–sequence-specific oligonucleotide) and NGS–based approaches to characterize gene content and haplotypic distribution. Genomic DNA was extracted from peripheral blood samples using standard protocols. The presence or absence of individual KIR genes was initially determined by PCR-SSO analysis, while allelic resolution and detailed haplotype assignment were further investigated using NGS.

For the NGS workflow, long-range PCR amplification of KIR and HLA class I loci was carried out using custom primer mixes targeting multiple KIR regions, including generic primers for KIR3DL3, KIR3DP1, and KIR2DL4 loci. Amplified products were verified by agarose gel electrophoresis (0.5–1% agarose), prior to library preparation.

NGS libraries were generated using NGSgo® workflow (GenDx, Utrecht, The Netherlands) following the manufacturer's instructions. Briefly, amplified DNA fragments underwent enzymatic fragmentation, end repair, and dA-tailing, followed by adapter ligation, and indexing PCR. Library purification and size selection were performed using magnetic-based purification (AMPure XP, Beckman Coulter). Indexed libraries were quantified, pooled equimolarly, and sequenced on an Illumina MiSeq platform (Illumina, San Diego, CA, USA).

Sequencing data were analyzed using CLC Genomics Workbench (Qiagen) and NGSengine® software (GenDx) for gene calling and haplotype reconstruction. KIR genes analyzed included KIR2DL1, KIR2DL2, KIR2DL3, KIR2DL4, KIR2DL5, KIR2DS1–2DS5, KIR3DL1–3DL3, KIR3DS1, and the pseudogenes KIR2DP1 and KIR3DP1. Gene content results were reported as presence or absence of each KIR gene, while full allelic resolution remained pending further validation.

KIR A and B haplotypes were assigned based on gene content following the classification criteria defined in the Immuno Polymorphism Database (IPD-KIR, EMBL-EBI). KIR genotyping results were integrated with NK-cell phenotypic data obtained by flow cytometry to explore potential associations between KIR gene content and NK-cell receptor expression.

In parallel, HLA class I genotyping (HLA-A, -B, and -C) was performed using the same NGSgo® library preparation workflow and MiSeq sequencing platform to assess potential KIR–HLA ligand interactions. HLA allele assignment and haplotype inference were conducted using NGSengine® software with reference to the IMGT/HLA Database (version 3.52.0). HLA-C alleles were classified into C1 (Asn80) or C2 (Lys80) groups according to the polymorphism at residue 80. The Bw4 epitope was determined at the HLA-B locus and at the HLA-A locus (specifically alleles A23, A24, and A*32). Patients were stratified according to HLA-C genotype (C1/C1, C1/C2, or C2/C2) and by the presence or absence of Bw4 ligands.

4.3.4 Molecular analyses

Targeted next-generation sequencing (NGS) was performed to analyze 40 genes and 29 fusion gene drivers associated with myeloid malignancies in samples from MDS and ICUS subjects. The analysis was conducted using the Oncomine™ Myeloid Research Assay (Thermo Fisher Scientific, Waltham, MA, USA) on the Thermo Fisher automated sequencing platform, which includes the Ion Chef™ and Ion S5 XL™ systems.

DNA and RNA were extracted from mononuclear cells isolated from BMA. Library preparation was performed using 20 ng of DNA and 100 ng of RNA, following the manufacturer's protocols. The mean sequencing depth of coverage achieved was approximately 2,500×, ensuring high sensitivity for variant detection.

Variant calling and filtering included pathogenic, likely pathogenic, and variants of unknown significance (VUS), based on a minimum variant coverage of 25 reads and a minimum allele frequency (AF) threshold of 1%. The limit of detection (LOD) for fusion gene transcripts was set at ≥0.1%.

Sequencing quality control was assessed using the Ion Torrent Suite™ and Ion Reporter™ software. Key parameters such as on-target percentage, coverage uniformity, and mean read depth were reviewed for each run, all of which met or exceeded the manufacturer's specifications for the Oncomine™ Myeloid Research Assay. Overall, the sequencing demonstrated robust analytical performance and high reproducibility across all samples analyzed.

4.4 Statistical analysis

Descriptive statistics were used to summarize demographic and clinical characteristics. Categorical variables were expressed as frequencies and percentages, while continuous variables were reported as medians with interquartile ranges (IQR) or full ranges, as appropriate. Comparisons between two independent groups were performed using the Mann–Whitney U test (Wilcoxon rank-sum test) for continuous variables and the chi-square test or Fisher's exact test for categorical variables, as applicable.

When more than two groups were analyzed (e.g., MDS, ICUS, and HD), pairwise non-parametric comparisons were performed. To account for multiple testing across immune parameters, p values were adjusted using the Benjamini–Hochberg false discovery rate (FDR) method. Continuous variables showed non-normal distributions and were therefore analyzed using non-parametric methods.

Even though adjustment for multiple comparisons was performed, the results remain exploratory in nature and should be interpreted with caution. All statistical analyses were conducted using R software (version 4.2.2; R Foundation for Statistical Computing, Vienna, Austria). All tests were two-sided, and $p < 0.05$ or FDR-adjusted $p < 0.05$ was considered statistically significant.

4.5 Ethical considerations

All participants provided written informed consent prior to enrollment, in accordance with the principles of the Declaration of Helsinki. The study protocol was reviewed and

approved by the Clinical Research Ethics Committee of Vall d'Hebron University Hospital (approval numbers 325/2018 and 460/2020). All procedures involving human samples and clinical data complied with the requirements of the European Union General Data Protection Regulation (GDPR) 2016/679 and the Spanish Organic Law 3/2018 on the Protection of Personal Data and Guarantee of Digital Rights. Participant confidentiality was strictly maintained throughout the study.

5. RESULTS

5.1 Subjects baseline characteristics

A total of 71 subjects were included in the study, from whom frozen BM supernatant samples were collected. Among them, 50 were diagnosed with MDS, 11 with ICUS, and 10 were HD. Baseline demographic and clinical characteristics are summarized in **Table 8.**

In the overall cohort, the median age was 75.0 years (range, 18–89), and 54.9% of subjects were male. Autoimmune disease was present in 4 participants (5.6%), including 3 with MDS and 1 with ICUS.

Table 8. Demographics and baseline laboratory characteristics at diagnosis.

	MDS (n= 50)	**ICUS (n= 11)**	**HD (n= 10)**	**Total (n= 71)**
Age, yrs Median (range)	80 (23-89)	73 (54-84)	40 (18-72)	75 (18-89)
Sex, n (%)				
Male	27 (54)	7 (63.6)	5 (50)	39 (54.9)
Female	23 (46)	4 (36.4)	5(50)	32 (45.1)
Hemoglobin, gr/dl Median (IQR)	9.9 (8.5–11.2)	11.2 (9.4–12.9)	14.1 (12.6–14.9)	10.3 (9.0–12.5)
Total WBC, $x10^9$/L Median (IQR)	3.82 (2.29–5.09)	3.94 (2.71–5.47)	6.21 (5.33–7.47)	4.15 (2.42–5.95)
ANC, $x10^9$/L Median (IQR)	1.95 (0.75–3.33)	1.90 (1.30–3.10)	3.36 (2.62–4.00)	2.40 (1.15–3.50)
Lymphocytes, $x10^9$/L Median (IQR)	1.30 (0.82–1.79)	1.20 (0.75–1.40)	2.33 (1.92–2.77)	1.40 (0.90–1.94)
Platelets, $x10^9$/L Median (IQR)	103.5 (64.5–171.0)	123.0 (87.0–224.5)	237.0 (212.5–306.8)	123.0 (71.3–208.0)

MDS, myelodysplastic syndromes; ICUS, idiopathic cytopenia of undetermined significance; HD, healthy donors; IQR, interquartile range; WBC, white blood cells; ANC, absolute neutrophil count; g/dL, grams per deciliter; ×10⁹/L, cells ×10⁹ per liter.

According to the WHO 2017 classification, 66.0% (33/50) of MDS participants were classified as MDS with single- or multilineage dysplasia (SLD/MLD), while 34.0% (17/50) had MDS with excess blasts (EB-1 or EB-2). Based on the IPSS-R 3.5 cut-off, 56.0% (28/50) were classified as LR-MDS and 44.0% as HR-MDS.

Very poor cytogenetic risk according to IPSS-R was identified in 10.0% of MDS patients (5/50). Somatic mutations at diagnosis were detected in 91.0% of cases. According to the IPSS-M classification, 24 of 44 evaluable patients (54.5%) were categorized as very low, low, or moderate-low risk, whereas the remaining 20 patients (45.5%) were classified as moderate-high, high, or very-high risk. **Table 9 and Supplementary S3.**

The median clinical follow-up for the study population was 25.4 months (IQR, 2.5–55.4), and 39/61 (64%) were alive as of January 2025. Patients in the ICUS group had a notably longer median follow-up of 58.5 months (IQR, 44.2 - 60.3) compared to MDS group, which presented a median follow-up of 14.8 months (IQR 1.9 - 43.3), with 62% of MDS alive at the last follow-up and 54% having received treatment. In the ICUS, 72.7% were alive and 18.2% treated after evolution to MDS.

During follow-up, disease progression was observed in 10 patients (14.0%), including progression from MDS to AML in seven patients, progression from LR to HR-MDS in one patient, and progression from ICUS to MDS in two patients.

Table 9. Stratification of MDS patients.

Classification System	Category	n (%)
WHO 2017 classification	MDS-SLD	1 (2.0)
	MDS-MLD	32 (64.0)
	MDS-EB-1	8 (16.0)
	MDS-EB-2	9 (18.0)
	SLD/MLD	**33 (66.0)**
	EB-1/EB-2	**17 (34.0)**
IPSS-R risk category	Very low	6 (12.0)
	Low	20 (40.0)
	Intermediate	12 (24.0)
	High	4 (8.0)
	Very high	8 (16.0)
	Low risk (very low + low)	**26 (52.0)**
	High risk (high + very high)	**12 (24.0)**
IPSS-R score (3.5 cut-off)	≤ 3.5	28 (56.0)
	> 3.5	22 (44.0)

NK, natural killer; MDS, myelodysplastic syndromes; ICUS, idiopathic cytopenia of undetermined significance; IPSS-R, Revised International Prognostic Scoring System, HD, healthy donors; IQR, interquartile range; CD, cluster of differentiation.

5.2 Main Findings

5.2.1 Immune cells subpopulation

5.2.1.1 NK cells

5.2.1.1.1 Phenotypic expression of NK cell receptors in BM

To characterize alterations in the NK cell compartment, we analyzed the frequency and maturation status of NK cell subsets, as well as the expression of NK cell receptors associated with inhibitory or activated phenotypes and the expression of their corresponding ligands on pathological cells in BM samples from MDS patients, ICUS patients, and HD. In addition, cytotoxic profiles were evaluated in MDS and ICUS patients, and all findings were analyzed in relation to disease risk stratification in MDS patients. NK cell phenotypic and functional analyses were performed on evaluable BM samples from a subset of patients, depending on sample availability and quality. NK phenotyping was available for 50 MDS patients, 10 ICUS patients, and 10 HD.

- **Frequency and maturation status of NK cell subsets**

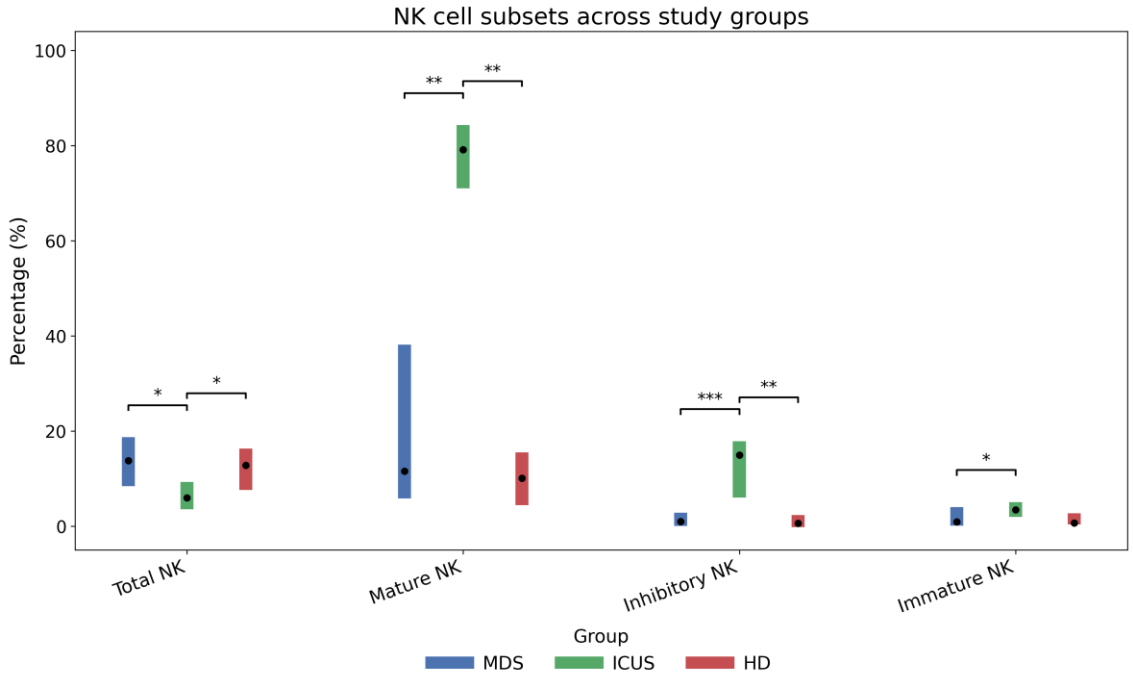
By flow cytometry, MDS patients showed a higher proportion of total NK cells, with a median frequency of 13.75% (IQR, 8.40–18.12), compared with ICUS patients [5.96% (IQR, 3.81–9.01); p = 0.01], while no significant difference was observed relative to HD [12.81% (IQR, 7.87–16.05); p = 0.20].

In contrast, ICUS patients exhibited a marked enrichment of mature NK cells ($CD56^{dim}CD16^{bright}$), accounting for 79.16% (IQR, 71.27–84.05) of NK cells, compared with MDS patients [11.57% (IQR, 6.08–37.92); p = 0.01] and HD [10.1% (IQR, 4.64–15.25); p = 0.01].

Similarly, the inhibitory NK cell subset ($CD56^{neg}CD16^{bright}$) was significantly expanded in the ICUS group [14.93% (IQR, 6.29–17.58)] in comparison to both MDS patients [1.00% (IQR, 0.29–2.58); p = 0.004] and HD [0.58% (IQR, 0.07–2.17); p = 0.03]. No significant differences in this subset were observed between MDS patients and HD (p = 0.65).

Furthermore, the immature NK cell subset ($CD56^{bright}CD16^{neg}$) was also increased in ICUS patients [3.41% (IQR, 2.23–4.78)] compared with MDS patients [1.00% (IQR, 0.35–3.74); p = 0.02] and showed a trend toward higher levels relative to HD [0.67% (IQR, 0.58–2.42); p = 0.06]. No significant difference in this subset was detected between MDS patients and HD (p = 0.80) **(Figure 7).**

Figure 7. Distribution of NK cell subpopulations across study groups.



Box-and-whisker plots represent the median and interquartile range (IQR) of total NK cells, mature NK cells ($CD56^{dim}CD16^{bright}$), inhibitory NK cells ($CD56^{neg}CD16^{bright}$), and immature NK cells ($CD56^{bright}$^$CD16^{neg}$) in patients with MDS, ICUS, and HD. Statistical comparisons were performed using non-parametric tests. Only statistically significant pairwise differences are shown and are indicated by brackets and asterisks ($p < 0.05$; $p < 0.01$; $p < 0.001$)

NK, natural killer; MDS, myelodysplastic syndromes; ICUS, idiopathic cytopenia of undetermined significance; HD, healthy donors; IQR, interquartile range; CD, cluster of differentiation.

- **Functional characterization of the NK cell compartment**

Within the NK cell compartment, distinct patterns of receptor expression were observed across the study groups. The expression of activating receptors, including NKp46, NKp30, NKG2C, NKG2D, and DNAM-1, was heterogeneous among MDS patients, ICUS patients, and HD.

Among the natural cytotoxicity receptors (NCRs), NKp46 expression was significantly increased in both MDS [49.45% (IQR, 0.01–75.99); $p = 0.05$] and ICUS [40.76% (IQR, 21.61–57.85); $p = 0.02$] compared with HD [1.47% (IQR, 0.01–15.82)], while no significant differences were observed between the MDS an ICUS ($p = 0.70$). NKp44 showed overall low expression across all groups but was significantly higher in MDS

[0.20% (IQR, 0.00–0.43); p = 0.005] and HD [0.29% (IQR, 0.15–20.26); p = 0.002] compared to ICUS, where it was virtually undetectable. NKp30 was consistently expressed across all groups without statistically significant differences.

Regarding receptors of the NKG2 family, NKG2C showed a significant reduction in both MDS [4.82% (IQR, 1.46–17.62); p = 0.05] and ICUS [3.38% (IQR, 0.00–9.54); p = 0.02] relative to HD [20.59% (IQR, 6.25–46.53)]. NKG2D expressions were preserved across all cohorts. Notably, DNAM-1, a critical receptor for tumor recognition, was significantly downregulated in ICUS [67.79% (IQR, 57.64–85.67)] compared to both MDS [96.06% (IQR, 89.20–98.67); p = 0.0002] and HD [95.44% (IQR, 91.52–97.29); p = 0.0006]. No significant differences were observed between MDS patients and HD (p = 0.80) **(Table 10).**

Table 10. Expression of activating NK cell receptors across study groups.

Activating Receptors	MDS (n=50)	ICUS (n=10)	HD (n=10)	MDS vs ICUS *p*	MDS vs HD *p*	ICUS vs HD *p*
NCR family, Median (IQR)						
NKp46 (335)	49.45 (0.01–75.9)	40.76 (21.6–57.8)	1.47 (0.01–15.8)	0.70	0.05	0.02
NKp30 (337)	44.5 (27.9–60.9)	47.5 (40.7–67.7)	45.0 (19.4–59.8)	0.33	0.89	0.57
NKp44 (336)	0.2 (0.0–0.4)	0.00 (0.0–0.00)	0.2 (0.1–20.2)	0.005	0.23	0.002
NKG2 family, Median (IQR)						
NKG2C	4.8 (1.4–17.6)	3.3 (0.0–9.54)	20.5 (6.2–46.5)	0.17	0.05	0.02
NKG2D	95.9 (90.8–98.3)	94.4 (83.5–96.0)	92.4 (86.1–97.1)	0.13	0.21	0.96
Others, Median (IQR)						
DNAM-1	96.0 (89.2–98.6)	67.7 (57.6–85.6)	95.4 (91.5–97.2)	0.0002	0.89	0.0006

The table summarizes the expression of activating receptors within the NK cell compartment in patients with MDS (n= 50), ICUS (n = 10), and HD (n= 10). Data is presented as median values with IQR. Pairwise comparisons between groups were performed using non-parametric tests, with corresponding p values reported for MDS vs

ICUS, MDS vs HD, and ICUS vs HD. Statistically significant differences are highlighted in bold.

MDS, myelodysplastic syndromes; ICUS, idiopathic cytopenia of undetermined significance; HD, healthy donors; NK, natural killer; NCR, natural cytotoxicity receptor; IQR, interquartile range; NKp30, natural cytotoxicity receptor 3 (CD337); NKp44, natural cytotoxicity receptor 2 (CD336); NKp46, natural cytotoxicity receptor 1 (CD335); NKG2C, natural killer group 2 member C; NKG2D, natural killer group 2 member D; DNAM-1, DNAX accessory molecule-1 (CD226).

To further characterize the regulatory landscape of NK cells, the analysis was extended to inhibitory receptors, including TIGIT, PD-1, NKG2A/CD94, and IRp60. Although heterogeneous expression patterns were observed and all receptors were detectable across the three study groups, immune checkpoint receptors such as TIGIT and PD-1 showed modest differences, with lower expression in MDS and ICUS compared with HD. These differences reached statistical significance in pairwise comparisons between MDS and ICUS and between MDS and HD, respectively. In contrast, no statistically significant differences were identified for the remaining inhibitory receptors. Finally, NK cell cytotoxic potential was assessed through the expression of perforin and granzyme B, which likewise did not differ significantly among groups. **(Table 11).**

Table 11. Expression of inhibitory NK cell receptors and cytotoxic markers.

Inhibitory Receptors	MDS (n=50)	ICUS (n=10)	HD (n=10)	MDS vs ICUS *p*	MDS vs HD *p*	ICUS vs HD *p*
NKG2A	72.0 (55.4–91.9)	84.1 (64.8–85.9)	73.6 (68.1–85.7)	0.5	0.9	0.5
TIGIT	40.1 (10.0–64.8)	43.5 (28.3–53.9)	69.2 (47.5–79.7)	0.9	0.05	0.07
PD-1	0.04 (0.0–0.4)	0.00 (0.0–0.0)	0.2 (0.03–2.5)	0.004	0.1	0.0002
IRp60	95.5 (89.2–98.6)	85.0 (57.6–85.6)	89.9 (91.5–97.2)	0.4	0.4	0.9
Perforin	34.7 (12.6–59.8)	42.6 (38.–54.6)	29.7 (18.9–43.5)	0.2	0.8	0.2
Granzyme	34.9 (17.2–68.1)	35.4 (26.5–38.4)	34.2 (22.7–58.0)	0.7	0.7	0.9

Data are presented as median and IQR. Pairwise comparisons were performed using non-parametric tests.

MDS, myelodysplastic syndromes; ICUS, idiopathic cytopenia of undetermined significance; HD, healthy donors; NK, natural killer; IQR, interquartile range; NKG2A, natural killer group 2 member A; TIGIT, T-cell immunoreceptor with Ig and ITIM domains; PD-1, programmed cell death protein 1; IRp60, inhibitory receptor protein 60.

- **Analysis of NK-cell ligands in the myeloid compartment**

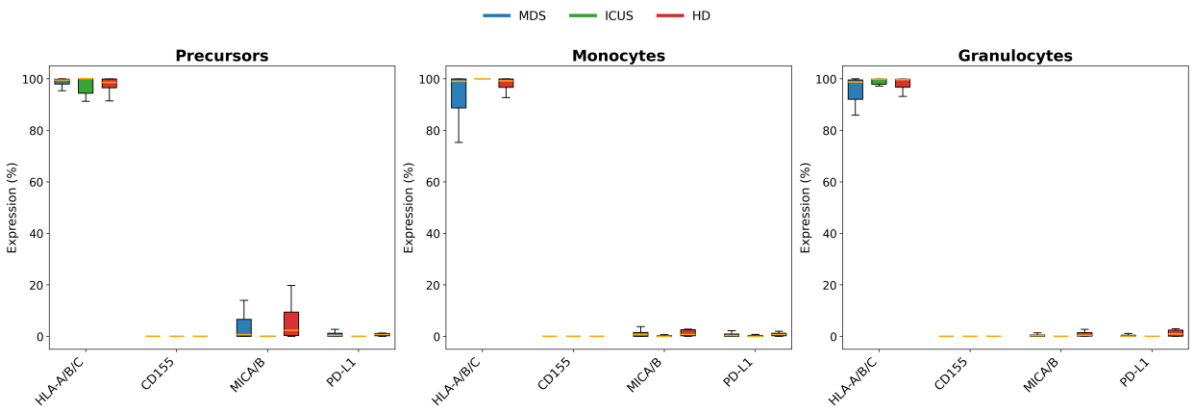
To evaluate the susceptibility of target cells to NK-mediated lysis, we analyzed the expression of key ligands on hematopoietic precursors, monocytes, and granulocytes. No loss of HLA-A/B/C was observed in any of the analyzed populations. CD155 was consistently absent, whereas PD-L1 (CD274) and MICA/B were significantly downregulated in ICUS compared to both MDS and HD, across all myeloid compartments. These findings are summarized in **Figure 8 and Supplementary Table S4.**

5.2.1.1.2 KIR phenotype and genotyping analysis in MDS patients

- *KIR phenotype:*

Phenotypic characterization of seven KIRs, including inhibitory receptors (3DL1, 2DL2/3, and 2DL1) and activating receptors (3DS1, 2DS1, 2DS4, and 2DS2), revealed

Figure 8. Differential expression of NK-cell ligands.



Boxplots show the percentage of positive cells for HLA-A/B/C, CD155, MICA/B, and PD-L1 (CD274) on hematopoietic precursors, monocytes, and granulocytes from patients with MDS, ICUS, and HD. Data are presented as median with (IQR, 25–75). Group comparisons were performed using the Mann–Whitney U test. Corresponding quantitative results and p-values are reported in Supplementary Table S4.

NK, natural killer; MDS, myelodysplastic syndromes; ICUS, idiopathic cytopenia of undetermined significance; HD, healthy donors; HLA, human leukocyte antigen; MICA/B, MHC class I polypeptide-related sequence A and B; PD-L1, programmed death-ligand 1 (CD274); IQR, interquartile range.

a significant divergence in activating receptor expression. MDS patients displayed lower expression of most activating KIRs (3DS1, 2DS1, 2DS4) compared to HD, with the exception of KIR2DS2, which was increased in MDS (p = 0.001) **(Table 12).**

Table 12. Activating KIR receptors in MDS and HD.

Activating KIRs	MDS median (IQR)	HD median (IQR)	MDS vs ICUS *p*	MDS vs HD *p*	ICUS vs HD *p*
KIR3DS1	0.00 (0.00–0.41)	5.98 (0.19–41.87)	0.01	0.005	0.0002
KIR2DS2	5.86 (1.32–13.82)	1.79 (0.00–4.65)	0.001	0.07	0.19
KIR2DS1	0.00 (0.00–0.00)	0.10 (0.00–0.33)	0.52	0.0004	0.18
KIR2DS4	31.02 (1.07–88.24)	81.14 (37.84–87.45)	0.002	0.19	0.001

Median percentage expression and IQR of activating KIRs in patients with MDS compared with HD. Pairwise comparisons between groups were performed using the Mann–Whitney U test. P values < 0.05 were considered statistically significant.

KIR, killer-cell immunoglobulin-like receptor; MDS, myelodysplastic syndromes; HD, healthy donors; IQR, interquartile range.

Strikingly, ICUS patients exhibited a highly restricted repertoire, with a near-complete absence of activating KIRs and a profile limited to inhibitory receptors **(Table 13).** This selective reduction of activating KIR expression in MDS, together with the preserved inhibitory KIR profile and the absence of activating KIRs in ICUS, may reflect differences in NK-cell education and licensing across disease states.

Table 13. KIR receptors expression.

Parameter	KIR nomenclature	Function	Haplotype	MDS median (IQR)	ICUS median (IQR)	HD median (IQR)	Overall *p*	MDS vs ICUS *p*	MDS vs HD *p*	ICUS vs HD *p*
158e2	**KIR3DS1**	**Activator**	**B**	0.00 (0.00–0.41)	0.00 (0.00–0.00)	5.98 (0.19–41.87)	0.0003	0.01	0.005	0.0002
158j	**KIR2DS2**	**Activator**	**B**	5.86 (1.32–13.82)	0.00 (0.00–0.83)	1.79 (0.00–4.65)	0.002	0.001	0.07	0.16
158h	**KIR2DS1**	**Activator**	**B**	0.00 (0.00–0.00)	0.00 (0.00–0.00)	0.10 (0.00–0.33)	0.002	0.52	0.0004	0.18
158i	**KIR2DS4**	**Activator**	**A**	31.02 (1.07–88.24)	0.00 (0.00–7.89)	81.14 (37.84–87.45)	0.002	0.002	0.19	0.001
158e1	**KIR3DL1**	**Inhibitory**	**A**	2.96 (0.00–11.44)	7.33 (0.73–20.21)	5.38 (1.18–10.47)	0.69	0.44	0.67	0.67
158b	**KIR2DL2/KIR2DL3**	**Inhibitory**	**B/A**	23.59 (5.04–44.50)	17.16 (15.00–38.50)	31.00 (14.89–44.97)	0.77	0.74	0.52	0.62
158a	**KIR2DL1**	**Inhibitory**	**A**	11.49 (2.83–27.96)	12.38 (8.50–18.90)	11.39 (1.83–47.33)	0.65	0.45	0.54	0.77

Median percentage expression and IQR, (25–75) of inhibitory KIRs in patients with MDS, ICUS, and HD. Overall comparisons were performed using the Kruskal–Wallis test, followed by pairwise Mann–Whitney U tests. Bold *p*-values indicate statistical significance ($p < 0.05$). KIR, killer-cell immunoglobulin-like receptor; MDS, myelodysplastic syndromes; ICUS, idiopathic cytopenia of undetermined significance; HD, healthy donors; IQR, interquartile range.

- *KIR genotype and KIR-ligand distribution*

To determine the genetic basis of these observations, KIR and HLA genotyping were performed in the MDS cohort (N =46). HLA typing was available as part of MDS pre-transplant evaluation. Consequently, KIR data were not obtained for the ICUS or HD cohorts. Following the definition of haplotypes based on the presence or absence of specific KIR genes, analysis revealed a predominance of group B–containing genotypes (Bx) 73.9% (34/46), whereas AA haplotype accounted for 26.1% (12/46). These findings are consistent with an expanded activating KIR repertoire in MDS cohort **(Figure 9).** Furthermore, the Bx group displayed marked heterogeneity, encompassing multiple centromeric and telomeric B configurations (e.g., Bx2, Bx3, Bx6, Bx7), reflecting the diversity of the activating KIR repertoire. The distribution of individual KIR genes across 46 MDS patients is detailed in **Supplementary Figure S5.**

Considering the critical role of KIR-HLA interactions in determining NK cell education and licensing, we characterized the KIR-ligand repertoire in the MDS group. We sought to determine whether a specific ligand background (e.g., HLA-C2 or Bw4 presence) could be associated with the phenotypic alterations observed in the NK cell subsets of MDS and ICUS patients. Characterization of the HLA ligand background in 43 MDS patients showed a balanced distribution of HLA-C groups, with frequencies of 32.6% for the C1/C1 genotype, 43.5% for C1/C2, and 17.4% for C2/C2. Regarding the KIR3DL1 receptor ligand, the Bw4 epitope (including Bw4+ HLA-A alleles such as A*23 and A*24) was present in 43.5% of the patients, while 50.0% were homozygous for Bw6.

In an integrative analysis of KIR and HLA genetics, we evaluated whether the presence of specific KIR haplotypes correlated with their cognate ligands. The most frequent integrative profile was the Bx haplotype combined with the C1/C2 genotype (39.5%).

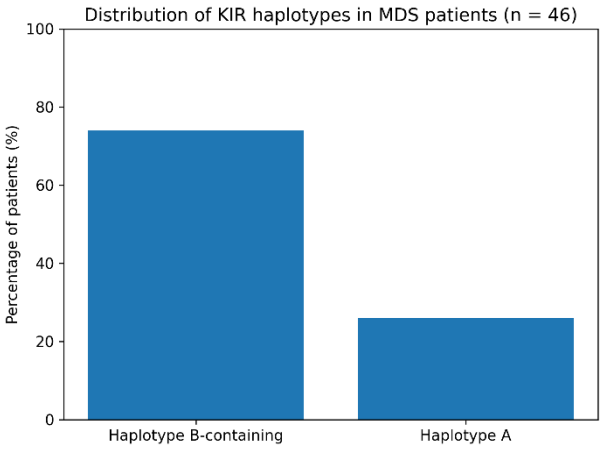
When assessing clinical outcomes, we observed that 75% of patients who underwent disease progression carried a Bx haplotype. Specifically, the Bx + C1/C1 combination exhibited the highest progression rate (14.2%), contrasting with the lack of progression in the Bx + C2/C2 group. These findings suggest that activating NK profile (Bx), when paired with specific HLA-C backgrounds (C1/C1), may influence the risk of disease transformation in MDS **(Figure 10)**.

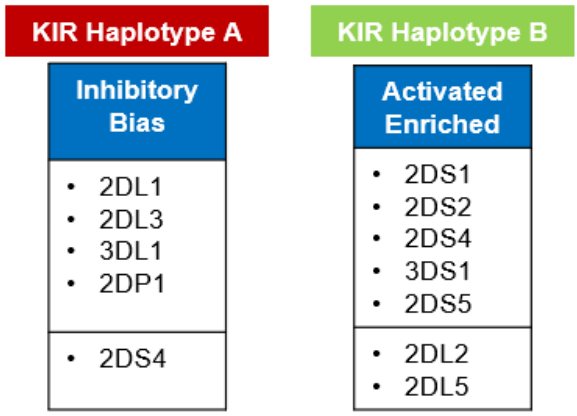
Figure 9. KIR gene repertoire and haplotype distribution.

A. KIR gene repertoire in MDS patients.

KIR gene	Function	Positive patients n (%)
Inhibitory		
2DL1	Inhibitory	45 (97.8)
2DL2	Inhibitory	28 (60.9)
2DL3	Inhibitory	43 (93.5)
2DL4	Inhibitory	46 (100)
2DL5	Inhibitory	27 (58.7)
3DL1	Inhibitory	43 (93.5)
3DL2	Inhibitory	46 (100)
3DL3	Inhibitory	46 (100)
Activating		
2DS1	Activating	22 (47.8)
2DS2	Activating	28 (60.9)
2DS3	Activating	16 (34.8)
2DS4	Activating	42 (91.3)
2DS5	Activating	17 (37.0)
3DS1	Activating	20 (43.5)
Pseudogenes		
2DP1	Pseudogene	45 (97.8)
3DP1	Pseudogene	46 (100)

B. Distribution of KIR haplotypes in MDS.





A. Frequency of inhibitory, activating, and pseudogene KIRs detected by genotyping in 46 evaluable MDS patients. Values represent the number and percentage of patients positive for each gene.

B. Distribution of KIR haplotypes, showing a predominance of haplotype B–containing genotypes (74.0%, 34/46) compared with haplotype A (26.0%, 12/46)

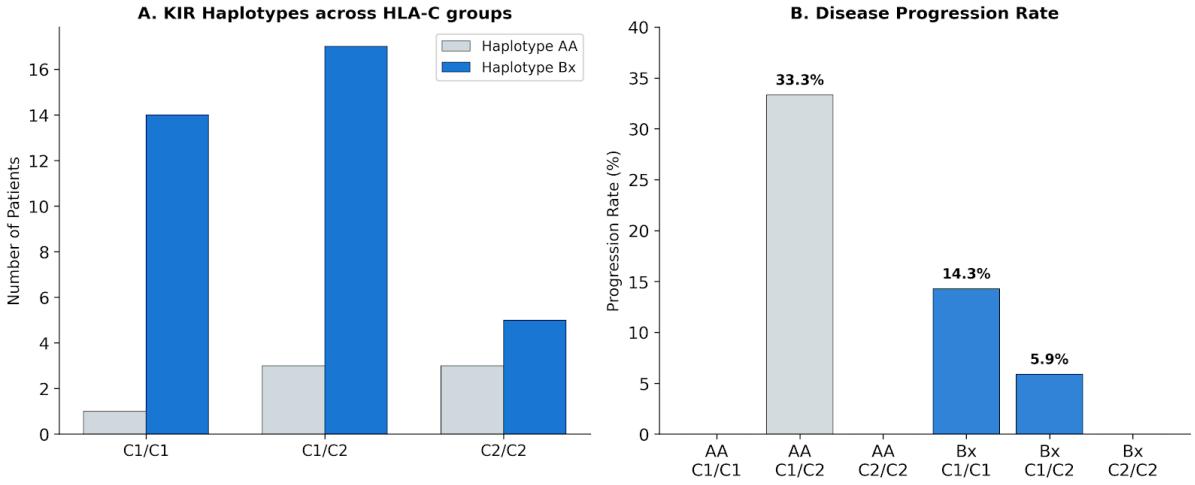
C. Schematic representation of KIR haplotype A and B architectures. Haplotype A is characterized by a predominance of inhibitory KIR genes, whereas haplotype B–containing genotypes include one or more activating KIRs

MDS, myelodysplastic syndromes; KIR, killer-cell immunoglobulin-like receptor.

Figure 10. Integrative immunogenetic analysis of KIR-HLA-C profiles and clinical outcomes.

KIR Haplotype	HLA-C Ligand	Total (n)	No Progression	Progression (Yes)	% Progression
AA	C1/C1	1	1	0	0%
AA	C1/C2	3	2	1	33.3%
AA	C2/C2	3	3	0	0%
Bx	C1/C1	14	12	2	14.3%
Bx	C1/C2	17	16	1	5.9%
Bx	C2/C2	5	5	0	0%
TOTAL		43	39	4	9.3%

Frequency of Disease Progression according to KIR-HLA-C Genotypes. Cross-tabulation of KIR haplotype groups and HLA-C ligand backgrounds. The table summarizes the total number of patients (n=43), absolute counts of stable disease versus progression, and the calculated progression risk for each immunogenetic profile.



A. Distribution of KIR Haplotypes across HLA-C Ligand Groups: Frequency of AA (inhibitory) and Bx (activating-rich) haplotypes within the C1/C1, C1/C2, and C2/C2 cohorts. The Bx haplotype predominated across all ligand backgrounds. B. Disease Progression Rate by Genetic Combination: Bar graph illustrating the percentage of patients within each specific KIR-HLA-C subgroup who experienced clinical disease progression. Data labels represent the progression rate relative to the total number of patients in each specific genetic bin.

MDS: Myelodysplastic Syndromes; KIR: Killer-cell Immunoglobulin-like Receptor; HLA: Human Leukocyte Antigen; C1/C2: HLA-C ligand groups based on the amino acid dimorphism at position 80.

5.2.1.1.3 NK cell phenotypic and functional differences according to risk stratification in MDS

We evaluated the frequency, maturation, and function of NK cells in MDS, stratified by IPSS-R risk. Our objective was to determine if disease risk correlates with specific NK cell exhaustion or cytotoxicity profile. Overall, NK cell phenotypes were highly heterogeneous across risk groups **(Supplementary Figure 1),** with no consistent, risk-specific modulation of individual receptors, despite some observable trends.

Notably, inhibitory NK cells ($CD56^{neg}CD16^{bright}$) were more frequent in LR-MDS [1.52% (IQR, 0.30–5.04)] compared with HR-MDS [0.51% (IQR, 0.25–1.18); p = 0.05]. Similarly, immature NK cell subsets ($CD56^{+}CD16^{neg}$) were significantly increased in LR-MDS [2.92% (IQR, 0.84–9.53)] relative to HR-MDS [0.41% (IQR, 0.16–0.82); p = < 0.001] **(Table 14).**

In contrast, TIGIT expression on NK cells showed a trend toward higher levels in HR-MDS [56.02% (IQR, 31.98–68.16)] compared with LR-MDS [24.46% (IQR, 5.41–56.44); p = 0.07]. Analysis of KIR expression by phenotype revealed a statistically significant increase in the activating receptor KIR2DS2 in HR-MDS [20.70% (IQR, 4.34–40.67)] compared with LR-MDS [2.21% (IQR, 0.33–7.42); p < 0.001]. Although not reaching statistical significance, higher expression levels of other activating (KIR2DS4) and inhibitory (KIR2DL2/2DL3 and KIR2DL1) KIR were also observed in HR-MDS **(Figure 11 and Supplementary table S6).**

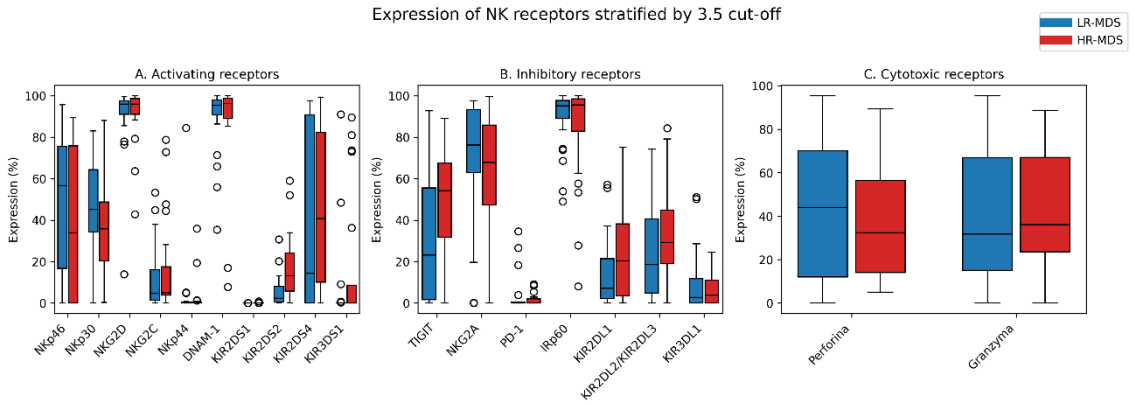
Table 14. NK cells frequency according to risk stratification.

Parameter	LR-MDS (≤ 3.5) Median (IQR)	HR-MDS (>3.5) Median (IQR)	*p* value
Total NK	15.65	10.80	0.40
	(7.77–18.70)	(9.15–15.87)	
Mature NK (CD56dim CD16bright)	15.31	9.78	0.60
	(2.83–86.29)	(7.39–16.13)	
Inhibitory NK (CD56negCD16+)	1.52	0.51	0.05
	(0.30–5.04)	(0.25–1.18)	
Immature NK (CD56+CD16neg)	2.92	0.41	0.00065
	(0.84–9.53)	(0.16–0.82)	
NK CD57+	5.68	6.62	0.06
	(2.33–7.05)	(5.54–9.65)	

Values are presented as median percentages with IQR. Comparisons between groups were performed using non-parametric statistical testing. NK cell subsets are expressed as a percentage of total lymphocytes. P values indicate comparisons between groups.

NK, natural killer; MDS, myelodysplastic syndromes; LR-MDS, low-risk myelodysplastic syndromes; HR-MDS, high-risk myelodysplastic syndromes; IQR, interquartile range; CD, cluster of differentiation.

Figure 11. NK receptor expression according to IPSS-R 3.5 risk cut-off.



(A) Activating receptors, (B) inhibitory receptors, and (C) cytotoxic molecules are shown for LR-MDS (blue) and HR-MDS (red). Box plots represent the IQR with the median indicated by the horizontal line; whiskers represent the full range of values. Group comparisons were performed using non-parametric statistical tests.

NK, natural killer; MDS, myelodysplastic syndromes; LR-MDS, low-risk myelodysplastic syndromes; HR-MDS, high-risk myelodysplastic syndromes; IPSS-R, Revised International Prognostic Scoring System; IQR, interquartile range; NKp46, natural cytotoxicity receptor 1; NKp44, natural cytotoxicity receptor 2; NKp30, natural cytotoxicity receptor 3; NKG2C, natural killer group 2 member C; NKG2D, natural killer group 2 member D; NKG2A, natural killer group 2 member A; DNAM-1, DNAX accessory molecule-1; TIGIT, T cell immunoreceptor with Ig and ITIM domains; PD-1, programmed cell death protein 1; KIR, killer cell immunoglobulin-like receptor.

5.2.1.2 T cells

5.2.1.2.1 Differential expression of T cell receptors in peripheral blood

We analyzed T-lymphocyte populations and subpopulations in peripheral blood. The overall frequencies of total lymphocytes, as well as B and T lymphocytes, were comparable across the three groups, MDS, ICUS, and HD. Likewise, no significant differences were observed in the proportions of $CD3^+CD4^+$ and $CD3^+CD8^+$ T cells among groups. Among the T-cell subpopulations analyzed, a trend toward increased $CD57^+$ T cells were observed in MDS [15.82% (IQR, 7.63–20.02)] compared with HD [8.12% (IQR, 5.27–11.76); p = 0.08].

Within the $CD4^+$ T-cell compartment, statistically significant differences were detected. $CD4^+$ memory T cells were increased in ICUS [44.89% (IQR, 22.28–55.62)] compared with HD [12.90% (IQR, 10.21–28.42); p = 0.02], with a trend toward higher levels relative to MDS [23.02% (IQR, 16.92–42.81); p = 0.09]. Similarly, $CD4^+$ effector memory T cells were higher in ICUS [11.78% (IQR, 6.38–15.91)], showing a trend toward significance compared with HD

[4.93% (IQR, 4.25–5.73); p = 0.08], while no difference was observed between ICUS and MDS (p = 0.42). In addition, $CD4^+CD57^+$ T cells were increased in both ICUS [4.49% (IQR, 1.89–6.96)] and MDS [2.58% (IQR, 1.00–5.27)] compared with HD [0.36% (IQR, 0.16–1.10); p = 0.04]. ICUS also exhibited a higher proportion of $CD4^+PD\text{-}1^+$ T cells [39.68% (IQR, 24.40–54.80)] compared with MDS [22.44% (IQR, 16.46–33.55); p = 0.04], whereas no differences were observed between ICUS and HD.

A similar pattern was observed within the $CD8^+$ T-cell compartment. ICUS and MDS showed higher proportions of $CD8^+$ memory, effector memory, and effector T cells compared with HD. Notably, PD-1 expression on $CD8^+$ T cells was significantly increased in ICUS [29.72% (IQR, 16.94–43.89)] compared with both MDS [12.35% (IQR, 6.43–20.30); p = 0.03] and HD [8.38% (IQR, 2.26–13.21); p = 0.02].

Finally, Th2 cells were decreased in ICUS [16.97% (IQR, 11.08–19.38)] compared with MDS [22.71% (IQR, 15.23–32.20); p = 0.03]. Comprehensive analysis of lymphocyte populations reveals a heterogeneous immune landscape. A summary of all analyzed populations is provided in **Table 15.**

- **T cell phenotypic differences according to risk stratification in MDS**

No major differences were observed in the expression of most immune markers in the fifty MDS patients. However, a statistically significant increase in $CD8^+$ effector T cells was detected in LR-MDS [18.19% (IQR, 8.23–36.48)] compared with HR-MDS [11.07% (IQR, 6.47–14.91); p = 0.03]. In contrast, Th2 cells were significantly increased in HR-MDS [29.73% (IQR, 22.44–33.41)] compared with LR-MDS [19.66% (IQR, 14.03–24.28); p = 0.01]. **(Figure 12)**

Table 15. Peripheral lymphocyte and T-cell subset distribution in MDS, ICUS, and HD.

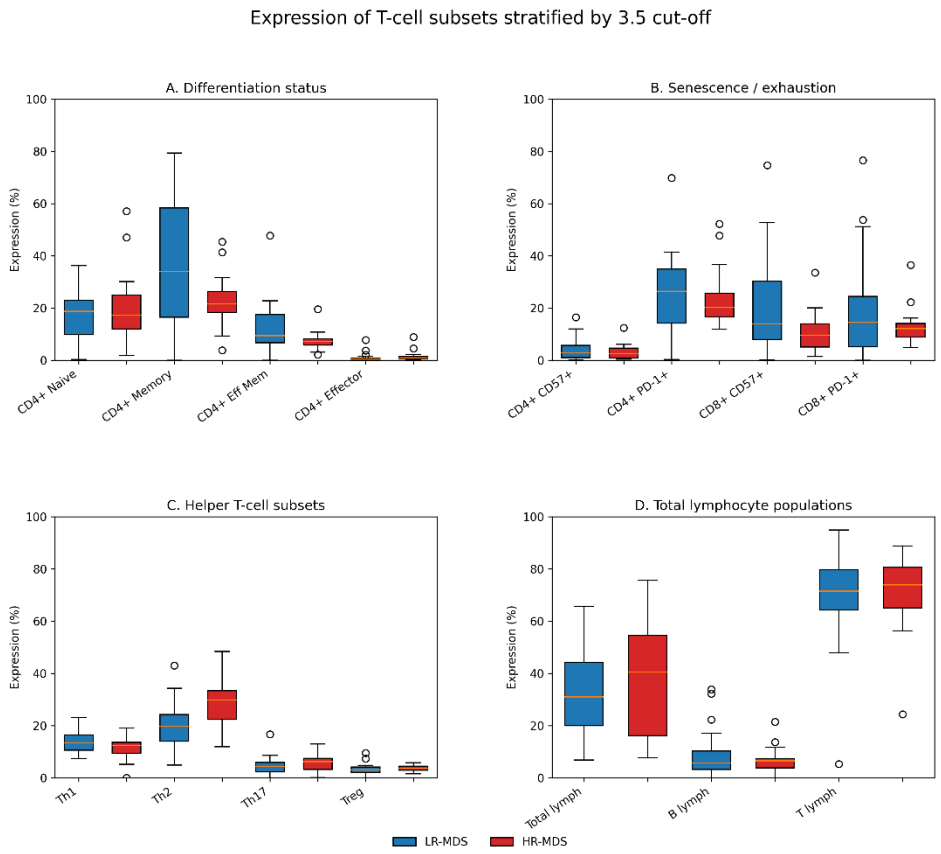
Parameter	MDS Median (IQR)	ICUS Median (IQR)	HD Median (IQR)	Overall p	MDS vs ICUS p	MDS vs HD p	ICUS vs HD p
Lymphocytes	33.4 (18.52–46.70)	30.48 (25.57–32.29)	35.26 (25.08–40.40)	0.81	0.59	0.98	0.47
Lymphocytes B	6.04 (3.65–9.68)	8.31 (5.60–24.37)	12.01 (4.11–21.47)	0.19	0.09	0.44	0.39
Lymphocytes T	72.2 (64.55–80.75)	73.72 (57.91–79.16)	69.62 (67.27–73.55)	0.65	0.70	0.42	0.43
γδ T cells	2.01 (1.08–5.71)	4.51 (2.67–9.19)	1.82 (1.45–2.37)	0.27	0.19	0.65	0.08
CD3+CD4+ T Cells	44.81 (32.57–51.59)	37.86 (36.24–43.99)	49.08 (41.73–51.55)	0.57	0.51	0.53	0.27
CD3+CD8+ T cells	21.79 (15.37–30.44)	22.98 (17.96–28.69)	17.73 (13.97–21.85)	0.38	0.75	0.25	0.13
CD57+ T cells	15.82 (7.63–20.02)	11.92 (11.52–12.32)	8.12 (5.27–11.76)	0.18	0.63	0.08	0.43
CD4+ Naive T cells	17.83 (9.84–24.14)	24.61 (12.20–28.91)	20.79 (15.74–23.27)	0.41	0.32	0.31	0.92
CD4+ Memory T cells	23.02 (16.92–42.81)	44.89 (22.28–55.62)	12.9 (10.21–28.42)	0.05	0.09	0.14	0.02
CD4+ Effector Memory T cells	7.71 (6.38–11.35)	11.78 (6.38–15.91)	4.93 (4.25–5.73)	0.16	0.42	0.08	0.21
CD4+ Effector T cells	0.56 (0.15–1.23)	0.53 (0.06–0.61)	0.32 (0.12–1.72)	0.87	0.67	0.72	0.87
CD4+CD57+ T cells	2.58 (1.00–5.27)	4.49 (1.89–6.96)	0.36 (0.16–1.10)	0.04	0.28	0.03	0.04
CD4+CD27+ T cells	0.12 (0.05–0.47)	1.47 (0.76–2.19)	0 (0.00–0.03)	0.08	0.78	0.03	0.28
CD4+ PD1+ T cells	22.44 (16.46–33.55)	39.68 (24.40–54.80)	28.36 (15.07–43.70)	0.12	0.04	0.56	0.54
CD8+ Naive T cells	2.67	3.78	4.19	0.36	0.13	0.98	0.68

	(1.22–5.63)	(3.58–12.00)	(0.86–9.55)				
CD8+ Memory T cells	3.16	7.43	1.04	0.05	0.20	0.06	0.02
	(1.71–7.00)	(3.56–19.03)	(0.42–3.02)				
CD8+ Effector Memory T cells	5.95	8.42	2.4	0.05	0.24	0.05	0.03
	(3.98–12.28)	(4.97–17.13)	(1.27–5.77)				
CD8+ Effector T cells	14.29	44.79	2.84	0.04	0.16	0.03	0.07
	(6.78–23.20)	(7.33–52.42)	(1.04–8.70)				
CD8+CD57+ T cells	11.13	26.89	3.65	0.27	0.24	0.26	0.30
	(5.85–20.77)	(7.07–32.44)	(1.29–29.64)				
CD8+CD27+ T cells	8.57	10.92	5.39	0.50	0.26	0.68	0.62
	(6.23–11.06)	(10.84–11.00)	(0.10–16.39)				
CD8+PD1+ T cells	12.35	29.72	8.38	0.03	0.03	0.19	0.02
	(6.43–20.30)	(16.94–43.89)	(2.26–13.21)				
Treg	3.36	3.58	3.67	0.94	0.93	0.78	0.72
	(2.21–4.39)	(2.19–4.35)	(2.26–4.92)				
Th1	13.18	15.46	16.83	0.25	0.10	0.45	0.97
	(9.87–15.16)	(13.01–19.03)	(6.79–18.97)				
Th2	22.71	16.97	17.72	0.09	0.03	0.37	0.54
	(15.23–32.20)	(11.08–19.38)	(15.52–26.32)				
Th17	4.72	5.36	4.26	0.93	0.75	0.93	0.71
	(2.83–6.61)	(3.46–5.84)	(3.72–5.83)				
Th1-17	3.48	5.14	3.36	0.48	0.28	0.75	0.24
	(1.74–6.26)	(3.96–6.32)	(2.58–4.95)				

Median percentages and IQR of lymphocyte populations and T cell subsets in MDS, ICUS, and HD. Overall comparisons were performed across the three groups, followed by pairwise comparisons using non-parametric tests.

MDS, myelodysplastic syndromes; ICUS, idiopathic cytopenia of undetermined significance; HD, healthy donors; IQR, interquartile range; Treg, regulatory T cells; Th, T helper cells; PD-1, programmed cell death protein 1; CD, cluster of differentiation.

Figure 12. Peripheral T cell subsets according to IPSS-R 3.5 risk cut-off.



Boxplots showing the distribution of peripheral blood T-cell subsets stratified into LR-MDS and HR-MDS using the IPSS-R 3.5 cut-off. Boxes represent the IQR with the median indicated by the horizontal line; whiskers represent the minimum and maximum values. Statistical comparisons between groups were performed using the Mann–Whitney U test. LR-MDS is shown in blue and HR-MDS in red.

MDS, myelodysplastic syndromes; LR-MDS, low-risk myelodysplastic syndromes; HR-MDS, high-risk myelodysplastic syndromes; IPSS-R, Revised International Prognostic Scoring System; IQR, interquartile range; Treg, regulatory T cells; Th, T helper cells; PD-1, programmed cell death protein 1; CD, cluster of differentiation.

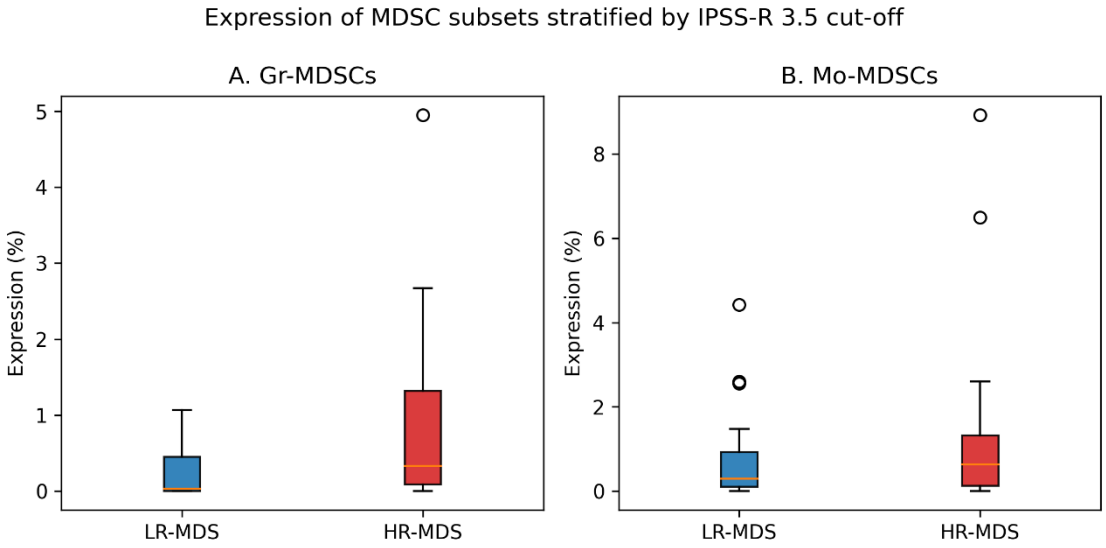
5.2.1.3 MDSCs

- **Expression in BM and its association with disease risk**

Finally, to complete the characterization of immune cell populations within the BM microenvironment, we evaluated the expression of MDSCs, distinguishing between granulocytic MDSCs (Gr-MDSCs; $CD11b^{+}CD33^{+}HLA\text{-}DR^{-}CD15^{+}CD14^{-}$) and monocytic MDSCs (Mo-MDSCs; CD11b⁺CD33⁺HLA-DR^low^CD15⁺CD14⁺). A total of 68 samples were available for this analysis, including 47 patients with MDS, 10 HD, and 11 ICUS.

MDSCs were low in all the patients and groups, and we did not identify any statistically significant difference among them. Comparing the MDSCs expression by IPSS-R 3.5cut-off we observed a statistically significant increase of Gr-MDSCs in HR-MDS [0.33% (IRQ, 0.09-1.32)] compared to LR-MDS [0.04% (IQR, 0.00- 0.45); p= <0.01], with moderate-to-large effect size. Mo-MDSCs showed a numerically higher median in HR-MDS, but no statistically significant difference (p = 0.37), with a small effect size **(Figure 13)**.

Figure 13. MDSCs according to IPSS-R risk category.



Population		LR-MDS (n = 26)	HR-MDS (n = 21)	p-value	Effect size (r_{rb})
Gr-MDSCs	Median	0.04	0.33	0.0028	0.51
	IQR	[0.00–0.45]	[0.09–1.32]		
Mo-MDSCs	Median	0.30	0.63	0.37	0.15
	IQR	[0.10–0.92]	[0.12–1.32]		

Boxplots showing the distribution of granulocytic (Gr-MDSCs) and monocytic (Mo-MDSCs) MDSCs according to IPSS-R risk category (LR-MDS ≤ 3.5; HR-MDS > 3.5). Boxes represent the IQR with median values; whiskers indicate minimum and maximum values, and dots represent outliers. Statistical comparisons between groups were performed using the non-parametric Mann–Whitney U test. Effect size was estimated using rank-biserial correlation (r_{rb}).

MDS, myelodysplastic syndromes; LR-MDS, low-risk myelodysplastic syndromes; HR-MDS, high-risk myelodysplastic syndromes; Gr-MDSCs, granulocytic myeloid-derived suppressor cells; Mo-MDSCs, monocytic myeloid-derived suppressor cells; IPSS-R, Revised International Prognostic Scoring System; IQR, interquartile range

5.2.2 Cytokines and chemokines

- **BM supernatants cytokine concentration**

To further characterize the inflammatory milieu of the BM microenvironment, cytokine concentrations were analyzed across the study groups. BM supernatant samples were collected from all subjects; however, evaluable cytokine data were available for 44 patients with MDS, 9 individuals with ICUS, and 7 HD. Overall, cytokine levels exhibited marked heterogeneity both between diagnostic categories and within individual groups. Although no statistically significant differences were identified, several cytokines showed consistent trends that may reflect underlying differences in immune regulation. Detailed cytokine concentrations are reported in **Table 16.**

Although CXCL9 (MIG), a chemokine produced by dendritic cells and macrophages within the tumor microenvironment and known to play a complex role in tumor progression, showed higher levels in MDS, no statistically significant differences were observed when compared with ICUS [29.08 pg/mL (IQR, 1.29–78.41) *vs* 17.14 pg/mL (IQR, 0–39.41); p= 0.4] or with HD [1.13 pg/mL (IQR, 1.13–42.64); p= 0.2].

CCL4, formerly known as macrophage inflammatory protein (MIP)-1β, has been implicated in modulation of the tumor microenvironment through the recruitment of cells that may promote tumorigenesis. In our study, CCL4 concentrations showed a trend toward higher levels in MDS samples, with a median of 11.60 pg/mL (IQR, 0–56.52), compared with ICUS samples, which exhibited a median of 0 pg/mL (IQR, 0–11.60); however, this difference did not reach statistical significance (p = 0.1).

Cytokines involved in T-cell differentiation and function, such as IL-2, were below the detection threshold in most MDS patients and individuals with ICUS, indicating a tendency toward lower levels in these groups. In contrast, IL-2 was detectable mainly in HD, who exhibited measurable concentrations 7.61 pg/mL (IQR, 0–7.61); however, this difference did not reach statistical significance (p = 0.2).

Detectable IL-6 concentrations in BM supernatant were observed in only ten subjects. Among these, 8/10 (80%) exhibited IL-6 levels ≥10 pg/mL, a threshold described in the literature as the upper limit of normal plasma concentrations. Notably, all eight subjects with elevated IL-6 levels were diagnosed with MDS. A similar pattern was observed for IL-8, a pro-inflammatory and pro-angiogenic cytokine involved in cell migration and cellular recruitment. Although no statistically significant differences in IL-8 concentrations were detected across diagnostic groups, 13/14 (92%) of subjects with elevated IL-8 levels (>9.4 ± 3.7 pg/mL) were diagnosed with MDS.

In contrast, IL-9, an interleukin involved in hematopoietic stem cell maturation, and IL-10, an immunosuppressive cytokine, were below the detection threshold in the majority of BM supernatant samples. Similarly, immunomodulatory cytokines including IFNα and TNFα were largely undetectable across the study population, with elevated concentrations (>50 pg/mL) observed in only two subjects, one with MDS and one HD.

Regarding the growth factors analyzed, epidermal growth factor (EGF) was detectable exclusively in HD samples, with a median concentration of 28.16 pg/mL (IQR, 6.80–37.40), whereas levels in MDS and ICUS samples were below the detection threshold. Hepatocyte growth factor (HGF) showed a trend toward higher concentrations in MDS samples, with a median of 479.1 pg/mL (IQR, 205.2–1053.0), compared with ICUS samples 201.4 pg/mL (IQR, 80.90- 322.60); p=0.1 and HD 105.0 pg/mL (IQR, 58.20 - 312.20); p=0.1 **(Figures 14).**

- **Cytokines and chemokines according to risk stratification in MDS**

We evaluated the concentrations of a broad panel of cytokines and chemokines in patients with MDS, stratified according to disease risk. A cutoff score of 3.5 was applied to classify patients as HR-MDS (n = 18, 41%) or LR-MDS (n = 26, 59%), providing a more balanced distribution between groups and enabling comparative analyses. Overall, most cytokines displayed comparable distributions between LR-MDS and HR-MDS, with substantial overlap and no statistically significant differences observed **(Supplementary Table S7).** Nevertheless, exploratory analyses revealed higher levels of IL-10, in HR-MDS [1.33 pg/mL (IQR, 1.08–1.67)] compared with LR-MDS [1.26 pg/mL (IQR, 1.12–1.41)], not statistically significant (p=0.07) **(Figure 15).**

Table 16. Cytokine and chemokines concentrations in BM supernatant samples.

Cytokines Median (IQR)	MDS pg/ml (n=44)	HD pg/ml (n=7)	p.value	MDS pg/ml (n=44)	ICUS pg/ml (n=9)	p.value
IL-1α	0.62(0-0.6375)	0.62(0.31-0.62)	0.48	0.62(0-0.6375)	0(0-0.62)	0.65
IL-1β	0.77(0-2.52)	2.52(1.48-2.52)	0.77	0.77(0-2.52)	2.52(0.64-2.52)	0.69
IL-1RA	139.9(0-3425)	36.4(18.2-36.4)	0.32	139.9(0-3425)	0(0-36.4)	0.23
IL-2	0(0-7.61)	7.61(0-7.61)	0.20	0(0-7.61)	0(0-7.61)	0.83
IL-3	13.84(0-20.5)	20.5(10.25-20.5)	0.61	13.84(0-20.5)	20.5(0-20.5)	0.66
IL-4	0(0-10.76)	10.76(0-10.76)	0.77	0(0-10.76)	0(0-10.76)	0.76
IL-5	0(0-10.62)	10.62(0-10.62)	0.47	0(0-10.62)	0(0-10.62)	0.59
IL-6	6.445(0-9.21)	9.21(0-71.04)	0.66	6.445(0-9.21)	0(0-9.21)	0.46
IL-7	0(0-1.1)	1.045(0-2.877)	0.73	0(0-1.1)	0(0-0.6351)	0.72
IL-8	3.61(0-7.292)	3.61(1.805-3.61)	0.51	3.61(0-7.292)	2.23(0-3.61)	0.28
IL-9	0(0-8.25)	8.25(0-8.25)	0.28	0(0-8.25)	0(0-8.25)	0.90
IL-10	1.295(1.115-1.418)	1.41(1.049-1.58)	0.97	1.295(1.115-1.418)	1.17(1.04-1.41)	0.25
IL-12	0(0-9)	9(0-9)	0.76	0(0-9)	0(0-9)	0.75
IL-13	0.48(0-3.7)	3.7(0-3.7)	0.71	0.48(0-3.7)	1.19(0-3.7)	0.67
IL-15	3.66(0.87-3.7)	3.7(1.812-6.02)	0.11	3.66(0.87-3.7)	3.62(0-3.7)	0.72
IL-17A (CTLA8)	0(0-2.3)	2.3(0-2.3)	0.41	0(0-2.3)	0(0-2.3)	0.74

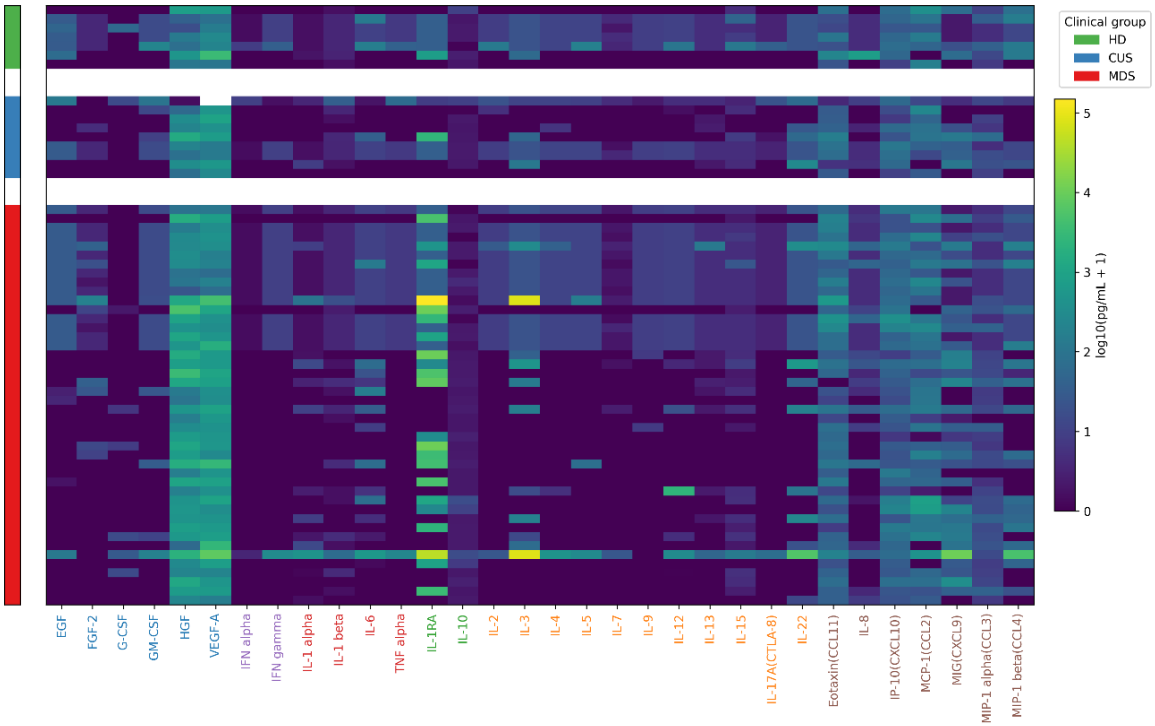
IFN-α	0(0-0.5)	0.5(0-0.5)	0.17	0(0-0.5)	0(0-0.5)	0.74
IFN-γ	0(0-8.56)	8.56(0-8.56)	0.96	0(0-8.56)	0(0-8.56)	0.76
TNF-α	0(0-6.3)	6.3(0-6.3)	0.95	0(0-6.3)	0(0-6.3)	0.77
Eotaxin (CCL11)	59.73(36.52-109.9)	22.63(17.47-90.66)	0.54	59.73(36.52-109.9)	41.24(29.17-73.33)	0.34
IP-10 (CXCL10)	50.05(21.88-72.91)	51.83(36.39-59.77)	0.44	50.05(21.88-72.91)	58.12(14.75-63.05)	0.40
MCP-1 (CCL2)	77.97(25.98-115.2)	96.35(36.36-154.7)	0.95	77.97(25.98-115.2)	47.32(28.09-88.77)	0.38
MIG (CXCL9)	29.08(1.295-78.41)	1.13(1.13-42.64)	0.28	29.08(1.295-78.41)	17.14(0-39.41)	0.49
MIP1-α (CCL3)	10.06(3.7-15.5)	9.71(5.165-23.43)	0.51	10.06(3.7-15.5)	8.4(3.7-15.6)	0.70
MIP1-β (CCL4)	11.6(0-56.52)	81.09(11.6-134.7)	0.81	11.6(0-56.52)	0(0-11.6)	0.15
EGF	0(0-28.91)	28.16(6.852-37.94)	0.16	0 (0 - 28.91)	0 (0 - 28.91)	0.70
FGF-2	0(0-2.73)	2.73(0-2.73)	0.50	0(0-2.73)	0(0-2.73)	0.40
G-CSF	0(0-0)	0(0-0)	0.15	0(0-0)	0(0-0)	0.99
GM-CSF	0(0-14.13)	14.13(0-14.13)	0.13	0(0-14.13)	8.57(0-14.13)	0.74
HGF	479.1(205.2-1053)	105.6(58.2-6-312.2)	0.11	479.1(205.2-1053)	201.4(80.9-322.6)	0.14
VEGF-A	491.2(341-812.8)	216.6(125.3-470.7)	0.72	491.2(341-812.8)	406.6(129.4-555.6)	0.28

The data provided presents the concentrations of various cytokines in the 3 different groups: MDS and control groups of HD and ICUS. The table includes median values and IQR for each cytokine studied, along with p-values indicating the statistical significance of the differences between

groups. Key Observations: Most cytokines across the board exhibit no significant differences between MDS and HD groups or their respective subsets. Cytokines and chemokines, exhibiting more pronounced differences, are detailed in the results section of the document.

MDS, myelodysplastic syndromes; HD, healthy donors; ICUS, idiopathic cytopenia of undetermined significance; IQR, interquartile range; IL, interleukin; IL-1RA, interleukin-1 receptor antagonist; IFN, interferon; TNF-α, tumor necrosis factor alpha; EGF, epidermal growth factor; FGF-2, fibroblast growth factor 2; G-CSF, granulocyte colony-stimulating factor; GM-CSF, granulocyte-macrophage colony-stimulating factor; HGF, hepatocyte growth factor; VEGF-A, vascular endothelial growth factor A; MCP-1 (CCL2), monocyte chemoattractant protein-1; MIP-1α (CCL3), macrophage inflammatory protein-1 alpha; MIP-1β (CCL4), macrophage inflammatory protein-1 beta; IP-10 (CXCL10), interferon gamma-induced protein-10; MIG (CXCL9), monokine induced by interferon gamma; Eotaxin (CCL11), eosinophil chemotactic protein.

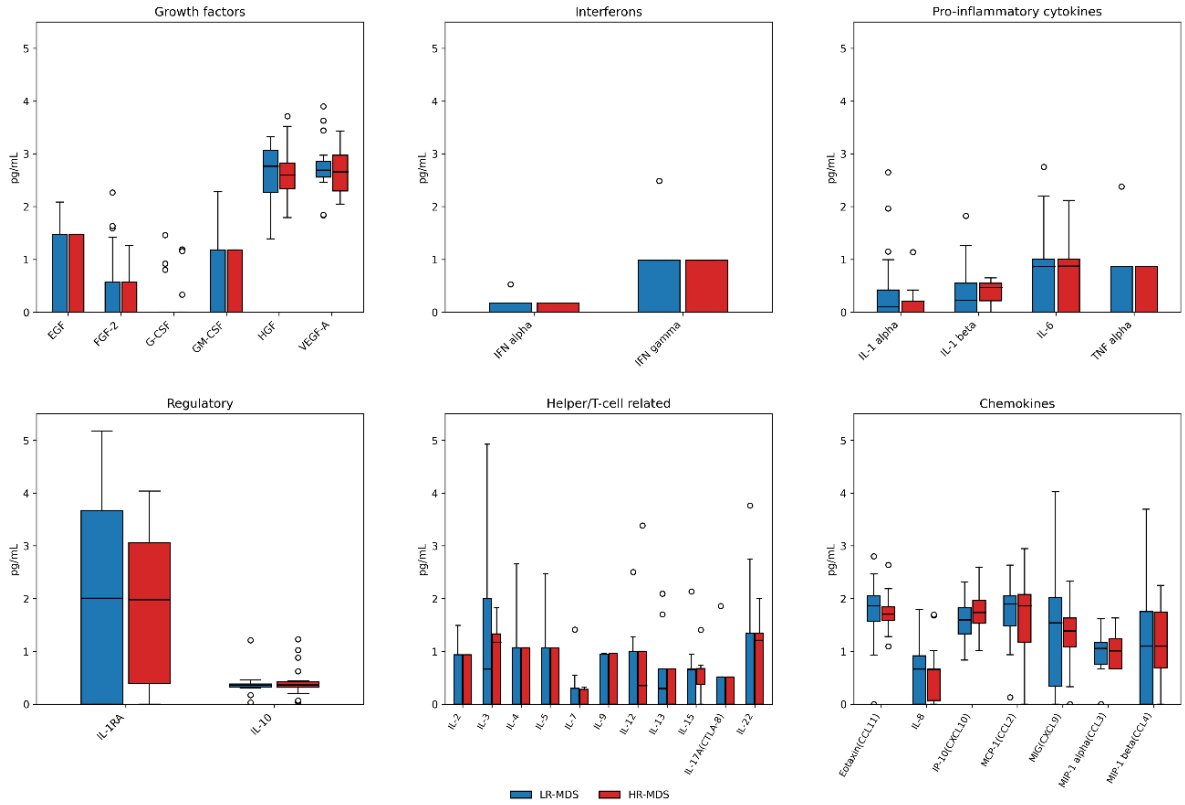
Figure 14. Cytokine expression profiles across study groups.



Heatmap showing cytokine concentrations in BM supernatant samples from HD, ICUS, and MDS. Cytokine levels were log10-transformed (pg/mL + 1). Samples are ordered by clinical group and indicated by the annotation bar, while cytokines are grouped and color-coded according to functional family.

HD, healthy donors; ICUS, idiopathic cytopenia of undetermined significance; MDS, myelodysplastic syndromes; pg/mL, picograms per milliliter.

Figure 15. Cytokine concentrations according to risk groups.



Boxplots showing cytokine concentrations in BM supernatant samples. Cytokine levels are expressed in pg/mL and were log-transformed for visualization as log10 (pg/mL + 1). Boxes represent the IQR with the median indicated by the horizontal line.

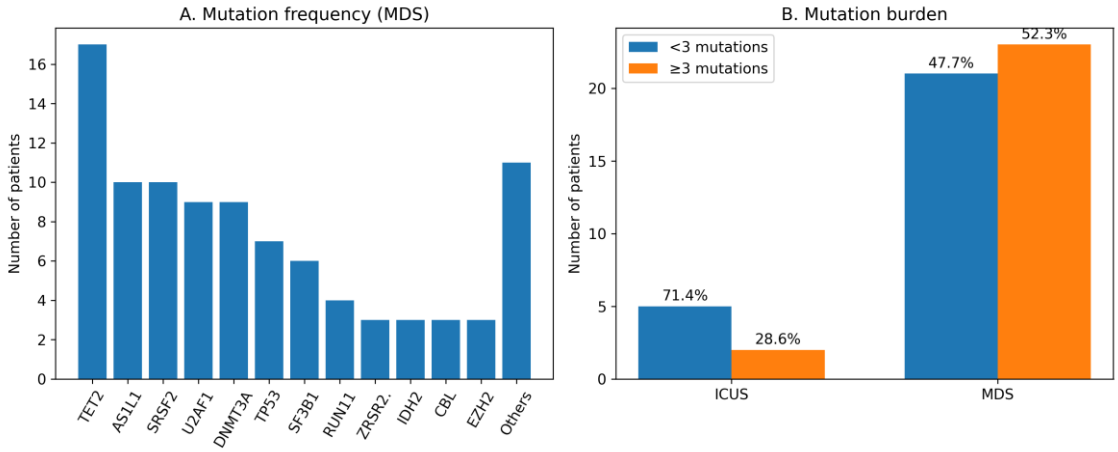
pg/mL, picograms per milliliter; IQR, interquartile range.

5.2.3 Mutational landscape in MDS and ICUS

5.2.3.1 Association with disease risk and immune profile

To characterize the genomic landscape of the cohort, mutational profiling was performed in 61 patients, including 50 with MDS and 11 with ICUS. HD was not included in this analysis, as mutational assessment is not applicable to this group. Somatic mutations were detected in 44 of 50 patients (88%) with MDS. The most frequently mutated genes were *TET2, DNMT3A, SRSF2, ASXL1, U2AF1, SF3β1*, and *TP53*, in agreement with previously published data. Among mutation-positive MDS patients, 52% harbored three or more somatic mutations **(Figure 16).**

Figure 16. MDS and ICUS genomic landscape.



(A) Frequency of pathogenic mutations detected in patients with MDS. Mutation frequency represents the number of patients harboring at least one pathogenic mutation in each gene. Rare mutations, defined as those present in fewer than three patients, were grouped as Others for visualization purposes. (B) Distribution of mutational burden according to diagnostic group. Mutation burden was evaluated only in patients with at least one detected mutation and categorized as <3 mutations or ≥3 mutations per patient. Percentages are calculated relative to the number of mutation-positive patients within each diagnostic group.

MDS, myelodysplastic syndromes; ICUS, idiopathic cytopenia of undetermined significance.

Within the ICUS group, 7 of 11 patients (63.6%) met criteria for CCUS. The mutational profile of these cases is detailed in **Figure 17**; notably, one patient exhibited a high mutational burden, defined as the presence of three or more somatic mutations.

Figure 17. Mutational profile of CCUS patients.

(A) Frequency and VAF of CUS somatic mutations

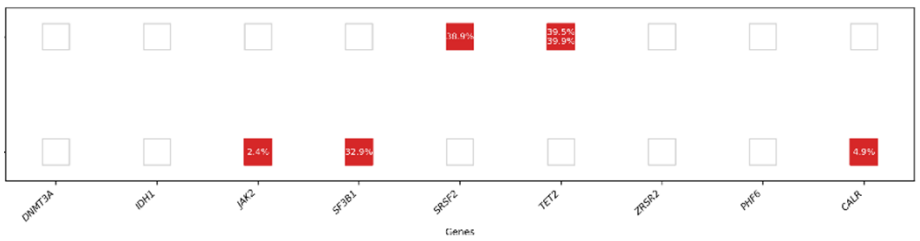
Mutation	Frequency (n)	VAF (%)
DNMT3A	1	4.5
	1	2.3
IDH1	1	3.7
JAK2	1	2.4
SF3β1	1	32.9
SRSF2	1	38.9
TET2	1	39.5
	1	39.9
ZRSR2	1	49.4
PHF6	1	39.8
CALR	1	4.9

A. Somatic mutations identified in CCUS, showing mutation frequency and VAF. Represents the number of patients harboring each mutation.

B. Mutational profile of CCUS patients with ≥3 somatic mutations. Filled squares indicate the presence of a mutation, and numbers within the squares represent the VAF (%).

CCUS, clonal cytopenia of undetermined significance; VAF, variant allele frequency.

(B). Mutational profile of CCUS with high mutational burden



To further investigate the potential impact of clonal architecture on immune dysregulation, immune profiles were analyzed according to mutational burden and mutational patterns. No significant differences were identified when comparing CCUS with ICUS.

When comparing MDS patients with detectable somatic mutations (MDS ^{Mut}) to those without detectable mutations (MDS ^{NoMut}), no significant differences were observed in most baseline clinical parameters, including hemoglobin levels, total white blood cell count, absolute neutrophil and lymphocyte counts, or BM blast percentage. Platelet counts, however, were significantly lower in the MDS ^{Mut} group (median 94.65 ×10⁹/L;

IQR, 63.75–127.5) compared with the MDS ^{NoMut} group (median 190 ×10⁹/L; IQR, 167.5–222.2; p = 0.004).

With respect to the immune compartment, MDS patients with mutations exhibited lower frequencies of several NK- and T-cell subsets. In particular, mature NK cells ($CD56^{dim}CD16^{bright}$) were reduced in the MDS ^{Mut} group compared with MDS ^{NoMut} patients (13.86%, IQR 7.02–54.28 vs. 85.48%, IQR 82.26–86.99; p = 0.003), along with inhibitory NK cells ($CD56^{neg}CD16^{bright}$) (0.96%, IQR 0.17–2.18 vs. 9.77%, IQR 6.29–10.98; p = 0.01). Similarly, lower proportions of naïve $CD8^+$ T cells (2.5%, IQR 0.87–5.53 vs. 9.6%, IQR 5.17–16.02; p = 0.01), memory $CD8^+$ T cells (3.0%, IQR 1.54–6.81 vs. 12.32%, IQR 6.53–21.02; p = 0.05), and $CD57^+CD8^+$ T cells (10.6%, IQR 5.24–20.56 vs. 28.53%, IQR 22.86–52.89; p = 0.008) were observed in the MDS ^{Mut} group.

No significant differences were detected in circulating cytokine concentrations between MDS ^{Mut} and MDS ^{NoMut} patients **(Table 17 and Supplementary Table S8).**

To further delineate immune differences between clonal cytopenias and overt myeloid neoplasia in the presence of somatic mutations, we compared the T-cell, NK-cell–related parameters and cytokines and chemokines between MDS^{Mut} and CCUS patients. In this exploratory analysis, CCUS patients exhibited higher frequencies of PD-1–expressing $CD4^+$ and $CD8^+$ T cells as well as increased proportions of immature NK cells, whereas DNAM-1 expression was higher in MDS ^{Mut}. These differences did not remain significant after false discovery rate correction (FDR) **(Figure 18).**

Consistent with previous analyses, no significant differences in clinical parameters or cytokine and chemokine concentrations were detected between mutated MDS and CCUS patients, although the limited size of the CCUS cohort warrants cautious interpretation.

Table 17. Immune cell subsets showing significant differences according to mutational status in MDS patients.

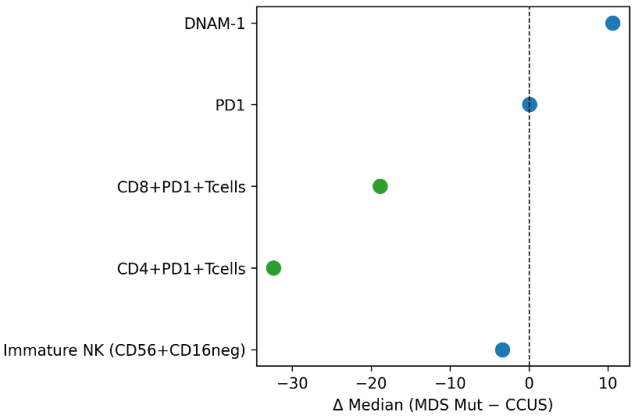
Variable		MDS^{Mut} (n=44)	MDS^{NoMut} (n=6)	p value
Mature NK cells ($CD56^{dim}CD16^{bright}$)	Median (%)	13.86	85.48	0.003
	IQR	7.02–54.28	82.26–86.99	
Inhibitory NK cells ($CD56^{neg}CD16^{bright}$)	Median (%)	0.96	9.77	0.01
	IQR	0.17–2.18	6.29–10.98	
Naïve $CD8^+$ T cells	Median (%)	2.5	9.6	0.01
	IQR	0.87–5.53	5.17–16.02	
Memory $CD8^+$ T cells	Median (%)	3.0	12.32	0.05

	IQR	1.54–6.81	6.53–21.02	
CD57⁺CD8⁺ T cells	Median (%)	10.6	28.53	0.008
	IQR	5.24–20.56	22.86–52.89	

Statistically significant differences between patients harboring at least one somatic mutation (MDS^{Mut}) and those without detectable mutations (MDS^{NoMut}). Data are presented as median percentages and IQR. Percentages represent the proportion of each immune subset within total lymphocytes. P values were calculated using the Mann–Whitney U test.

MDS, myelodysplastic syndromes; NK, natural killer; IQR, interquartile range.

Figure 18. Immune parameters with observed differences between mutated MDS and CCUS.



Difference in median values (Δ median; MDS^{Mut} − CCUS) for selected T cell (green) and NK cell (blue) parameters. Positive values indicate higher expression in mutated MDS^{Mut}, whereas negative values indicate higher levels in CCUS. CCUS patients exhibited higher frequencies of inhibitory receptors. The vertical dashed line represents no difference (Δ = 0). Findings are exploratory and did not remain statistically significant after FDR correction.

MDS, myelodysplastic syndromes; MDS^{Mut}, mutated MDS patients; CCUS, clonal cytopenia of undetermined significance; NK, natural killer; FDR, false discovery rate; Δ, difference in median values.

Although this difference did not reach statistical significance, we observed a trend toward higher concentrations of soluble growth factors such as VEGF-A in mutated MDS compared with CCUS (median 479.4 pg/mL, IQR 339.40–773.60 vs. 268.0 pg/mL, IQR 127.60–472.00; p = 0.07) **(Figure 19)**.

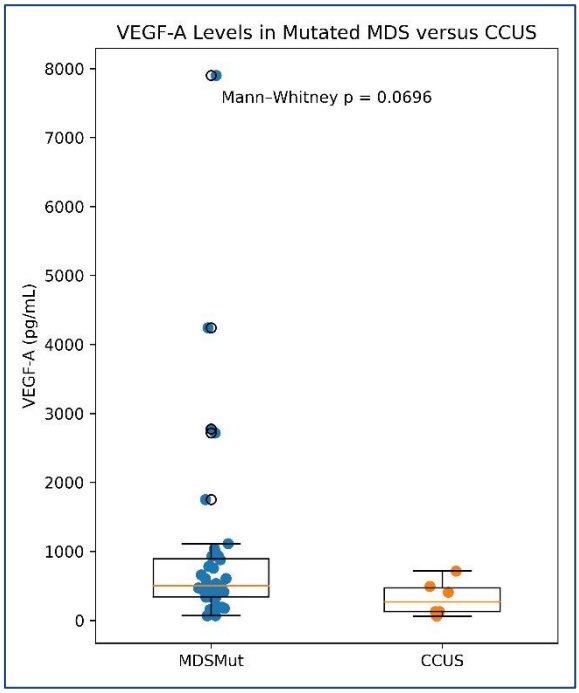


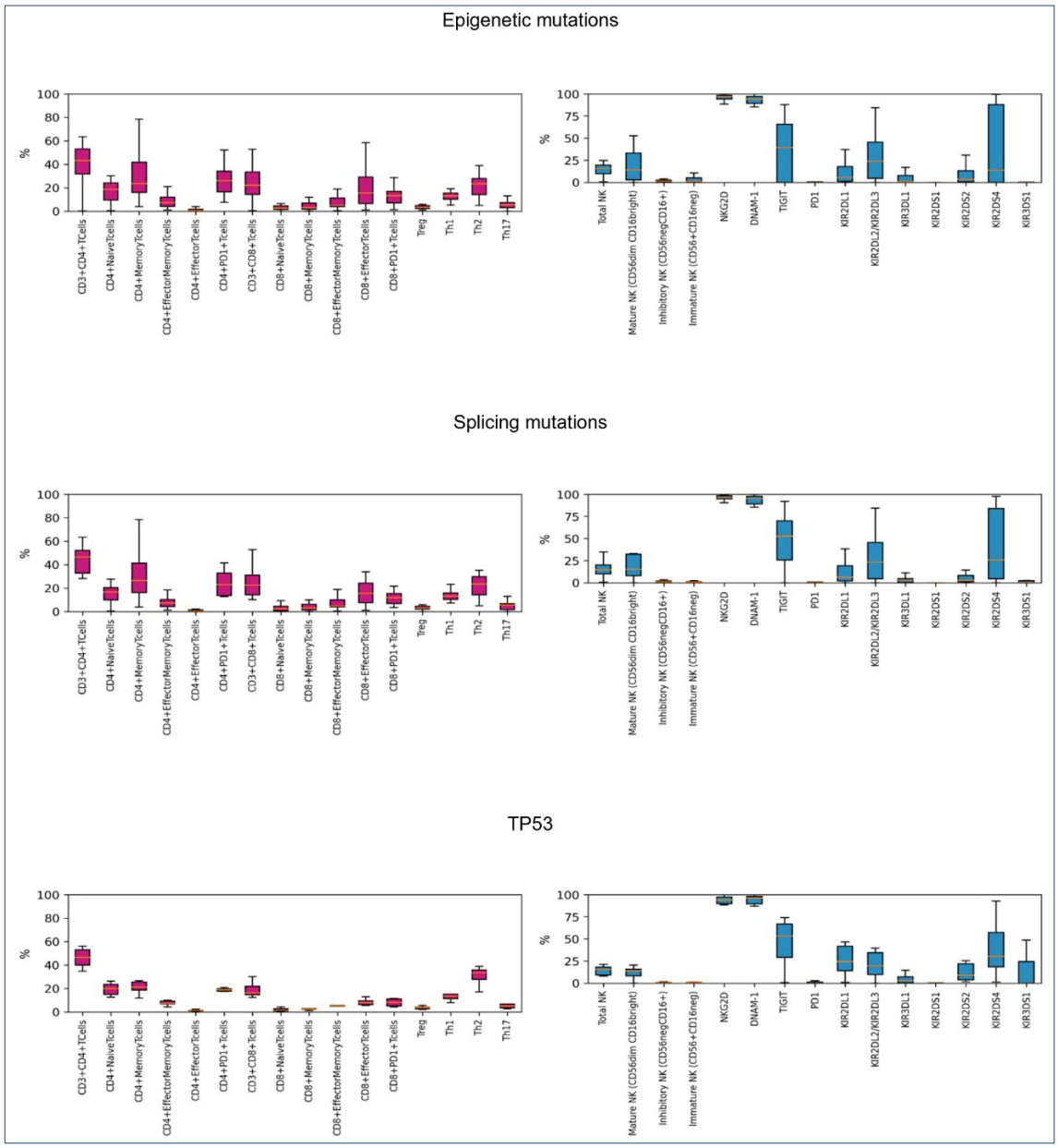
Figure 19. VEGF-A levels in mutated MDS versus CCUS.

Boxplots represent median and IQR, with whiskers indicating minimum and maximum values. Individual points correspond to single patients. Analysis includes only cases harboring at least one somatic mutation for both groups. VEGF-A concentrations are expressed in pg/mL. Statistical comparison was performed using the two-sided Mann–Whitney U test. VEGF-A: Higher median in MDS^{Mut} vs CCUS but did not reach statistical significance (p = 0.06). Strong right-skew and outliers suggest biological heterogeneity.

MDS, myelodysplastic syndromes; MDS^{Mut}, mutated MDS patients; CCUS, clonal cytopenia of undetermined significance; VEGF-A, vascular endothelial growth factor A; IQR, interquartile range; pg/mL, picograms per milliliter.

In addition, immunomodulatory cytokines including IFN-α, IFN-γ, and TNF-α were detected at low concentrations in the BM supernatant of CCUS patients, whereas in MDS^{Mut} their levels were largely below the assay detection limit **(Supplementary Table S9).** In our analysis of MDS patients with somatic mutations, we categorize them into distinct genetic profiles to explore potential associations with different immune profiles. We identified three main groups based on their genetic alterations: epigenetic regulation mutations (*TET2, DNMT3a*, and *ASXL1*; n=25), splicing mutations (*SRSF2, SF3β1*, *U2AF1*; n= 18), and *TP53* mutations (n=6). This stratification aimed to elucidate potential correlations between genetic profiles and immune profiles. Most patients presented epigenetic regulation mutations, and no significant changes were observed when comparing different groups **(Figure 20).**

Figure 20. Immune subpopulation distribution according to MDS mutational category.



Distribution of T cell (red) and NK cell (blue) subpopulations in MDS stratified by mutational category: epigenetic mutations (*TET2, DNMT3A, ASXL1*), splicing mutations (*SRSF2, SF3β1, U2AF1*), and *TP53*. Percentages represent the frequency of each subpopulation within total lymphocytes. The y-axis is harmonized (0–100%) across panels to allow comparison between groups. Boxes represent median and IQR; whiskers indicate the range of observed values, excluding outliers.

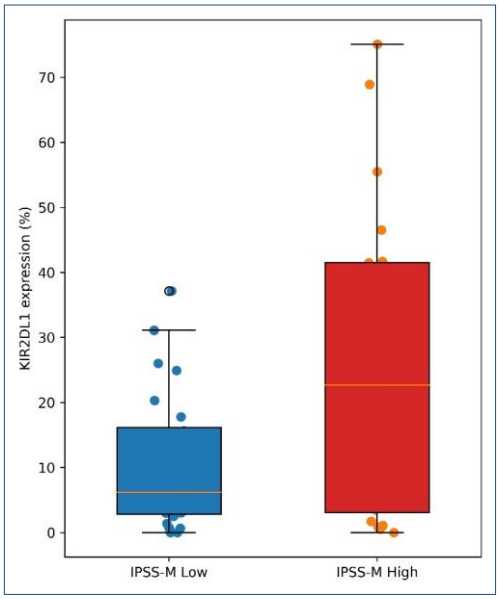
MDS, myelodysplastic syndromes; NK, natural killer; IQR, interquartile range.

Finally, to determine whether immune and clinical features differ according to mutational risk as defined by IPSS-M, we compared MDS patients classified as low risk (very low,

low, and moderate-low; n = 24) with those classified as high risk (moderate-high, high, and very high; n = 20). Overall, no significant differences were observed across the majority of immune parameters between IPSS-M risk groups. A nominally significant increase in the inhibitory NK receptor KIR2DL1 expression was observed in high-risk patients (median 22.69%, IQR 3.06–41.54) compared with low-risk patients (median 6.18%, IQR 2.83–16.15; p = 0.03); however, this association did not remain significant after correction for multiple testing (FDR = 0.20) **(Figure 21)**.

The limited size of several subgroups substantially constrains statistical power; consequently, neither the absence of differences nor nominally significant associations can be considered definitive. As most findings did not withstand correction for multiple testing, these results should be interpreted with caution and regarded as exploratory.

Figure 21. KIR2DL1 expression according to IPSS-M risk in MDS.



Boxplots represent median and IQR, with whiskers indicating minimum and maximum values. Each dot represents an individual patient. IPSS-M Low corresponds to Very Low, Low, and Moderate Low categories, whereas IPSS-M High includes Moderate High, High, and Very High. KIR2DL1 expression is shown as a percentage of NK cells. Statistical comparison was performed using the two-sided Mann–Whitney U test. KIR2DL1 is significantly increased in IPSS-M High MDS (p = 0.03), with markedly broader dispersion.

MDS, myelodysplastic syndromes; KIR2DL1, killer-cell immunoglobulin-like receptor 2DL1; NK, natural killer; IPSS-M, Molecular International Prognostic Scoring System; IQR, interquartile range

5.3 Follow-up of MDS patients

5.3.1 Immune phenotypic and functional differences

Finally, we conducted a one-year follow-up (1y-FU) BMA analysis in 19 patients with MDS. Among them, 13 had a complete and evaluable immunophenotypic assessment available at both diagnosis and 1y-FU and were included in the paired analysis.

During follow-up, only two patients experienced clinical deterioration characterized by worsening cytopenia, one progressed to AML, while the other developed more profound cytopenia without leukemic transformation. Nine patients received treatment during the follow-up period, six of whom achieved a clinical response, including the patient who had progressed to AML and was evaluated at the last follow-up.

Regarding immune phenotypes, no significant differences were observed in the overall frequency of BM NK cells or in most functional NK cell parameters between diagnosis and 1y-FU. Similarly, the distribution of peripheral blood T cell subsets remained largely stable over time **(Supplementary Table 10)**.

However, we identified statistically significant reductions at 1y-FU in $CD8^+$ memory T cells and Tregs. In addition, granzyme B expression significantly decreased during follow-up. Detailed paired analyses are presented in **Table 18.**

Table 18. Summary of the immune subpopulations over time.

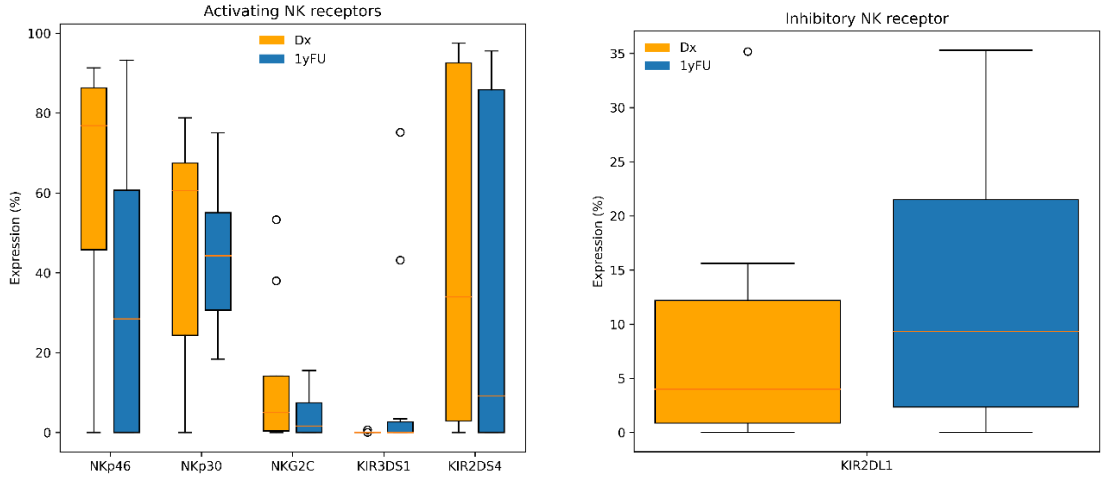
Variable		Diagnosis (n=13)	1y-FU (n=13)	p value
Memory CD8+ Tcells	Median (%)	9.95	7.60	0.03
	IQR	5.15–17.84	2.77–15.67	
Treg	Median (%)	3.36	2.56	0.04
	IQR	3.08–4.50	2.23–3.74	
Granzyme B	Median (%)	49.05	15.76	0.05
	IQR	20.00–61.05	11.30–27.39	

Shows variables with statistically significant differences at 1y-FU. Data are presented as median percentages and IQR. Percentages represent the proportion of each immune subset within total lymphocytes. Comparisons were performed using the paired Wilcoxon signed-rank test.

MDS, myelodysplastic syndromes; 1y-FU, 1-year follow-up; IQR, interquartile range; Treg, regulatory T cells.

In the paired analysis of NK cell receptors, several dynamic trends were observed. Expression of the inhibitory receptor KIR2DL1 increased from 4.00% at diagnosis (IQR, 0.87–12.20) to 9.32% at 1y-FU (IQR, 2.36–21.51; p = 0.17). Among activating receptors, NKp46 showed a marked numerical decline, decreasing from 76.84% at diagnosis (IQR, 45.81–86.31) to 28.46% at 1y-FU (IQR, 0.03–60.66; p = 0.11). A similar downward trend was observed for NKG2C, which decreased from 5.04% (IQR, 0.38–14.11) to 1.65% (IQR, 0.00–7.43; p = 0.06), approaching statistical significance. Additional non-significant reductions were observed for KIR2DS4 that decreased from 33.95% (IQR, 2.88–92.59) at diagnosis to 9.20% at 1y-FU (IQR, 0.00–85.81; p = 0.87) and NKp30 decreased from 60.61% (IQR, 24.35–67.49) to 44.30% (IQR, 30.64–55.04; p = 0.43). In contrast, NKG2D expression remained stable over time (97.59% [IQR, 95.26–98.76] vs. 97.61% [IQR, 93.09–98.45]; p = 1.00). Overall, although several receptors displayed directional changes, none reached statistical significance in this limited paired cohort **Figure 22.**

Figure 22. Longitudinal changes in NK receptor expression from diagnosis to one-year follow-up.



Expression of the inhibitory NK receptor KIR2DL1 and activating NK receptors (NKp46, NKp30, NKG2C, KIR3DS1, and KIR2DS4) in BM samples at diagnosis and 1yFU. Boxplots showing median and IQR; whiskers represent the minimum and maximum values. Comparisons were performed using the paired Wilcoxon signed-rank test, including only patients with evaluable measurements at both time points (n = 13).

MDS, myelodysplastic syndromes; 1y-FU, 1-year follow-up; IQR, interquartile range; Treg, regulatory T cells.

6. DISCUSSION

Overall, our findings partially support the hypothesis of the present study, since the pattern of immune alterations observed was more heterogeneous and nuanced than initially anticipated. Rather than identifying a single pattern of immune abnormalities, our data showed dynamic changes in the BM niche, not only with quantitative changes in its composition, but also progressive imbalance with higher risks and mutational burden. The strongest findings in our data support the hypothesis that NK cells dysfunction or exhaustion accompanied by the expansion of MDSCs occur in HR-MDS.

The principal findings were seen in ICUS displaying a highly cytotoxic and activated NK cell profile, characterized by enrichment of mature $CD56^{dim}CD16^{bright}$ NK cells (79.16%), but with a reduced DNAM-1 expression compared with MDS and HD. MDS showed marked NK cell heterogeneity, without a uniform receptor-level signature across risk categories, although HR-MDS exhibited features suggestive of exhaustion like higher Gr-MDSCs and a trend toward increase expression of TIGIT (56.02%).

Most cytokines did not differ significantly across groups, although subtle shifts toward immunosuppressive mediators (e.g., IL-10) were observed in HR-MDS. Mutational burden was associated with quantitative immune alterations, including reduced mature NK cells and decreased naïve and memory $CD8^+$ T-cell subsets in MDS^{Mut}.

Although causality cannot be established in this cross-sectional analysis, immune differences were often subtle and did not consistently withstand multiple testing correction, underscoring biological heterogeneity and limited subgroup sizes. Collectively, the coexistence of suppressor cell expansion and altered NK cell receptor profiles supports a model in which immune dysregulation in MDS is not driven by a single dominant pathway but rather reflects dynamic interactions between clonal hematopoiesis, inflammatory signaling, and immune exhaustion [136-138].

At the same time, the marked differences observed between ICUS and overt MDS provide additional insight into the temporal dynamics of immune remodeling.

- **NK Cell compartment: clonal cytopenias versus overt MDS**

One of the most relevant observations of this study was the quantitative redistribution of NK cell subsets in ICUS compared with overt MDS. Patients with ICUS exhibited a predominance of mature $CD56^{dim}CD16^{bright}$ NK cells, together with an expansion of $CD56^{neg}CD16b^{right}$ subsets, whereas MDS patients displayed significantly reduced frequencies of these populations relative to ICUS. Importantly, total NK-cell percentages did not differ substantially between MDS and healthy donors, indicating that the major

difference resides not in overall NK cell abundance but in subset composition and differentiation state.

The enrichment of mature $CD56^{dim}CD16^{bright}$ NK cells in ICUS suggests relative preservation of terminal NK differentiation. These cells represent the principal cytotoxic effector compartment and are typically characterized by high perforin and granzyme content and efficient target-cell killing. In this context, ICUS may represent an early clonal state in which immune surveillance remains partially intact and capable of exerting pressure on emerging abnormal hematopoietic progenitors. Conversely, the reduction of mature cytotoxic NK cells observed in MDS, particularly in mutation-positive cases, is consistent with impaired NK maturation. This interpretation is consistent with prior reports describing defective NK cell differentiation, altered receptor repertoires, and impaired cytotoxic function in MDS [139-143]. Hejazi *et al*. investigated NK cell subpopulations in peripheral blood by flow cytometry in 75 patients with MDS and 30 age-matched healthy controls. Their results demonstrated a similar skewing of NK cell subsets, characterized by expansion of $CD56^{bright}$ NK cells and preferential expression of early-acquired KIRs (KIR2DL2/3), together with reduced expression of late-acquired KIRs (KIR2DL1, KIR3DL1), supporting a model of incomplete or defective NK-cell maturation in MDS [144].

In contrast, our study did not demonstrate an increased proportion of $CD56^{bright}$ NK cells in MDS patients, suggesting that the classical maturation-arrest phenotype may not be uniformly present, particularly in cohorts enriched for lower-risk disease [145-146]. These differences may reflect variability in disease stage, risk composition, or methodological approaches. Importantly, progressive NK cell dysfunction has been reported not only in overt MDS but also in related clonal cytopenias, supporting a broader model of gradual immune dysregulation accompanying clonal evolution rather than a single-step defect in terminal differentiation [147-148].

Beyond subset distribution, alterations were also observed at the receptor level. DNAM-1 (CD226), a key activating receptor involved in recognition of malignant myeloid cells [149], was significantly reduced in ICUS compared with both MDS and healthy donors. DNAM-1 plays a central role in NK-cell–mediated tumor surveillance through interaction with its ligands CD155 and CD112 [150-151]. Experimental models have demonstrated that sustained ligand engagement may induce receptor internalization or adaptive downmodulation, thereby modulating NK cell responsiveness within tumor microenvironments. In principle, therefore, reduced DNAM-1 expression could reflect chronic receptor engagement and activation-induced remodeling [152–154].

However, several aspects of our dataset limit this interpretation. First, CD155 expression was undetectable in the analyzed cell populations across all groups. Although absence of detection does not exclude low-level or compartment-restricted expression, ligand-driven internalization of DNAM-1 cannot be directly demonstrated in this cohort. Second, no activation markers or functional degranulation assays were available to support recent NK cell activation. Third, TIGIT expression, a competitive inhibitory receptor sharing ligands with DNAM-1, did not differ between ICUS and MDS and was in fact lower in both disease groups compared with healthy donors. PD-1 expression was absent in ICUS, and only modest, non-significant changes were observed in other inhibitory markers such as NKG2A. Collectively, these findings do not support a clear exhaustion phenotype nor provide direct evidence of activation-induced receptor modulation [149, 155].

Therefore, while the DNAM-1 axis appears altered in ICUS, the biological meaning of this alteration remains open to interpretation. Reduced DNAM-1 expression in the setting of preserved mature NK cell proportions may reflect early receptor repertoire reprogramming occurring during clonal hematopoiesis. Alternatively, it could represent subtle dysregulation of activating pathways preceding overt functional impairment. In contrast, in established MDS, the reduction of mature NK subsets together with previously described functional defects suggests a more advanced stage of immune disruption [156,157]. The cross-sectional phenotypic nature of the present analysis does not allow discrimination between activation-induced modulation, inhibitory reprogramming, altered maturation dynamics, or emerging functional dysfunction as the primary mechanism underlying DNAM-1 downregulation in ICUS. These findings underscore the need for functional assays and ligand profiling to clarify the stage-specific biological consequences of DNAM-1 pathway alteration during myeloid disease evolution [158].

Downregulation of activating receptors, NKG2D and DNAM-1 expression in BM-derived NK cells from MDS patients was reportedly associated with elevated blast counts and high-risk disease [159-162]. In contrast, no changes in the surface of NK cells from peripheral blood were seen, and other studies investigating peripheral blood NK cells from MDS patients have reported loss of activating receptors like the NCRs (NKp30, NKp46) expression [163-164].

In our study, the analysis of NCRs revealed a distinct but partially overlapping pattern between ICUS and overt MDS. NKp46 expression was significantly increased in both MDS and ICUS compared with healthy donors, with no significant differences observed between the two disease groups. NKp46 is considered the dominant activating NCR and plays a central role in NK-cell–mediated cytotoxicity against malignant targets. Its

upregulation in both clonal cytopenia and overt MDS suggests that early and established clonal hematopoiesis are associated with remodeling of the NCR compartment rather than global loss of activating receptors. In MDS, NKp46 expression could be preserved, but despite this, impairment of cytolytic function can be seen, likely driven by compromised downstream signaling and concurrent defects in DNAM-1 and CD155 axis [156, 165-166]. NK cell activation relies on the integration of multiple synergistic signals to surpass a functional threshold [167-168]. The DNAM-1/CD155 axis is a critical co-stimulatory pathway that amplifies the signals generated by natural cytotoxicity receptors like NKp46. In MDS, a dissociation occurs, NKp46 may remain expressed, but the loss of the DNAM-1 prevents the cell from achieving the signal strength necessary for degranulation [169]. Our data supports this functional dissociation, as evidenced by the statistically significant reduction in Granzyme B expression ($p= 0.05$) at follow-up, suggesting that even when activating receptors remain on the surface, the cells become progressively unarmed and unable to execute their cytolytic program [152,160,163].

The lack of significant differences in NKp30 and the globally low expression of NKp44 further reinforces that NCR dysregulation in this setting is selective. Rather than a coordinated downregulation of the NCR family, the data suggests receptor-specific modulation. This selective pattern weakens the hypothesis of generalized NK exhaustion and favors, instead, the interpretation of receptor repertoire reshaping as part of an adaptive or dysregulated differentiation process [170].

The reduction of NKG2C in both ICUS and MDS provides an additional layer of insight. Because NKG2C is associated with adaptive or memory-like NK-cell subsets, particularly expanded in response to CMV infection, its contraction in both disease states suggests that impairment of this compartment may occur early, even before overt morphological dysplasia develops. The role of NKG2C is to mediate strong activating signals that enhance NK cell cytotoxicity against malignant myeloid cells, including those expressing CD33, a common myeloid antigen [164]. Importantly, the reduction coexists in ICUS with preserved proportions of mature cytotoxic NK subsets, indicating that phenotypic maturation and adaptive specialization may be dissociated processes [167].

Taken together, our data indicates remodeling of NK-cell differentiation and selective activating receptor pathways across the continuum from clonal cytopenia to overt MDS.

Finally, the KIR phenotype adds a complementary layer to the DNAM-1/NCR findings by pointing to a broader remodeling of NK-cell “education” and activation thresholds in clonal cytopenias and overt MDS. In our study, an imbalance in activating KIR availability differs between ICUS and MDS. This pattern is consistent with the idea that, in these

disease contexts, NK cells may lose (or failing to acquire) activating inputs [171, 172]. A key observation is the restricted activating KIR repertoire in ICUS, with near-absent expression and a profile limited to inhibitory KIRs, aligning with an early clonal state where NK differentiation may look preserved at the subset level, but functional breadth is already narrowed [170].

In our study, the picture in MDS patients appears more heterogeneous, with selective shifts in specific activating KIRs rather than a uniform increase or decrease. This heterogeneity fits with MDS being biologically diverse, associated with decreased activating KIR gene expression, reduced repertoire complexity, and significant heterogeneity in KIR genotypes [173-174]. Our MDS cohort was enriched for lower-risk disease, which can resemble clonal cytopenias more than advanced MDS in immune architecture. In that setting, it is plausible that the KIR profile reflects a mixture of trajectories: some patients retaining partial activating KIR expression, others showing patterns closer to ICUS, and a subset potentially showing compensatory expression of particular activating KIRs [172]. The net effect is an “uneven remodeling” rather than a single directional change. Due to the differences in population sizes and predominance of LR-MDS, changes could be misinterpreted. Therefore, it is reasonable to frame that KIR findings could be indicative of repertoire restriction and remodeling rather than definitive evidence of stage-specific licensing failure [175].

Ligand–receptor interactions are critical determinants of NK-cell–mediated lysis of MDS blasts; however, published data remain inconsistent. Epling-Burnette *et al*. reported that approximately 30% of MDS blasts expressed the NKG2D ligands MICA/B [174]. In partial agreement with this observation, our study detected higher MICA/B expression in MDS compared with ICUS, in which no expression was observed. Nevertheless, the overall levels were low and comparable to those detected in HD, suggesting that the quantitative increase in MDS may be modest and of uncertain biological significance.

In contrast, Carlsten *et al*. described rare expression of NKG2D ligands (MICs and ULBPs) in the BM of MDS patients and instead identified expression of the DNAM-1 ligands CD155 and CD112, highlighting the potential importance of the DNAM-1–CD155/CD112 axis in NK-cell–mediated cytotoxicity against MDS blasts [153]. Notably, in our cohort, CD155 expression was not detected, as previously discussed.

Taken together, these discrepancies may reflect differences in patient risk composition, sample source (BM versus peripheral blood), detection methods, or disease heterogeneity. They also underscore the complexity of NK–tumor interactions in MDS

and suggest that the relative contribution of NKG2D- versus DNAM-1–mediated pathways may vary across disease stages and biological contexts [176].

- **KIR genotypic landscape and its impact on NK cell education in MDS**

The combined phenotypic and genotypic KIR analyses reveal a nuanced and somewhat paradoxical landscape in MDS. At the surface-expression level, MDS patients demonstrate a selective reduction of several activating KIRs (KIR3DS1, KIR2DS1) compared with HD, while inhibitory KIR expression remains largely preserved. This pattern suggests that early states may be associated with narrowing of activating breadth without overt disruption of inhibitory licensing frameworks [175]. Our study provides a comprehensive characterization of the NK cell compartment in MDS, revealing a complex interplay between this receptor expression and the underlying genetic background.

Importantly, genotyping in MDS patients reveals a predominance of B-containing haplotypes (74%), which are classically enriched in activating KIR genes. At first glance, this might appear inconsistent with the phenotypic data showing reduced surface expression of activating KIRs in MDS compared with HD. However, this apparent discrepancy likely reflects a dissociation between genetic potential and phenotypic realization [177]. This genetic potential contrasts with the phenotypic exhaustion and reduced expression of activating receptors like NKG2C and DNAM-1 observed in our functional analysis, supporting the hypothesis of a chronic activation-induced exhaustion within the BM microenvironment.

The presence of activating KIR genes does not guarantee uniform expression across the NK cell compartment. Instead, receptor expression is regulated by stochastic promoter activity, epigenetic mechanisms, and education-dependent selection. KIR gene expression is inherently stochastic, meaning that individual NK cells randomly express different combinations of KIRs, due to promoter activity that is variably silenced or activated by DNA methylation and chromatin accessibility, resulting in a clonally distributed and highly diverse KIR repertoire within the NK cell population [178-181]. Epigenetic regulation further modulates which KIR genes are transcribed, and this is altered in MDS [182].

NK cell "licensing," shapes the functional NK cell repertoire by favoring the survival and maturation of NK cells whose KIRs interact with self-HLA ligands. Activating KIRs participate in this process, but their expression can render NK cells hyporesponsive if not balanced by inhibitory signals, and the presence of activating KIR genes does not guarantee their expression or function in all NK cells [182].

Furthermore, the integrative analysis of KIR and their cognate HLA-C ligands highlight a potential genetic risk factor for disease evolution that extends beyond gene content alone. We observed that 75% of patients who progressed to more advanced stages carried a Bx haplotype, with the Bx + C1/C1 combination showing the highest progression rate (14.3%). This specific immunogenetic profile, characterized by a high density of activating KIRs in a low-affinity ligand environment, might result in inadequate NK cell 'licensing' or education, leading to impaired immunosurveillance against the dysplastic clone. While the limited number of progression events precludes definitive statistical associations, these trends suggest that KIR-HLA-C genotyping could provide additional prognostic value beyond standard clinical scores. Serio *et al*. found a decreased frequency of the activating KIR2DS1/C2 mismatch combination in both MDS, and aplastic anemia patients compared to controls, suggesting that loss of this activating interaction may predispose immune-mediated BM failure [(183)].

Stringaris *et al*. reported that KIR haplotype composition may represent an independent risk factor in MDS, with haplotype A, characterized by a predominance of inhibitory KIR genes, associated with worse outcomes, with a higher risk of progression to MDS and AML [(48)]. They also described that the median number of activating genes was lower in MDS compared to healthy controls, and the same was seen in secondary AMLs compared to de novo AML and healthy controls. Furthermore, our integration of HLA-A alleles (specifically A*23) to define the Bw4 ligand status allowed for a more precise characterization of the KIR3DL1-Bw4 axis. This is consistent with Zhen *et al*. [(184)], who demonstrated that the KIR3DL1-HLA-Bw4 interaction confers a protective effect against MDS development. The inclusion of HLA-A in our analysis ensures that patients who would otherwise be classified as 'missing ligand' are correctly identified, providing a more robust framework for assessing immune surveillance.

However, in our cohort, the predominance of B-containing haplotypes suggests that the genetic framework for a broader activating KIR repertoire is largely preserved. Compared to the restricted activating KIR repertoire observed in ICUS patients, the expanded Bx profile in MDS may represent a late-stage immune attempt to control clonal expansion, which ultimately fails due to the immunosuppressive landscape, as evidenced by the concurrent downregulation of NKp46 and DNAM-1 [(185)].

This apparent dissociation implies that NK cell education in MDS may not be primarily limited by gene content, but rather by altered differentiation dynamics or microenvironment-driven modulation. Therefore, the decoupling between genotype and surface phenotype may reflect a disturbed education process where the absence of

strong inhibitory "licensing" signals (as seen in the Bx + C1/C1 group) fails to tune the NK cells for effective antitumor killing [183].

Importantly, the predominance of LR-MDS in our cohort may attenuate differences that could be more pronounced in advanced disease. Furthermore, genotyping was only available for MDS patients, limiting direct comparison across groups. Therefore, while the data supports altered NK cell education dynamics in MDS, they should be interpreted as evidence of qualitative remodeling of activation thresholds rather than definitive licensing failure [175]. These findings align with prior evidence of altered NK differentiation and impaired cytotoxicity in MDS and complements reports that deficits in other activating axes (DNAM-1/NKG2D) and ligand availability can further uncouple receptor expression from effective antitumor killing [176].

- **Risk Stratification: from inflammation to exhaustion**

Risk-stratified analysis supports the concept that progression in MDS is not characterized by a single, uniform receptor-level shift within the immune niche. No discrete phenotypic signature clearly distinguishes LR-MDS from HR-MDS. Rather, disease evolution appears to involve gradual immune remodeling, with coordinated changes that align with the emerging framework of transition from an inflammatory, immune-reactive environment in early disease toward compensatory immunosuppression in higher-risk stages.

The absence of a consistent, risk-specific receptor signature is not unexpected in MDS, given the biological heterogeneity of the disease [6]. Immune phenotypes in MDS frequently exhibit substantial within-group variability, a feature that becomes more pronounced in modest and unbalanced cohorts. Accordingly, NK- and T-cell phenotypes in our dataset were highly heterogeneous across IPSS-R risk categories. Nevertheless, despite this variability and the lack of a single defining marker, several converging features in our analysis suggest a trajectory toward progressive immune exhaustion in HR-MDS.

NK cells demonstrated a trend toward higher TIGIT expression in HR-MDS together with a significant increase in the activating receptor KIR2DS2 and suggestive elevations in additional KIRs. The coexistence of enhanced activating receptor expression and checkpoint upregulation may suggest a state of chronic immune stimulation accompanied by compensatory inhibitory signaling. Rather than indicating effective hyperactivation, this profile is more consistent with functional restraint, in which persistent antigenic pressure drives simultaneous activation signals and checkpoint-mediated modulation [186].

Previous studies have reported increased TIGIT expression in peripheral blood in association with MDS progression, concomitant with reduced NK- and T-cell effector function [187], supporting the interpretation that checkpoint upregulation may mark emerging immune exhaustion in higher-risk disease.

Moreover, MDSCs have been identified as key contributors to immune dysfunction, ineffective hematopoiesis, and disease progression in MDS [188-190]. Kittang *et al*. reported increased levels of circulating MDSCs in patients with MDS, with significantly higher frequencies in high-risk categories compared with low-risk patients and age-matched healthy donors. Furthermore, they observed that patients with higher BM blast percentages exhibited greater MDSC expansion compared with those with <5% blasts and healthy controls, supporting an association between disease burden and suppressor cell accumulation [191].

In our cohort, we observed a statistically significant expansion of granulocytic MDSCs in HR-MDS (median 0.33% vs. 0.04%, p= 0.0028), with a moderate-to-large effect size, whereas monocytic MDSCs showed only a numerical increase without statistical significance. These findings suggest that higher-risk disease is characterized by enhanced cell-mediated immunosuppression, potentially contributing to risk stratification independently of soluble cytokine levels [192].

This pattern is consistent with accumulating evidence indicating that MDSC expansion is enriched in advanced or biologically aggressive MDS and plays a central role in shaping the immunosuppressive microenvironment [188]. Mechanistically, MDSCs suppress NK- and T-cell effector function through multiple pathways, including arginase activity, reactive oxygen species production, secretion of inhibitory cytokines such as IL-10 and TGF-β, and engagement of immune checkpoint ligands. This provides a biologically plausible link between the observed increase in TIGIT expression and the expansion of granulocytic MDSCs in HR-MDS, supporting a coordinated shift toward immune restraint in higher-risk disease [193-195].

Regarding soluble mediators, the cytokine panel showed substantial overlap between LR- and HR-MDS. Across the 32-plex assay, no cytokine remained significant after FDR correction, and even unadjusted p-values did not demonstrate consistent differences. Most analytes exhibited overlapping interquartile ranges, minimal median shifts, and uniformly high q-values (~0.99–1.00). These findings indicate the absence of a robust, risk-specific systemic cytokine signature in BM.

This observation is consistent with prior reports indicating that circulating cytokine levels in MDS are highly heterogeneous and often poorly correlated with IPSS-R categories, particularly when assessed in peripheral blood rather than within the BM microenvironment. Although inflammatory cytokines are frequently elevated in MDS compared with healthy controls, risk-stratified differences are typically modest and may not withstand correction for multiple testing [49,196, 197]

Despite the lack of statistical significance, certain directional trends merit cautious mechanistic consideration. HR-MDS demonstrated a subtle increase in IL-10 (Δ +0.07 pg/mL), although overlapping distributions preclude firm conclusions. IL-10 is a well-established immunoregulatory cytokine associated with suppression of NK- and T-cell effector function, expansion of regulatory circuits, and MDSC-mediated immune inhibition [198]. Even minor upward shifts in IL-10, particularly when considered alongside increased granulocytic MDSCs and checkpoint upregulation, may reflect a gradual drift toward an immunoregulatory milieu.

Similarly, HR-MDS exhibited a modest numerical increase in IP-10 (CXCL10). As an IFN-γ–inducible chemokine, IP-10 is linked to chronic inflammatory signaling, T-cell trafficking, and sustained immune activation [199]. The coexistence of slightly higher IP-10 levels, increased TIGIT expression, and expanded Gr-MDSCs may be compatible with a scenario of chronic antigenic stimulation followed by compensatory inhibitory regulation, rather than acute inflammatory escalation [186].

Importantly, no clear increase in classical pro-inflammatory mediators such as IL-6, TNF-α, or IFN-γ was observed between risk groups. This contrasts with simplified models proposing a linear transition from inflammatory LR disease to overtly immunosuppressive HR disease driven by escalating cytokine production [200-201].

Overall, the subtle cytokine differences between LR- and HR-MDS reinforce the notion that immune dysregulation in MDS could be more strongly reflected by changes in cellular composition and receptor dynamics than by overt systemic cytokine storms.

- **Mutational burden and immune remodeling**

In this cohort, somatic mutations were identified in the majority of MDS patients, and more than half of mutation-positive cases carried three or more lesions, reflecting the degree of clonal complexity typical of established disease. The distribution of recurrently mutated genes parallel to the canonical MDS genomic spectrum, supporting that the associated immune findings arise within a representative biological context rather than an atypical genetic subset [99].

Stratification by mutational status revealed a pattern of contraction within cytotoxic compartments. MDS^{Mut} patients displayed reduced frequencies of mature NK cells ($CD56^{dim}CD16^{bright}$) and diminished $CD8^+$ T-cell subsets, particularly $CD57^+$ effector populations. These immune changes coincided with significantly lower platelet counts, suggesting that increasing clonal burden is linked not only to hematopoietic impairment but also to attenuation of cytotoxic immune maintenance.

Several non-mutually exclusive mechanisms may underline this association. Expanding clones could promote sustained antigenic or innate immune stimulation through aberrant splicing products, neoantigens, or damage-associated signals, ultimately, leading to differentiation arrest or functional exhaustion of NK and $CD8^+$ T cells. Alternatively, mutations affecting epigenetic regulators may alter transcriptional programs in both hematopoietic and stromal compartments, reshaping the marrow microenvironment in ways that limit cytotoxic cell survival or maturation [202-206]. Importantly, these cellular alterations occurred without significant differences in measured cytokine concentrations between MDS^{Mut} and MDS^{NoMut} groups, which could indicate that the remodeling process is not driven by broad systemic inflammatory shifts. Rather, it appears to reflect changes in cellular composition, local signaling, or licensing dynamics within the marrow niche. Extrinsic and intrinsic immunological factors might severely impair immune surveillance and contribute to clonal immune escape. Genomic alterations appear to make an independent contribution to the clonal evolution and progression of MDS [207-210].

A trend toward higher VEGF-A levels in mutation-positive MDS suggests that pro-angiogenic and immunoregulatory pathways may become increasingly relevant as clonal complexity expands, potentially fostering a microenvironment less conducive to effective cytotoxic surveillance. VEGF-A has been implicated in ineffective hematopoiesis, enhanced marrow angiogenesis, and disease progression in MDS, and elevated expression has been associated with adverse clinical outcomes, particularly in higher-risk categories [211–213].

However, the prognostic impact of VEGF-A appears to be context-dependent. Some studies have reported associations between VEGF-A expression and longer survival in selected LR-MDS cohorts, underscoring the biological heterogeneity of the disease and suggesting that VEGF-A may exert differential effects depending on disease stage, risk profile, and microenvironmental context [213].

Notably, immune parameters did not segregate according to mutational categories (epigenetic, splicing, or *TP53*). This lack of genotype-specific patterns in our data implies that cumulative clonal burden, rather than individual driver mutations, exerts the

dominant influence on immune architecture as describe in the literature [214-216]. However, limited subgroup sizes, particularly for *TP53*-mutated cases, reduce statistical power and preclude definitive conclusions [207, 217]. Similarly, stratification by IPSS-M risk revealed only a nominal increase in inhibitory KIR2DL1 expression in higher-risk disease that did not withstand correction for multiple testing, underscoring the exploratory nature of these associations. This finding should be interpreted in the context of prior work showing that higher-risk MDS, particularly disease enriched for adverse mutations such as TP53, is associated with marked biologic aggressiveness and immune impairment. Nevertheless, while molecular risk stratification has been extensively studied, direct phenotypic assessment of individual KIR receptors across molecular risk groups remains scarce. Thus, the apparent increase in KIR2DL1 observed in our higher-risk subgroup should be regarded as hypothesis-generating rather than definitive and warrant validation in larger, molecularly annotated cohorts [217- 220].

Taken together, the findings support a model in which immune dysregulation in MDS is not defined by a single dominant pathway, but rather by progressive and context-dependent remodeling of the BM immune niche [221]. In earlier disease states, this process appears to involve alterations in NK cell differentiation and receptor repertoire in the setting of a relatively limited cytokine signal, whereas higher-risk disease is associated with a more suppressive immune configuration, including increased checkpoint expression and expansion of suppressive Gr-MDSCs [193].

Notably, in our cohort these changes occurred without robust soluble cytokine signature, suggesting that immune evolution in MDS may be shaped more by changes in cellular composition, receptor dynamics, and local microenvironmental interactions than by overt inflammatory amplification alone [171]. The coexistence of activating receptor expression with inhibitory checkpoint signals further supports a model of sustained immune pressure followed by compensatory restraint, consistent with progressive functional exhaustion [222- 223].

Overall, these data reinforce the concept that immune alterations in MDS unfold along a continuum shaped by clonal complexity, disease risk, and microenvironmental pressure rather than by a single fixed immune defect [136, 221]. This integrated perspective provides a framework for understanding how immune surveillance may be progressively recalibrated during disease evolution, from early perturbations in NK-cell differentiation and receptor balance to more advanced states characterized by immune restraint and suppressive niche remodeling [171, 224].

These observations align with previous work describing immune dysregulation in MDS as a multifaceted and stage-dependent process. Prior studies have emphasized defective NK-cell differentiation, altered receptor repertoires, checkpoint upregulation, and expansion of suppressive myeloid populations, particularly in advanced disease [193]. However, unlike some earlier reports describing clear maturation arrest signatures or strong systemic inflammatory gradients, we did not observe a uniform receptor-level pattern. Such differences may be attributable to cohort composition, particularly the predominance of LR-MDS in our population, as well as differences in sampling compartment, methodological platforms, and statistical correction approaches. Unexpectedly, activating KIR genotypes were frequent despite reduced or heterogeneous phenotypic expressions, suggesting that genetic potential and functional deployment may be dissociated in MDS. Rather than reflecting simple receptor loss, this pattern may indicate disturbed NK cell education or context-dependent regulation of receptor expression, although these mechanisms remain incompletely characterized and require validation in larger studies integrating genotype, phenotype, and function [225- 226].

The principal strengths of our study lie in its integrative design, which combines detailed phenotypic NK cell analysis, KIR genotyping, HLA matching, quantification of MDSCs, and multiplex cytokine profiling within the same cohort. Moreover, the evaluation of these parameters directly in the BM provides a descriptive yet biologically relevant assessment of the immune landscape within the disease niche. This systems-level approach allows for a more comprehensive interpretation of immune remodeling across disease stages. In addition, the application of non-parametric statistical methods with correction for multiple testing strengthens the reliability of negative findings and reduces the risk of overinterpreting exploratory associations.

Nevertheless, several limitations must be acknowledged. The cohort size, particularly within stratified and control subgroups, limits statistical power and may have obscured subtle yet biologically meaningful differences. The predominance of LR-MDS cases may also attenuate contrasts that could be more evident in cohorts enriched for advanced disease. The cross-sectional design precludes causal inference and does not allow evaluation of longitudinal immune evolution during disease progression. Additionally, the absence of parallel peripheral blood analyses limits our ability to contextualize BM findings and assess compartment-specific immune dynamics. Finally, the lack of functional assays prevents direct conclusions regarding cytotoxic capacity, checkpoint responsiveness, or the presence of true exhaustion states, restricting interpretation to phenotypic associations.

Within the broader scientific conversation, our study supports a refined model of immune evolution in MDS: rather than a binary inflammatory-to-immunosuppressive switch, disease progression appears to involve gradual recalibration of NK-cell education, checkpoint balance, and suppressive cellular expansion, occurring even in the absence of dramatic systemic cytokine changes. This perspective contributes to a more nuanced understanding of immune dynamics in clonal hematopoiesis and MDS progression and may inform future studies exploring stage-specific immunomodulatory interventions.

The primary aim of this study was to characterize the immune landscape of the BM niche in MDS and to explore how immune alterations correlate with disease progression. We hypothesized that advancing disease risk would be associated with coordinated shifts in soluble mediators, immune-cell composition, and receptor expression profiles. Instead, our results revealed marked heterogeneity: soluble cytokine levels showed no consistent risk-specific pattern, and cellular differences between low- and HR-MDS were present but subtle. These findings do not support a single dominant immunological signature of progression. Rather, they underscore the intrinsic biological variability that defines MDS.

Although the immediate clinical impact for hematologists may appear modest, the study is significant for several reasons. First, it focuses on the BM microenvironment, an underexplored compartment compared with peripheral blood, thereby contributing data directly from the disease niche where clonal evolution unfolds. Second, it reinforces the concept that immune dysregulation in MDS is complex, compartment-specific, and not adequately captured by isolated biomarkers. By demonstrating heterogeneity rather than a simplistic inflammatory-to-suppressive switch, this work adds nuance to the current understanding of immune remodeling in MDS and cautions against overreliance on single-parameter immune readouts.

Several important questions remain unanswered. Longitudinal studies are needed to track immune evolution within the same patients across risk transitions and treatment exposure. Functional assays, including NK cytotoxicity, degranulation capacity, checkpoint blockade responsiveness, and suppressor-cell inhibition experiments should be integrated with phenotypic profiling to clarify biological relevance. Single-cell transcriptomic and spatial analyses of the BM niche allow resolution of clonal–immune cell interactions and better define microenvironmental signaling networks. Stratification by molecular risk (e.g., mutational profile and clonal burden) rather than IPSS-R alone reveals more biologically meaningful immune correlations. Finally, interventional studies targeting checkpoint pathways or MDSCs must incorporate immune monitoring frameworks capable of detecting subtle niche remodeling.

In summary, this study suggests that immune alterations in MDS BM are heterogeneous, context-dependent, and not defined by overt cytokine dysregulation. The key contribution is not the identification of a single predictive immune marker, but the demonstration that immune remodeling in MDS is complex and requires more precise, integrative methodologies. The take-home message is clear: understanding MDS progression demands deeper, longitudinal, and functionally informed interrogation of the BM immune niche with better comparisons and impact to the peripheral blood changes, because in this disease, the signal lies not in dramatic shifts, but in subtle and evolving recalibration of the immune ecosystem.

7. CONCLUSIONS

1) MDS is characterized by a measurable remodeling of the immune landscape. Alterations in NK cell differentiation, receptor expression shifts, and T cell subsets fluctuations demonstrate that immune dysregulation is an integral biological component of the disease, rather than a secondary epiphenomenon.
2) The BM cytokine milieu exhibits substantial heterogeneity. Observed trends in pro-inflammatory and immunomodulatory mediators suggest a microenvironment that concurrently promotes chronic inflammation and immunosuppressive signaling.
3) A distinct dissociation exists between KIR genotypes. The prevalence of B-containing haplotypes despite reduced activating KIR expression underscores the role of epigenetic regulation and NK cell education in limiting effective immune surveillance.
4) Somatic mutations and immune remodeling coexist within a unified biological framework. While associations were limited by cohort size, the data indicates that inflammatory signaling and immune dysfunction are intertwined with the molecular evolution of the disease.
5) Risk stratification using the IPSS-R 3.5 cutoff reveals that immune dysfunction correlates with disease progression. While differences between risk groups are modest, specific immunological changes in advanced stages suggest that immune profiling, especially when integrated with molecular risk, could significantly complement current prognostic systems.

8. FUTURE DIRECTIONS

The results presented in this thesis highlight the relevance of immune dysregulation in the pathophysiology of MDS. Given the marked biological heterogeneity of the disease, future research should focus on improving disease stratification by integrating immune profiling with genomic and molecular characterization. Such approaches may help clarify disease mechanisms and identify biomarkers associated with treatment response or resistance, ultimately contributing to more accurate patient stratification and more rational therapeutic selection.

From a translational perspective, these findings may also inform the development of biomarker-driven clinical trials and novel therapeutic strategies. A deeper understanding of the interaction between clonal hematopoiesis and immune surveillance could help explain treatment failure in a subset of patients and support the design of more personalized treatment approaches, ultimately improving outcomes for individuals with MDS.

9. REFERENCES

1. Hasserjian RP, Germing U, Malcovati L. Diagnosis and classification of myelodysplastic syndromes. Blood. 2023;142(26):2247-2257. doi: 10.1182/blood.2023020078
2. Khoury JD, Solary E, Abla O, *et al*. The 5th edition of the World Health Organization Classification of Haematolymphoid Tumours: Myeloid and Histiocytic/Dendritic Neoplasms. Leukemia. 2022;36(7):1703-1719. doi:10.1038/s41375-022-01613-1
3. Arber DA, Orazi A, Hasserjian RP, *et al*. ICC 2022: International Consensus Classification for Myelodysplastic Neoplasms. Blood. 2022;140(11):1200-1228. doi:10.1182/blood.2022015850
4. Steensma DP. Historical perspectives on myelodysplastic syndromes. Leukemia research. 2012; 1441-1452. 10.1016/j.leukres.2012.08.007
5. Toprak S. Past, present and future in low-risk myelodysplastic syndrome. Front. Med. 9:967900. doi: 10.3389/fmed.2022.967900.
6. Garcia-Manero G. Myelodysplastic syndromes: 2023 update on diagnosis, risk stratification, and management. Am J Hematol. 2023;98(8):1307-1325. doi:10.1002/ajh.26984
7. Besa EC. Myelodysplastic syndrome (MDS): epidemiology. Medscape. Updated October 1, 2022.
8. Marsà A, Ascanio M, Díaz-García J, *et al*. Epidemiology, management, and economic impact of acute myeloid leukemia and myelodysplastic syndrome in Spain at the hospital level: a claims database analysis. Journal of Medical Economics. 2020. 10.1080/13696998.2020.1840180.
9. Kouroukli O, Symeonidis A, Foukas P, *et al*. Bone marrow immune microenvironment in myelodysplastic syndromes. *Cancers (Basel)*. 2022;14(22):5656. doi:10.3390/cancers14225656.
10. Cazzola M. Myelodysplastic syndromes. *N Engl J Med.* 2020;383(14):1358-1374. doi:10.1056/NEJMra1904794.
11. Sperling AS, Gibson CJ, Ebert BL. The genetics of myelodysplastic syndrome: from clonal haematopoiesis to secondary leukaemia. *Nat Rev Cancer.* 2017;17(1):5-19. doi:10.1038/nrc.2016.112
12. Sekeres MA, Taylor J. Diagnosis and treatment of myelodysplastic syndromes: a review. *JAMA.* 2022;328(9):872-880. doi:10.1001/jama.2022.14578.
13. Pierro F, Fazio M, Murdaca G, *et al*. Oxidative stress and mitochondrial dysfunction in myelodysplastic syndrome: roles in development, diagnosis,

prognosis, and treatment. *Int J Mol Sci.* 2025;26(13):6415. doi:10.3390/ijms26136415.

14. Balaian E, Wobus M, Bornhäuser M, *et al*. Myelodysplastic syndromes and metabolism. *Int J Mol Sci.* 2021;22(20):11250. doi:10.3390/ijms222011250.
15. Franceschi C, Garagnani P, Parini P, *et al*. Inflammaging: a new immune-metabolic viewpoint for age-related diseases. Nat Rev Endocrinol. 2018;14(10):576-590. doi:10.1038/s41574-018-0059-4.
16. Teissier T, Boulanger E, Cox LS. Interconnections between inflammageing and immunosenescence during ageing. Cells. 2022;11(3):359. doi:10.3390/cells11030359.
17. Chambers ES, Akbar AN. Can blocking inflammation enhance immunity during aging? J Allergy Clin Immunol. 2020;145(5):1323-1331. doi:10.1016/j.jaci.2020.03.016.
18. Fülöp T, Witkowski JM, Olivieri F, *et al*. The integration of inflammaging in age-related diseases. Semin Immunol. 2018; 40:17-35. doi:10.1016/j.smim.2018.09.003.
19. Dugan B, Conway J, Duggal NA. Inflammaging as a target for healthy ageing. *Age Ageing.* 2023;52(2):afac328. doi:10.1093/ageing/afac328.
20. Lee G, Lee GS. Potential role of inflammasomes in aging. Int J Mol Sci. 2025;26(14):6768. doi:10.3390/ijms26146768.
21. Giunta S, Wei Y, Xu K, *et al*. Cold-inflammaging: when a state of homeostatic imbalance associated with aging precedes the low-grade pro-inflammatory state (inflammaging): meaning, evolution, inflammaging phenotypes. Clin Exp Pharmacol Physiol. 2022;49(9):925-934. doi:10.1111/1440-1681.13686.
22. Van Beek AA, Van den Bossche J, Mastroberardino PG, de Winther MPJ, Leenen PJM. Metabolic alterations in aging macrophages: ingredients for inflammaging? Trends Immunol. 2019;40(2):113-127. doi:10.1016/j.it.2018.12.007.
23. Rasa SMM, Annunziata F, Krepelova A, *et al*. Inflammaging is driven by upregulation of innate immune receptors and systemic interferon signaling and is ameliorated by dietary restriction. *Cell Rep.* 2022;39(13):111017. doi:10.1016/j.celrep.2022.111017.
24. Walker KA, Basisty N, Wilson DM, *et al*. Connecting aging biology and inflammation in the omics era. J Clin Invest. 2022;132(14):e158448. doi:10.1172/JCI158448.
25. Singh A, Schurman SH, Bektas A, *et al*. Aging and inflammation. Cold Spring Harb Perspect Med. 2024;14(6):a041197. doi:10.1101/041197.

26. Villaume MT, Savona MR. Pathogenesis and inflammaging in myelodysplastic syndrome. Haematologica. 2025;110(2):283-299. doi:10.3324/haematol.2023.284944.
27. Rodriguez-Sevilla JJ, Colla S. Inflammation in myelodysplastic syndrome pathogenesis. Semin Hematol. 2024;61(6):385-396. doi:10.1053/j.seminhematol.2024.09.005.
28. Balaian E, Wobus M, Bornhäuser M, *et al*. Myelodysplastic syndromes and metabolism. Int J Mol Sci. 2021;22(20):11250. doi:10.3390/ijms222011250.
29. Heibl S, Stauder R, Pfeilstöcker M. Is myelodysplasia a consequence of normal aging? Curr Oncol Rep. 2021;23(12):142. doi:10.1007/s11912-021-01136-5.
30. Grants JM, Wegrzyn J, Hui T, *et al*. Altered microRNA expression links IL-6 and TNF-induced inflammaging with myeloid malignancy in humans and mice. Blood. 2020;135(25):2235-2251. doi:10.1182/blood.2019003105.
31. Trowbridge JJ, Starczynowski DT. Innate immune pathways and inflammation in hematopoietic aging, clonal hematopoiesis, and MDS. J Exp Med. 2021;218(7):e20201544. doi:10.1084/jem.20201544.
32. Sallman DA, List A. The central role of inflammatory signaling in the pathogenesis of myelodysplastic syndromes. Blood. 2019;133(10):1039-1048. doi:10.1182/blood-2018-10-844654.
33. Kawano Y, Kawano H, LaMere M, *et al*. IL-1R1 and IL-18 signals regulate mesenchymal stromal cells in an aged murine model of myelodysplastic syndromes. Blood. 2025; Apr 10;145(15):1632-1644.doi: 10.1182/blood.2024024818.
34. Datar GK, Goodell MA. Where there's smoke, there's fire: inflammation drives MDS. Trends Immunol. 2020;41(7):558-560. doi:10.1016/j.it.2020.05.007.
35. Barreyro L, Chlon TM, Starczynowski DT. Chronic immune response dysregulation in MDS pathogenesis. Blood. 2018;132(15):1553-1560. doi:10.1182/blood-2018-03-784116.
36. Banerjee T, Calvi LM, Becker MW, *et al*. Flaming and fanning: the spectrum of inflammatory influences in myelodysplastic syndromes. Blood Rev. 2019; 36:57-69. doi:10.1016/j.blre.2019.04.004.
37. Shi X, Zheng Y, Xu L, *et al*. The inflammatory cytokine profile of myelodysplastic syndromes: a meta-analysis. Medicine (Baltimore). 2019;98(22):e15844. doi:10.1097/MD.0000000000015844.
38. Kitagawa M, Saito I, Kuwata T, *et al*. Overexpression of tumor necrosis factor (TNF)-alpha and interferon (IFN)-gamma by bone marrow cells from participants

with myelodysplastic syndromes. Leukemia. 1997;11(12):2049-2054. doi:10.1038/sj.leu.2400844.

39. Xiong H, Yang XY, Han J, *et al*. Cytokine expression patterns and mesenchymal stem cell karyotypes from the bone marrow microenvironment of participants with myelodysplastic syndromes. Braz J Med Biol Res. 2015;48(3):207-213. doi:10.1590/1414-431X20144051.
40. Lynch OF, Calvi LM. Immune dysfunction, cytokine disruption, and stromal changes in myelodysplastic syndrome: a review. Cells. 2022;11(3):580. doi:10.3390/cells11030580
41. Rodriguez-Sevilla JJ, Colla S. T-cell dysfunctions in myelodysplastic syndromes. Blood. 2024;143(14): 1329–1343. doi:10.1182/blood.2023023166.
42. Li X, Zou C, Xiang X, *et al*. Myelodysplastic neoplasms (MDS): pathogenesis and therapeutic prospects. *Biomolecules.* 2025;15(6):761. doi:10.3390/biom15060761
43. Hoff FW, Madanat YF. Molecular drivers of myelodysplastic neoplasms (MDS): classification and prognostic relevance. Cells. 2023;12(4):627. doi:10.3390/cells12040627.
44. Zhang W, Xie X, Mi H, *et al*. Abnormal populations and functions of natural killer cells in participants with myelodysplastic syndromes. Oncol Lett. 2018;15(4):5497-5504. doi:10.3892/ol.2018.8062
45. Cianga VA, Campos Catafal L, Cianga P, *et al*. Natural killer cell subpopulations and inhibitory receptor dynamics in myelodysplastic syndromes and acute myeloid leukemia. Front Immunol. 2021; 12:665541. doi:10.3389/fimmu.2021.665541
46. Hejazi M, Manser AR, Fröbel J, *et al*. Impaired cytotoxicity associated with defective natural killer cell differentiation in myelodysplastic syndromes. Haematologica. 2015;100(5):643-652. doi:10.3324/haematol.2014.118679
47. Arellano-Ballestero H, Sabry M, Lowdell MW. A killer disarmed: natural killer cell impairment in myelodysplastic syndrome. Cells. 2023;12(4):633. doi:10.3390/cells12040633
48. Stringaris K, Marin D, Barrett AJ, *et al*. KIR gene haplotype: an independent predictor of clinical outcome in MDS participants. *Blood.* 2016;128(24):2819-2823. doi:10.1182/blood-2016-05-713099
49. Serio B, Selleri C, Maciejewski JP. Impact of immunogenetic polymorphisms in bone marrow failure syndromes. Mini Rev Med Chem. 2011;11(6):544-552. doi:10.2174/138955711795843356.
50. Howe EC, Wlodarski M, Ball EJ, *et al*. Killer immunoglobulin-like receptor genotype in immune-mediated bone marrow failure syndromes. Exp Hematol. 2005;33(11):1357-1362. doi:10.1016/j.exphem.2005.07.005

51. Majcherek M, Przeorski K, Mroczkowska-Bękarciak A, *et al*. Integrating molecular alterations with immunophenotype and clinical characteristics in myelodysplastic syndromes: a single-center study. Int J Mol Sci. 2025;26(15):7382. doi:10.3390/ijms26157382.
52. Cheung NK, Hsu KC. Genotyping natural killer immune checkpoints to discover biomarkers of response. Clin Cancer Res. 2018;24(1):3-5. doi:10.1158/1078-0432.CCR-17-2884.
53. Bernson E, Hallner A, Sander FE, *et al*. Impact of killer-immunoglobulin-like receptor and human leukocyte antigen genotypes on the efficacy of immunotherapy in acute myeloid leukemia. Leukemia. 2017;31(12):2552-2559. doi:10.1038/leu.2017.151
54. Chiereghin C, Travaglino E, Zampini M, *et al*. The genetics of myelodysplastic syndromes: clinical relevance. Genes (Basel). 2021;12(8):1144. doi:10.3390/genes12081144.
55. Adès L, Itzykson R, Fenaux P. Myelodysplastic syndromes. Lancet. 2014;383(9936):2239-2252. doi:10.1016/S0140-6736(13)61901-7.
56. Cazzola M, Della Porta MG, Malcovati L. The genetic basis of myelodysplasia and its clinical relevance. Blood. 2013;122(25):4021-4034. doi:10.1182/blood-2013-09-381665.
57. Pellagatti A, Boultwood J. The molecular pathogenesis of the myelodysplastic syndromes. Eur J Haematol. 2015;95(1):3-15. doi:10.1111/ejh.12515.
58. Bernard E, Tuechler H, Greenberg PL, *et al*. Molecular International Prognostic Scoring System for myelodysplastic syndromes. N Engl J Med Evid. 2022;1(7) doi:10.1056/EVIDoa2200008
59. Yang X, Zhao H, Wu H, *et al*. Analysis of gene mutation characteristics and its correlation with prognosis in participants with myelodysplastic syndromes. *Clin Chim Acta.* 2024; 554:117789. doi:10.1016/j.cca.2024.117789.
60. Hu C, Wang X. Predictive and prognostic value of gene mutations in myelodysplastic syndrome treated with hypomethylating agents: a meta-analysis. *Leuk Lymphoma.* 2022;63(10):2336-2351. doi:10.1080/10428194.2022.2070913.
61. Della Porta MG, Gallì A, Bacigalupo A, *et al*. Clinical effects of driver somatic mutations on the outcomes of participants with myelodysplastic syndromes treated with allogeneic hematopoietic stem-cell transplantation. *J Clin Oncol.* 2016;34(30):3627-3637. doi:10.1200/JCO.2016.67.3616.
62. Komrokji RS, Lanino L, Ball S, *et al*. Data-driven, harmonised classification system for myelodysplastic syndromes: a consensus paper from the International

Consortium for Myelodysplastic Syndromes. Lancet Haematol. 2024 Nov;11(11):e862-e872. 10.1016/S2352-3026(24)00251-5.

63. Itzykson R, Kosmider O, Fenaux P. Somatic mutations and epigenetic abnormalities in myelodysplastic syndromes. *Best Pract Res Clin Haematol.* 2013;26(4):355-364. doi:10.1016/j.beha.2014.01.001.
64. Sarchi M, Clough CA, Gallì A, *et al*. Distinct routes of clonal progression in SF3B1-mutant myelodysplastic syndromes. Blood Adv. 2025 Jun 24;9(12):3044-3055. 10.1182/bloodadvances.2024014965.
65. Konishi T, Sadato D, Toya T, *et al*. Impact of gene alterations on clinical outcome in young adults with myelodysplastic syndromes. Sci Rep. 2023;13(1):2641. doi:10.1038/s41598-023-29794-4.
66. Maurya N, Mohanty P, Dhangar S, *et al*. Comprehensive analysis of genetic factors predicting overall survival in myelodysplastic syndromes. Sci Rep. 2022;12(1):5925. doi:10.1038/s41598-022-09864-9.
67. Kusne Y, Xie Z, Patnaik MM. Clonal hematopoiesis: molecular and clinical implications. *Leuk Res.* 2022; 113:106787. doi:10.1016/j.leukres.2022.106787.
68. Dunn WG, McLoughlin MA, Vassiliou GS. Clonal hematopoiesis and hematological malignancy. J Clin Invest. 2024;134(19): e180065. doi:10.1172/JCI180065.
69. Zhang Q, Yim R, Lee P, *et al*. Implications of clonal hematopoiesis in hematological and non-hematological disorders. Cancers (Basel). 2024;16(23):4118. doi:10.3390/cancers16234118.
70. Gibson CJ, Steensma DP. New insights from studies of clonal hematopoiesis. Clin Cancer Res. 2018;24(19):4633-4642. doi: 10.1158/1078-0432.CCR-17-3044.
71. Osman A, Patel JL. Diagnostic challenge and clinical dilemma: the long reach of clonal hematopoiesis. Clin Chem. 2021;67(8):1062-1070. doi:10.1093/clinchem/hvab105.
72. Marnell CS, Bick A, Natarajan P. Clonal hematopoiesis of indeterminate potential (CHIP): linking somatic mutations, hematopoiesis, chronic inflammation and cardiovascular disease. J Mol Cell Cardiol. 2021; 161:98-105. doi: 10.1016/j.yjmcc.2021.07.004.
73. Kunimoto H, Nakajima H. Clonal hematopoiesis: molecular basis and clinical relevance. Leuk Res. 2020; 98:106457. doi: 10.1016/j.leukres.2020.106457.
74. Valent P. ICUS, IDUS, CHIP and CCUS: diagnostic criteria, separation from MDS and clinical implications. Pathobiology. 2019;86(1):30-38. doi:10.1159/000489042
75. Osman AEWG. When are idiopathic and clonal cytopenias of unknown significance (ICUS or CCUS)? Hematology Am Soc Hematol Educ Program. 2021;2021(1):399-404. doi:10.1182/hematology.2021000272.

76. Malcovati L, Cazzola M. The shadowlands of MDS: idiopathic cytopenias of undetermined significance (ICUS) and clonal hematopoiesis of indeterminate potential (CHIP). Hematology Am Soc Hematol Educ Program. 2015; 2015:299-307. doi:10.1182/asheducation-2015.1.299.
77. Schroeder T, Ruf L, Bernhardt A, *et al*. Distinguishing myelodysplastic syndromes (MDS) from idiopathic cytopenia of undetermined significance (ICUS): HUMARA unravels clonality in a subgroup of participants. Ann Oncol. 2010;21(11):2267-2271. doi:10.1093/annonc/mdq233.
78. Gallì A, Todisco G, Catamo E, *et al*. Relationship between clone metrics and clinical outcome in clonal cytopenia. Blood. 2021;138(11):965-976. doi:10.1182/blood.2021011323.
79. Choi EJ, Cho YU, Hur EH, *et al*. Clinical implications and genetic features of clonal cytopenia of undetermined significance compared to lower-risk myelodysplastic syndrome. Br J Haematol. 2022;198(4):703-712. doi:10.1111/bjh.18273.
80. Cargo C, Bernard E, Beinortas T, *et al*. Predicting cytopenias, progression, and survival in participants with clonal cytopenia of undetermined significance: a prospective cohort study. Lancet Haematol. 2024;11(1): e51-e61. doi:10.1016/S2352-3026(23)00340-X.
81. Kwok B, Hall JM, Witte JS, *et al*. MDS-associated somatic mutations and clonal hematopoiesis are common in idiopathic cytopenias of undetermined significance. Blood. 2015;126(21):2355-2361. doi:10.1182/blood-2015-08-667063.
82. Ferrone CK, McNaughton AJM, Rashedi I, *et al*. A lower frequency of spliceosome mutations distinguishes clonal cytopenias of undetermined significance from low-risk myelodysplastic syndromes, despite inherent similarities in genomic, laboratory, and clinical features. Mod Pathol. 2023;36(3):100068. doi: 10.1016/j.modpat.2022.100068.
83. Schanz J, Tüchler H, Solé F, *et al*. New comprehensive cytogenetic scoring system for primary myelodysplastic syndromes and oligoblastic acute myeloid leukemia after MDS derived from an international database merge. J Clin Oncol. 2012 Mar 10;30(8):820-829. 10.1200/JCO.2011.35.6394.
84. Xie Z, Komrokji R, Al Ali N, *et al*. Risk prediction for clonal cytopenia: multicenter real-world evidence. Blood. 2024;144(19):2033-2044. doi:10.1182/blood.2024024756.
85. Greenberg PL, Stone RM, Abaza Y, *et al*. Myelodysplastic syndromes, version 2.2025: featured updates to the NCCN guidelines. J Natl Compr Canc Netw. 2025;23(3):66–75. doi:10.6004/jnccn.2025.0013.

86. Arber DA, Orazi A, Hasserjian R, *et al*. The 2016 revision to the World Health Organization classification of myeloid neoplasms and acute leukemia. Blood. 2016;127(20):2391–2405. doi:10.1182/blood-2016-03-643544.
87. Hasserjian RP, Orazi A, Orfao A, *et al*. The International Consensus Classification of myelodysplastic syndromes and related entities. Virchows Arch. 2022;482(1):1–18. doi:10.1007/s00428-022-03417-1.
88. Komrokji RS, Lanino L, Ball S, *et al*. Data-driven, harmonised classification system for myelodysplastic syndromes: a consensus paper from the International Consortium for Myelodysplastic Syndromes. Lancet Haematol. 2024;11(11): e862–e872. 10.1016/S2352-3026(24)00251-5.

Correction: Lancet Haematol. 2024;11(12):e886. 10.1016/S2352-3026(24)00339-9

89. Aakash F, Gisriel SD, Zeidan AM, *et al*. Contemporary approach to the diagnosis and classification of myelodysplastic neoplasms/syndromes recommendations from the International Consortium for Myelodysplastic Neoplasms/Syndromes (MDS [icMDS]). Mod Pathol. 2024;37(12):100615. 10.1016/j.modpat.2024.100615

90. National Comprehensive Cancer Network. Myelodysplastic syndromes. NCCN Clinical Practice Guidelines in Oncology. 2026 Jan 12. Available online: https://www.nccn.org

91. Bennett JM, Catovsky D, Daniel MT, *et al*. Proposals for the classification of the myelodysplastic syndromes. Br J Haematol. 1982;51(2):189–199. doi:10.1111/j.1365-2141. 1982.tb02771. x.
92. Valcárcel D, Sanz G, Ortega M, *et al*. Use of newer prognostic indices for patients with myelodysplastic syndromes in the low and intermediate-1 risk categories: a population-based study. Lancet Haematol. 2015 Jun;2(6):e260–e266. 10.1016/S2352-3026(15)00067-8.
93. Vardiman JW, Harris NL, Brunning RD. The World Health Organization (WHO) classification of the myeloid neoplasms. Blood. 2002;100(7):2292–2302. doi:10.1182/blood-2002-04-1199.
94. Vardiman JW, Thiele J, Arber DA, *et al*. The 2008 revision of the World Health Organization (WHO) classification of myeloid neoplasms and acute leukemia: rationale and important changes. Blood. 2009;114(5):937–951. doi:10.1182/blood-2009-03-209262.
95. Greenberg P, Cox C, LeBeau MM, *et al*. International scoring system for evaluating prognosis in myelodysplastic syndromes. Blood. 1997;89(6):2079–88

96. Greenberg PL, Tuechler H, Schanz J, *et al*. Revised International Prognostic Scoring System for Myelodysplastic Syndromes. Blood. 2012;120(12):2454–65. doi:10.1182/blood-2012-03-420489.
97. Montoro J, Pomares H, Villacampa G, *et al*. Dichotomization of the new revised international prognostic scoring system for a better clinical stratification of participants with myelodysplastic syndromes. Leuk Lymphoma. 2019; 60:1522-7.
98. Pfeilstocker M, Tuechler H, Sanz G, *et al*. Time-dependent changes in mortality and transformation risk in MDS. Blood. 2016; 128:902-10.
99. Voso MT, Fenu S, Latagliata R, *et al*. Revised International Prognostic Scoring System (IPSS-R) Predicts Survival and Leukemic Evolution of Myelodysplastic Syndromes Significantly Better Than IPSS and WHO Prognostic Scoring System: Validation by the Gruppo Romano Mielodisplasie Italian Regional Database. J Clin Oncol. 2013;31(21):2671–7. doi:10.1200/JCO.2012.48.0764.
100. Bernard E, Tuechler H, Greenberg PL, *et al*. Molecular International Prognostic Scoring System for Myelodysplastic Syndromes. NEJM Evid. 2022;1(7): EVIDoa2200008. doi:10.1056/EVIDoa2200008.
101. Aguirre LE, Al Ali N, Sallman DA, *et al*. Assessment and validation of the Molecular International Prognostic Scoring System for myelodysplastic syndromes. Leukemia. 2023;37(7):1530-1539. doi:10.1038/s41375-023-01910
102. Sauta E, Robin M, Bersanelli M, *et al*. Real-world validation of Molecular International Prognostic Scoring System for myelodysplastic syndromes. J Clin Oncol. 2023;41(15):2827-2842. doi:10.1200/JCO.22.01784.
103. Lee WH, Tsai MT, Tsai CH, *et al*. Validation of the Molecular International Prognostic Scoring System in participants with myelodysplastic syndromes defined by International Consensus Classification. Blood Cancer J. 2023;13(1):120. doi:10.1038/s41408-023-00894-8.
104. Sabile JMG, Kaempf A, Tomic K, *et al*. A retrospective validation of the IPSS-M molecular score in primary and therapy-related myelodysplastic syndromes (MDS). Leuk Lymphoma. 2023;64(10):1689-1694. doi:10.1080/10428194.2023. 2232491.
105. Zamanillo I, Poza M, Ayala R, *et al*. Impact of IPSS-M implementation in real-life clinical practice. Front Oncol. 2023; 13:1199023. doi:10.3389/fonc.2023. 1199023.
106. Huang N, Song Y, Wu L, *et al*. Validation and improvement of the Molecular International Prognostic Scoring System in Chinese participants with myelodysplastic syndromes. Ann Hematol. 2025;104(1):193-206. doi:10.1007/s00277-024-06162-4.
107. Schulz F, Kellersmann C, Betz B, *et al*. Comparison of prognostication by IPSS-M, IPSS-R and AIPSS-MDS in the context of limited availability of molecular data in

daily clinical practice. Ann Hematol. 2025;10.1007/s00277-025-06570-0. doi:10.1007/s00277-025-06570-0.

108. Chernak B, Ali A, Jan A, *et al*. External validation of the Molecular International Prognostic Scoring System (IPSS-M) for myelodysplastic syndromes. J Clin Oncol. 2023;41(Suppl 16):7056. doi: 10.1200/JCO.2023.41.16_suppl.7056.
109. Kewan T, Bewersdorf JP, Gurnari C, *et al*. When to use which molecular prognostic scoring system in the management of participants with MDS? Best Pract Res Clin Haematol. 2023;36(4):101517. doi: 10.1016/j.beha.2023.101517.
110. Montoro MJ, Palomo L, Haferlach C, *et al*. Influence of TP53 gene mutations and their allelic status in myelodysplastic syndromes with isolated 5q deletion. Blood. 2024 Oct 17;144(16):1722–1731. 10.1182/blood.2024023840
111. Hellström-Lindberg ES, Kröger N. Clinical decision-making and treatment of myelodysplastic syndromes. Blood. 2023;142(26):2268–81. doi:10.1182/blood.2023020079.
112. Karel D, Valburg C, Woddor N, *et al*. Myelodysplastic neoplasms (MDS): the current and future treatment landscape. Curr Oncol. 2024;31(4):1971–93. doi:10.3390/curroncol31040148.
113. Carraway HE, Saygin C. Therapy for lower-risk MDS. *Hematology Am Soc Hematol Educ Program*. 2020;2020(1):426–33. doi:10.1182/hematology.20200001
114. Randall MP, DeZern AE. The management of low-risk myelodysplastic syndromes: current standards and recent advances. Cancer J. 2023;29(3):152–9. doi:10.1097/PPO.0000000000000655.
115. Platzbecker U, Della Porta MG, Santini V, *et al*. Efficacy and safety of luspatercept versus epoetin alfa in erythropoiesis-stimulating agent-naive, transfusion-dependent, lower-risk myelodysplastic syndromes (COMMANDS): interim analysis of a phase 3, open-label, randomised controlled trial. Lancet. 2023;402(10399):373–85. doi:10.1016/S0140-6736(23)00874-7.
116. Santini V, Consagra A. How to use luspatercept and erythropoiesis-stimulating agents in low-risk myelodysplastic syndrome. Br J Haematol. 2025;207(1):15–26. doi:10.1111/bjh.20126.
117. Grupo Español de Síndromes Mielodisplásicos (GESMD). Guía española de manejo de los síndromes mielodisplásicos de bajo riesgo. 2026.
118. Bouchla A, Papageorgiou SG, Kotsianidis I, *et al*. Real-life experience of luspatercept in transfusion-dependent lower-risk myelodysplastic syndrome participants. Br J Haematol. 2025;207(1):101–9. doi:10.1111/bjh.20102.
119. Platzbecker U, Götze KS, Kiewe P, *et al*. Long-term efficacy and safety of luspatercept for anemia treatment in participants with lower-risk myelodysplastic

syndromes: the phase II PACE-MDS study. J Clin Oncol. 2022;40(33):3800–7. doi:10.1200/JCO.21.02476.

120. Sébert M. Next-generation therapy for lower-risk MDS. Hematology Am Soc Hematol Educ Program. 2023;2023(1):59–64. doi:10.1182/hematology.2023000520.
121. Platzbecker U, Santini V, Fenaux P, *et al*. Imetelstat in participants with lower-risk myelodysplastic syndromes who have relapsed or are refractory to erythropoiesis-stimulating agents (IMerge): a multinational, randomised, double-blind, placebo-controlled, phase 3 trial. Lancet. 2024;403(10423):249–60. doi:10.1016/S0140-6736(23)01724-5.
122. Abaza Y, DeZern AE. Imetelstat: a new addition to the therapeutic landscape of lower-risk MDS. Blood. 2025;145(5):469–74. doi:10.1182/blood.2024025702.
123. Kim N, Pulte ED, Ehrlich LA, *et al*. US Food and Drug Administration approval summary: imetelstat for selected participants with low- to intermediate-1-risk myelodysplastic syndromes with transfusion-dependent anemia. J Clin Oncol. 2025; JCO2501369. doi:10.1200/JCO-25-01369
124. Mina A, Komrokji R. How I treat higher-risk MDS. Blood. 2025;145(18):2002–11. doi:10.1182/blood.2024025271.
125. Montalban-Bravo G, Garcia-Manero G. Myelodysplastic syndromes: 2018 update on diagnosis, risk-stratification and management. Am J Hematol. 2018;93(1):129–47. doi:10.1002/ajh.24930.
126. Garcia-Manero G, Chien KS, Montalban-Bravo G. Myelodysplastic syndromes: 2021 update on diagnosis, risk stratification and management. Am J Hematol. 2020;95(11):1399–420. doi:10.1002/ajh.25950.
127. Fenaux P, Platzbecker U, Adès L. How we manage adults with myelodysplastic syndrome. Br J Haematol. 2020;189(6):1016–27. doi:10.1111/bjh.16206.
128. Singh A, Carraway HE. Overview of the management of higher-risk myelodysplastic syndromes. Cancer J. 2023;29(3):160–7. doi:10.1097/PPO.0000000000000664.
129. Fenaux P, Mufti GJ, Hellström-Lindberg E, *et al*. Efficacy of azacitidine compared with that of conventional care regimens in the treatment of higher-risk myelodysplastic syndromes: a randomised, open-label, phase III study. Lancet Oncol. 2009;10(3):223–32. doi:10.1016/S1470-2045(09)70003-8.
130. Garcia-Manero G, McCloskey J, Griffiths EA, *et al*. Oral decitabine-cedazuridine versus intravenous decitabine for myelodysplastic syndromes and chronic myelomonocytic leukaemia (ASCERTAIN): a registrational, randomised,

crossover, pharmacokinetics, phase 3 study. Lancet Haematol. 2024;11(1): e15–26. doi:10.1016/S2352-3026(23)00338-1.

131. Kim N, Norsworthy KJ, Subramaniam S, *et al*. FDA approval summary: decitabine and cedazuridine tablets for myelodysplastic syndromes. Clin Cancer Res. 2022;28(16):3411–6. doi: 10.1158/1078-0432.CCR-21-4498.
132. Dhillon S. Decitabine/cedazuridine: first approval. Drugs. 2020;80(13):1373–8. doi:10.1007/s40265-020-01389-7.
133. Thota S, Oganesian A, Azab M, *et al*. Role of cedazuridine/decitabine in the management of myelodysplastic syndrome and chronic myelomonocytic leukemia. Future Oncol. 2021;17(16):2077–87. doi:10.2217/fon-2020-1210.
134. Zeidan AM, Zhao R, Epstein RS, *et al*. Oral decitabine and cedazuridine for the treatment of myelodysplastic syndromes: an integrated review of clinical, economic and patient-centered evidence. Expert Rev Anticancer Ther. 2025; doi:10.1080/14737140.2025.2544859.
135. Sekeres MA, Cutler C. How we treat higher-risk myelodysplastic syndromes. Blood. 2014;123(6):829–36. doi:10.1182/blood-2013-08-496935.
136. Ganan-Gomez I, We, Y, Starczynowski D, *et al*. (2015). Deregulation of innate immune and inflammatory signaling in myelodysplastic syndromes. *Leukemia, 29*, 1458-1469. https://doi.org/10.1038/leu.2015.69.
137. Vegivinti C, Keesari P, Veeraballi S, *et al*. (2023). Role of innate immunological/inflammatory pathways in myelodysplastic syndromes and AML: a narrative review. *Experimental Hematology & Oncology, 12*. https://doi.org/10.1186/s40164-023-00422-1.
138. Vallelonga V, Gandolfi F, Ficara F, *et al*. (2023). Emerging Insights into Molecular Mechanisms of Inflammation in Myelodysplastic Syndromes. *Biomedicines, 11*. https://doi.org/10.3390/biomedicines11102613.
139. Aggarwal N, Swerdlow SH, TenEyck SP, *et al*. Natural killer cell (NK) subsets and NK-like T-cell populations in acute myeloid leukemias and myelodysplastic syndromes. Cytometry B Clin Cytom. 2016;90(4):349–357.
140. Arellano-Ballestero H, Sabry M, Lowdell MW. A killer disarmed: Natural killer cell impairment in myelodysplastic syndrome. Cells. 2023;12(4):633. doi:10.3390/cells12040633.
141. Zhang W, Xie X, Mi H, *et al*. Abnormal populations and functions of natural killer cells in patients with myelodysplastic syndromes. Oncol Lett. 2018;15(4):5497–5504.
142. Rodríguez-Sevilla J, Ganan-Gomez I, Kumar B, *et al*. (2025). Natural killer cells' functional impairment drives the immune escape of pre-malignant clones in early-

stage myelodysplastic syndromes. *Nature Communications, 16*. https://doi.org/10.1038/s41467-025-58662-0.

143. Ganan-Gomez I, Kumar B, Sevilla J, *et al*. (2023). Mutant Natural Killer Cell Dysfunction Enables the Immune Escape of Premalignant MDS Cell Clones. *Blood*. https://doi.org/10.1182/blood-2023-184349.
144. Hejazi M, Manser AR, Fröbel J, *et al*. Impaired cytotoxicity associated with defective natural killer cell differentiation in myelodysplastic syndromes. Haematologica. 2015;100(5):643–652.
145. Rai R, Feld J, Sheppard R, *et al*. (2024). Bone Marrow-Derived CD57+ NK and NK-like T-Cells Expand in Lower-Risk MDS and Are Implicated in Driving Bone Marrow Failure. *Blood*. https://doi.org/10.1182/blood-2024-210271.
146. Feld J, Rai R, Wiatrowski K, *et al*. (2025). Bone marrow CD57+ LGL cells comprised of NK and CD8 T cells drive bone marrow failure in Myelodysplastic Syndromes. *Blood*. https://doi.org/10.1182/blood-2025-5619.
147. Mukaida N, Sasaki SI, Baba T. CCL4 Signaling in the Tumor Microenvironment. Adv Exp Med Biol. 2020; 1231:23-32. doi: 10.1007/978-3-030-36667-4_3.
148. Wang Y, Feng Z, Li L, *et al* (2025). Advances in the role of NK cells in MDS immune dysfunction and antitumor research. *Frontiers in Immunology, 16*. https://doi.org/10.3389/fimmu.2025.1511616.
149. Liu K, Liu Y, Xiong H, *et al* (2025). The Immune Regulatory Functions of CD226 and Its Implications in Immune-Mediated Diseases. *Biomolecules, 15*. https://doi.org/10.3390/biom15071007.
150. Andrade L, Smyth M, & Martinet L. (2014). DNAM-1 control of natural killer cells functions through nectin and nectin-like proteins. *Immunology and Cell Biology, 92*. https://doi.org/10.1038/icb.2013.95.
151. Tahara-Hanaoka S, Shibuya K, Onoda Y, *et al*. (2004). Functional characterization of DNAM-1 (CD226) interaction with its ligands PVR (CD155) and nectin-2 (PRR-2/CD112). *International immunology, 16 4*, 533-8. https://doi.org/10.1093/intimm/dxh059.
152. Saunders PM, Oates CVL, Hare R, *et al*. CD155 density on target cells drives divergent natural killer cell responses owing to DNAM-1 loss. J Immunol. 2025 Nov 4; vkaf293. doi:10.1093/jimmun/vkaf293.
153. Carlsten M, Norell H, Bryceson YT, *et al*. Primary human tumor cells expressing CD155 impair tumor targeting by down-regulating DNAM-1 on NK cells. J Immunol. 2009 Oct 15;183(8):4921–4930. doi:10.4049/jimmunol.0901226.

154. Du X, de Almeida P, Manieri N, *et al*. CD226 regulates natural killer cell antitumor responses via phosphorylation-mediated inactivation of transcription factor FOXO1. Proc Natl Acad Sci U S A. 2018;115(22): E11771–E11780.
155. Lu H, Zhao X, Liu L, *et al* (2025). Increased TIGIT expression correlates with impaired NK cell function in diffuse large B-cell lymphoma. *Frontiers in Oncology, 15*. https://doi.org/10.3389/fonc.2025.1551061.
156. Wang Y, Chen C, Dong F, *et al*. (2015). NK cells play a significant role in immunosurveillance at the early stage of MLL-AF9 acute myeloid leukemia via CD226/CD155 interactions. *Science China Life Sciences, 58*, 1288 - 1298. https://doi.org/10.1007/s11427-015-4968-3.
157. Ma P, & Sun W. (2023). Integrated single-cell and bulk sequencing analyses with experimental validation identify the prognostic and immunological implications of CD226 in pan-cancer. *Journal of Cancer Research and Clinical Oncology, 149*, 14597 - 14617. https://doi.org/10.1007/s00432-023-05268-y.
158. Garcia L, Gangadharan A, Banerjee P, *et al*. (2025). Overcoming CD226-related immune evasion in acute myeloid leukemia with CD38 CAR-engineered NK cells. *Cell reports, 44*, 115122 - 115122. https://doi.org/10.1016/j.celrep.2024.115122.
159. Carlsten M, Baumann BC, Simonsson M, *et al*. Reduced DNAM-1 expression on bone marrow NK cells associated with impaired killing of CD34+ blasts in myelodysplastic syndrome. Leukemia. 2010;24(9):1607-1616. doi:10.1038/leu.2010.149.
160. Kearney CJ, Ramsbottom KM, Voskoboinik I, *et al*. Loss of DNAM-1 ligand expression by acute myeloid leukemia cells renders them resistant to NK cell killing. Oncoimmunology. 2016;5(8): e1196308. doi:10.1080/2162402X.2016.1196308.
161. Kiladjian JJ, Bourgeois E, Lobe I, *et al*. Cytolytic function and survival of natural killer cells are severely altered in myelodysplastic syndromes. Leukemia. 2006;20(3):463-470. doi: 10.1038/sj.leu.2404080
162. Paolini R, Molfetta R. Dysregulation of DNAM-1-mediated NK cell anti-cancer responses in the tumor microenvironment. Cancers. 2023;15(18):4616. doi:10.3390/cancers15184616.
163. Qian S, Zhou Y, Jin Z, *et al*. Advancements in the study of the immune molecule NKp46 in immune system-related diseases. Clin Rev Allergy Immunol. 2024.
164. Chiu E, Felices M, Cichocki F, *et al*. Anti-NKG2C/IL-15/anti-CD33 killer engager directs primary and iPSC-derived NKG2C NK cells to target myeloid leukemia. Mol Ther. 2021 Dec 1;29(12):3410-3421. doi: 10.1016/j.ymthe.2021.06.018.

165. Kiladjian J, Bourgeois E, Lobe I, *et al* (2006). Cytolytic function and survival of natural killer cells are severely altered in myelodysplastic syndromes. *Leukemia, 20*, 463-470. https://doi.org/10.1038/sj.leu.2404080.

166. Barrow A, Martin C, & Colonna M (2019). The Natural Cytotoxicity Receptors in Health and Disease. *Frontiers in Immunology, 10*. https://doi.org/10.3389/fimmu.2019.00909.

167. Chen S, Zhu, H, & Jounaidi Y (2024). Comprehensive snapshots of natural killer cells functions, signaling, molecular mechanisms and clinical utilization. *Signal Transduction and Targeted Therapy, 9*. https://doi.org/10.1038/s41392-024-02005-w.

168. El-Sherbiny Y, Meade J, Holmes, T, *et al* (2007). The requirement for DNAM-1, NKG2D, and NKp46 in the natural killer cell-mediated killing of myeloma cells. *Cancer research, 67 18*, 8444-9. https://doi.org/10.1158/0008-5472.can-06-4230.

169. Bryceson YT, March ME, Ljunggren HG, *et al.* Synergy among receptors on resting NK cells for the activation of natural cytotoxicity and cytokine secretion. Blood. 2006 Jan 1;107(1):159–166. 10.1182/blood-2005-04-1351

170. Pazina T, Shemesh A, Brusilovsky M, *et al* (2017). Regulation of the Functions of Natural Cytotoxicity Receptors by Interactions with Diverse Ligands and Alterations in Splice Variant Expression. *Frontiers in Immunology, 8*. https://doi.org/10.3389/fimmu.2017.00369.

171. Liu Z, Guo Y, Huang L, *et al* (2022). Bone marrow mesenchymal stem cells regulate the dysfunction of NK cells via the T cell immunoglobulin and ITIM domain in patients with myelodysplastic syndromes. *Cell Communication and Signaling: CCS, 20*. https://doi.org/10.1186/s12964-022-00985-2.

172. Rascle P, Woolley G, Jost S, *et al*. (2023). NK cell education: Physiological and pathological influences. *Frontiers in Immunology, 14*. https://doi.org/10.3389/fimmu.2023.1087155.

173. Manser AR, Weinhold S, Uhrberg M. Human KIR repertoires: shaped by genetic diversity and evolution. Immunol Rev. 2015 Sep;267(1):178-96. doi:10.1111/imr.12316.

174. Epling-Burnette PK, Bai F, Painter JS, *et al*. Reduced natural killer (NK) function associated with high-risk myelodysplastic syndrome (MDS) correlates with increased inhibitory ligand expression for NK cells. Blood. 2007;109(11):4816-4824. doi:10.1182/blood-2006-07-035519.

175. Imširović V, Wensveen F, Polić B, *et al* (2024). Maintaining the Balance: Regulation of NK Cell Activity. *Cells, 13*. https://doi.org/10.3390/cells13171464.

176. Marangio C, Milito N, Putro E, *et al* (2025). NKG2D triggering hampers DNAM-1-mediated signaling in human NK cells. *Frontiers in Immunology, 16*. https://doi.org/10.3389/fimmu.2025.1575059.
177. Boudreau J, & Hsu K (2018). Natural Killer Cell Education and the Response to Infection and Cancer Therapy: Stay Tuned. *Trends in immunology, 39 3*, 222-239. https://doi.org/10.1016/j.it.2017.12.001.
178. Trompeter HI, Gómez-Lozano N, Santourlidis S, *et al*. Three structurally and functionally divergent kinds of promoters regulate expression of clonally distributed killer cell Ig-like receptors (KIR), of KIR2DL4, and of KIR3DL3. J Immunol. 2005;174(7):4135-4143.
179. van Bergen J, Stewart CA, van den Elsen PJ, *et al*. Structural and functional differences between the promoters of independently expressed killer cell Ig-like receptors. Eur J Immunol. 2005;35(7):2191-2199.
180. Salem MA, Varkey A, Estrada MD, *et al*. Gene regulatory programs of NK cells show that NCAM1 (CD56) and KIRs are controlled by genetically polymorphic distal regulatory elements. Eur J Immunol. 2026 Feb;56(2): e70142. doi:10.1002/eji.70142.
181. Boudreau JE, Hsu KC. Natural killer cell education in human health and disease. Curr Opin Immunol. 2018 Feb; 50:102-111. doi: 10.1016/j.coi.2017.11.003.
182. Sleiman M, Brons NH, Kaoma T, *et al*. NK cell killer Ig-like receptor repertoire acquisition and maturation are strongly modulated by HLA class I molecules. J Immunol. 2014 Mar 15;192(6):2602-10. doi:10.4049/jimmunol.1302843.
183. Serio B, Selleri C, Maciejewski JP. Impact of immunogenetic polymorphisms in bone marrow failure syndromes. Mini Rev Med Chem. 2011 Jun;11(6):544-52. doi: 10.2174/138955711795843356.
184. Zhen JX, Tang SB, Lu JW, *et al*. KIR3DL1 and HLA-Bw4 Interaction Showed a Favorable Role in Patients with Myelodysplastic Syndromes in Chinese Southern Han. Biomed Res Int. 2020; 2020:6458319.
185. Boy M, Bisio V, Zhao L, *et al*. (2023). Myelodysplastic Syndrome associated TET2 mutations affect NK cell function and genome methylation. *Nature Communications, 14*. https://doi.org/10.1038/s41467-023-36193-w.
186. Bernard E, Hasserjian R, Greenberg P, *et al*. (2023). Molecular Taxonomy of Myelodysplastic Syndromes and Its Clinical Implications. *Blood*. https://doi.org/10.1182/blood-2023-186863.
187. Meng F, Li L, Lu F, *et al*. Overexpression of TIGIT in NK and T cells contributes to tumor immune escape in myelodysplastic syndromes. Front Oncol. 2020 Aug 7; 10:1595. doi:10.3389/fonc.2020.01595.

188. Velegraki M, Stiff A, Papadaki HA, *et al*. Myeloid-derived suppressor cells: new insights into the pathogenesis and therapy of MDS. J Clin Med. 2022 Aug 21;11(16):4908. doi:10.3390/jcm11164908.
189. Chen X, Eksioglu EA, Zhou J, *et al*. Induction of myelodysplasia by myeloid-derived suppressor cells. J Clin Invest. 2013 Nov;123(11):4595-611. doi:10.1172/JCI67580.
190. Kapor S, Santibanez JF. Myeloid-derived suppressor cells and mesenchymal stem/stromal cells in myeloid malignancies. J Clin Med. 2021 Jun 24;10(13):2788. doi:10.3390/jcm10132788.
191. Kittang AO, Kordasti S, Sand KE, *et al*. Expansion of myeloid derived suppressor cells correlates with number of T regulatory cells and disease progression in myelodysplastic syndrome. Oncoimmunology. 2016;5(2): e1062208. doi:10.1080/2162402X.2015.1062208.
192. Peng X, Zhu X, Di T, *et al*. The yin-yang of immunity: immune dysregulation in myelodysplastic syndrome with different risk stratification. Front Immunol. 2022 Sep 23; 13:994053. doi:10.3389/fimmu.2022.994053.
193. Alhajahjeh A, Stahl M, Kim TK, *et al*. Contemporary understanding of myeloid-derived suppressor cells in the acute myeloid leukemia (AML) and myelodysplastic syndrome (MDS) tumor microenvironment. Expert Rev Anticancer Ther. 2025 May;25(5):435-456. doi:10.1080/14737140.2025.2483855.
194. Gunes EGG, Rosen ST, Querfeld C. The role of myeloid-derived suppressor cells in hematologic malignancies. Curr Opin Oncol. 2020 Sep;32(5):518-526. doi:10.1097/CCO.0000000000000662.
195. Bhardwaj V, Ansell SM. Modulation of T-cell function by myeloid-derived suppressor cells in hematological malignancies. Front Cell Dev Biol. 2023 Apr 5; 11:1129343. doi:10.3389/fcell.2023.1129343.
196. Wang YH, Hou HA, Lin CC, *et al*. A CIBERSORTx-based immune cell scoring system could independently predict the prognosis of patients with myelodysplastic syndromes. Blood Adv. 2021 Nov 23;5(22):4535-4548. doi:10.1182/bloodadvances.2021005141.
197. Wang YH, Lin CC, Yao CY, *et al*. Immune signatures of bone marrow cells can independently predict prognosis in patients with myelodysplastic syndrome. Br J Haematol. 2022 Jan;196(1):156-168. doi:10.1111/bjh.17837.
198. Lopes MR, Traina F, de Melo Campos P, *et al*. IL10 inversely correlates with the percentage of $CD8^+$ cells in MDS patients. Leuk Res. 2013 May;37(5):541-6. doi: 10.1016/j.leukres.2013.01.019.

199. Yaseen MM, Abuharfeil NM, Darmani H, *et al*. Mechanisms of immune suppression by myeloid-derived suppressor cells: the role of interleukin-10 as a key immunoregulatory cytokine. Open Biol. 2020 Sep;10(9):200111. doi:10.1098/rsob.200111.
200. Pardanani A, Finke C, Lasho TL, *et al*. IPSS-independent prognostic value of plasma CXCL10, IL-7 and IL-6 levels in myelodysplastic syndromes. Leukemia. 2012 Apr;26(4):693-699. doi:10.1038/leu.2011.251.
201. Warlick ED, Miller JS. Myelodysplastic syndromes: the role of the immune system in pathogenesis. Leuk Lymphoma. 2011 Nov;52(11):2045-9. doi:10.3109/10428194.2011.584002.
202. Chen L, Bian Y, Pronk E, *et al*. An inflammatory T-cell–stromal axis contributes to hematopoietic stem/progenitor cell failure and clonal evolution in human myelodysplastic syndrome. Nat Commun. 2025;16(1):10042. doi:10.1038/s41467-025-65802-z.
203. Prummel KD, Woods K, Kholmatov M, *et al*. Inflammatory stromal and T cells mediate human bone marrow niche remodeling in clonal hematopoiesis and myelodysplasia. Nat Commun. 2025;16(1):10042. doi:10.1038/s41467-025-65803-y.
204. Belizaire R, Wong WJ, Robinette ML, *et al*. Clonal haematopoiesis and dysregulation of the immune system. Nat Rev Immunol. 2023 Sep;23(9):595-610. doi:10.1038/s41577-023-00843-3.
205. Xiong B, Nie Y, Yu Y, *et al*. Reduced miR-16 levels are associated with VEGF upregulation in high-risk myelodysplastic syndromes. J Cancer. 2021 Jan 30;12(7):1967-1977. doi:10.7150/jca.52455.
206. Wimazal F, Krauth MT, Vales A, *et al*. Immunohistochemical detection of vascular endothelial growth factor (VEGF) in the bone marrow in patients with myelodysplastic syndromes: correlation between VEGF expression and the FAB category. Leuk Lymphoma. 2006 Mar;47(3):451-460. doi:10.1080/10428190500353083.
207. Albakri, M. (2025). TP53-mutated MDS and AML: immune dysregulation, tumor microenvironment, and emerging therapeutic strategies. *Frontiers in Oncology, 15*. https://doi.org/10.3389/fonc.2025.1655486.
208. Gurnari C, Durmaz A, Kroger B, *et al*. (2023). Somatic and Germline HLA Determinants of Immune Surveillance and Escape in Myelodysplastic Syndromes. *Blood*. https://doi.org/10.1182/blood-2023-178890.
209. Rodríguez-Sevilla J, & Colla S (2024). T cell dysfunctions in myelodysplastic syndromes. *Blood*. https://doi.org/10.1182/blood.2023023166.

210. Majcherek M, Przeorski K, Mroczkowska-Bękarciak A, *et al*. (2025). Integrating Molecular Alterations with Immunophenotype and Clinical Characteristics in Myelodysplastic Syndromes: A Single-Center Study. *International Journal of Molecular Sciences, 26*. https://doi.org/10.3390/ijms26157382.
211. Gianelli U, Fracchiolla NS, Bucciarelli P, *et al*. High levels of vascular endothelial growth factor protein expression are associated with an increased risk of transfusion dependence in myelodysplastic syndromes. Am J Clin Pathol. 2013 Mar;139(3):380-387. doi:10.1309/AJCP5O3YBKTGGWNQ.
212. Kalitin N, Dudina G, Kostritsa N, *et al*. Evaluation of VEGF and VEGFR gene expression as prognostic markers in low and intermediate-1 risk patients with myelodysplastic syndromes. Oncol Lett. 2023 Mar;25(3):95. doi:10.3892/ol.2023.13681.
213. Invernizzi R, Travaglino E, Della Porta MG, *et al*. Vascular endothelial growth factor overexpression in myelodysplastic syndrome bone marrow cells: biological and clinical implications. Leuk Lymphoma. 2017 Jul;58(7):1711-1720. doi:10.1080/10428194.2016.1262030.
214. Menssen, A., & Walter, M. (2020). Genetics of Progression from MDS to Secondary Leukemia. *Blood*. https://doi.org/10.1182/blood.2019000942.
215. Ogawa, S. (2019). Genetics of MDS. *Blood, 133 10*, 1049-1059. https://doi.org/10.1182/blood-2018-10-844621.
216. Montes P, Bernal M, Campo L, *et al*. (2019). Tumor genetic alterations and features of the immune microenvironment drive myelodysplastic syndrome escape and progression. *Cancer Immunology, Immunotherapy, 68*, 2015 - 2027. https://doi.org/10.1007/s00262-019-02420-x.
217. Sallman D, McLemore A, Aldrich A, *et al*. (2020). TP53 mutations in myelodysplastic syndromes and secondary AML confer an immunosuppressive phenotype. *Blood*. https://doi.org/10.1182/blood.2020006158.
218. Lindsley RC, Saber W, Mar BG, *et al*. Prognostic mutations in myelodysplastic syndrome after stem-cell transplantation. N Engl J Med. 2017; 376:536-47.
219. Hou HA, Tsai CH, Lin CC, *et al*. Incorporation of mutations in five genes in the revised International Prognostic Scoring System can improve risk stratification in the patients with myelodysplastic syndrome. Blood Cancer J. 2018; 8:39.
220. Grob T, Al Hinai ASA, Sanders MA, *et al*. Molecular characterization of mutant TP53 acute myeloid leukemia and high-risk myelodysplastic syndrome. Blood. 2022; 139:2347-54.

221. Comont T, Treiner E, Vergez F. From immune dysregulations to therapeutic perspectives in myelodysplastic syndromes: a review. Diagnostics (Basel). 2021; 11:1080.
222. Khan M, Arooj S, Wang H. NK cell-based immune checkpoint inhibition. Front Immunol. 2020; 11:167.
223. Jia H, Yang H, Xiong H, *et al*. NK cell exhaustion in the tumor microenvironment. Front Immunol. 2023; 14:1078390.
224. Moiseev I, Tcvetkov NY, Epifanovskaya OS, *et al*. Landscape of alterations in the checkpoint system in myelodysplastic syndrome and implications for prognosis. PLoS One. 2022;17: e0278970.
225. Dębska-Zielkowska J, Moszkowska G, Zieliński M, *et al*. KIR receptors as key regulators of NK cells activity in health and disease. Cells. 2021; 10:1777.
226. Schetelig J, Baldauf H, Koster L, *et al*. Haplotype motif-based models for KIR-genotype informed selection of hematopoietic cell donors fail to predict outcome of patients with myelodysplastic syndromes or secondary acute myeloid leukemia. Front Immunol. 2021; 11:608278.

10. APPENDICES

10.1 Funding

This work was supported by research funding from the Instituto de Salud Carlos III awarded to the principal investigator Dr. David Valcárcel (Reference: PI17/01088).

10.2 Supplementary Tables

Supplementary Table 1. Lymphocyte subpopulations.

Lymphocyte T sub-populations	
T cells	$CD45^+$ $CD3^+$
$CD4^+$ T cells	$CD45^+$ $CD3^+$ $CD4^+$
$CD8^+$ T cells	$CD45^+$ $CD3^+$ $CD8^+$
Naive T cells	CCR7+ CD45RA+ CD27++ CD28 ++
Central Memory T cells	CCR7+, CD45RA-, CD27+++, CD28+++
Effector Memory T cells	CCR7-, CD45RA-, CD27+, CD28-
Effector T cells	CCR7-, CD45RA+, CD27-, CD28-
T cell $PD1^+$	$CD45^+$ $CD3^+$ $CD4^+$/$CD8^+$ $PD1^+$
Treg	CD3+ CD4+ CD25++ CD127+/low
Th1	CD3+ CD4+ CXCR3+ CCR6-
Th2	CD3+ CD4+ CXCR3- CCR6-
Th17	CD3+ CD4+ CXCR3- CCR6+

This table provides a comprehensive overview of the diverse T lymphocytic populations under investigation and their characterization, performed by flow cytometry.

CD, cluster of differentiation; CCR7, C–C chemokine receptor type 7; CXCR3, C–X–C chemokine receptor type 3; CCR6, C–C chemokine receptor type 6; PD-1, programmed cell death protein 1; Treg, regulatory T cells; Th, T helper cells; RA, CD45RA isoform of leukocyte common antigen; TCR, T-cell receptor; FCM, flow cytometry.

Supplementary Table 2. Multiparametric flow cytometry panels used for immune cell profiling.

A. Panel: Myelodysplasia diagnostic

FIT-C	PE	ECD	PC5.5	PC7	APC	APC-A700	APC-A750	PB	KO
CD11b	CD15	CD16	CD117	CD10	CD13	CD34	CD33	HLA-DR	CD45
CD35	CD300e	CD64	CD117	CD14	CD7	CD34	CD56	HLA-DR	CD45
CD71	CD105	CD38	CD117	CD235a	CD36	CD34	CD33	HLA-DR	CD45

B. Panel: T-cell and NK identification

PB	KO	FITC	PE	ECD	PC5.5	PC7	APC	APC-A700	APC-A750
CD57	CD45	CD8	CD56	CD3	CD4	TCR*gd*	CD16	CD19	CD27
	CD45	CD127	CD183	CD3	CD4	CD196	CD25		
CD57	CD45	CD45RA	CD197	CD28	CD279	CD27	CD4	CD8	CD3

* Duraclone® IM T Cell Subsets

C. Panel: NK receptor repertoire

FIT-C	PE	ECD	PC5.5	PC7	APC	APC -A700	APC -A750	PB	KO
Control	Control	Control	Control	Control	Control	Control	Control	Control	Control
CD34	CD94	CD3	CD244	CD159a	CD133	CD56	CD117	HLA-DR	CD45
CD158b	CD158e1	CD3	CD158b1/b2,j		CD158e1/e2	CD56	CD16		CD45
	TIGIT	CD3		CD158a,h	CD158a	CD56	CD16		CD45
	CD335 NKp46	CD3	CD244		CD158i	CD56	CD16	CD337 NKp30	CD45
	CD159c NKG2C	CD3		CD159a NKG2A	CD314 NKG2D	CD56	CD16	CD336 NKp44	CD45
CD95	CD300a Irp60	CD3		CD279 PD1	CD226 DNAM	CD56	CD161		CD45
	Granzyma B	CD3				CD56	CD16	Perforina	CD45

D. Panel: NK Ligand expression

FIT-C	PE	ECD	PC5.5	PC7	APC	APC-A700	APC-A750	PB	KO
HLA-ABC	CD155	CD13	CD117	CD274	MIC A/B	CD34	CD33	HLA-DR	CD45

E. Panel: Myeloid-derived suppressor cells (MDSC)

FIT-C	PE	ECD	PC5.5	PC7	APC	APC-A700	APC-A750	PB	KO
CD11b	CD15	CD19 CD3 CD56	CD117	CD14	CD16	CD34	CD33	HLA-DR	CD45

Multiparametric flow cytometry antibody panels used for immune phenotyping. The table summarizes fluorochrome–antibody combinations and clones, used for characterization of myelodysplastic bone marrow populations, NK-cell ligands, lymphocyte subsets, myeloid-derived suppressor cells, and NK-cell receptor repertoire.

FITC, fluorescein isothiocyanate; PE, phycoerythrin; ECD, energy-coupled dye; PC5.5, phycoerythrin–cyanine 5.5; PC7, phycoerythrin–cyanine 7; APC, allophycocyanin; APC-A700, allophycocyanin–Alexa Fluor 700; APC-A750, allophycocyanin–Alexa Fluor 750; PB, Pacific Blue; KO, Krome Orange; HLA, human leukocyte antigen; TCRγδ, T-cell receptor gamma/delta; NK, natural killer; MDSC, myeloid-derived suppressor cell; PD-1, programmed cell death protein 1 (CD279); DNAM-1, DNAX accessory molecule 1 (CD226); NKG2A/C/D, natural killer group 2 receptor family members A, C, and D; NKp30, NKp44, NKp46, natural cytotoxicity receptors 3, 2, and 1; MIC A/B, MHC class I polypeptide-related sequence A and B; Irp60, inhibitory receptor protein 60.

Supplementary Table 3. Detailed cytogenetic and molecular risk stratification of MDS patients.

Risk classification	Category	n (%)
IPSS-R cytogenetic risk (N= 50)	Very good	4 (8.0)
	Good	32 (64.0)
	Intermediate	9 (18.0)
	Poor	0 (0.0)
	Very poor	5 (10.0)
IPSS-M risk category (N= 44) *	Very low	5 (11.4)
	Low	15 (34.1)
	Moderate-low	4 (9.1)
	Moderate-high	7 (15.9)
	High	4 (9.1)
	Very high	9 (20.5)
	Low risk (VL + L + ML)	**24 (54.5)**
	High risk (MH + H + VH)	**20 (45.5)**

* IPSS-M was available for 44 evaluable MDS patients

Data are presented as number of patients and percentage of the total cohort. For IPSS-M, risk groups were also aggregated into low-risk (very low, low, and moderate-low) and high-risk (moderate-high, high, and very high) categories. IPSS-M classification was available for 44 evaluable patients.

MDS, myelodysplastic syndromes; IPSS-R, Revised International Prognostic Scoring System; IPSS-M, Molecular International Prognostic Scoring System; VL, very low; L, low; ML, moderate-low; MH, moderate-high; H, high; VH, very high.

Supplementary Table 4. Expression of NK cell ligands on hematopoietic precursors and myeloid cells in ICUS, MDS, and healthy donors.

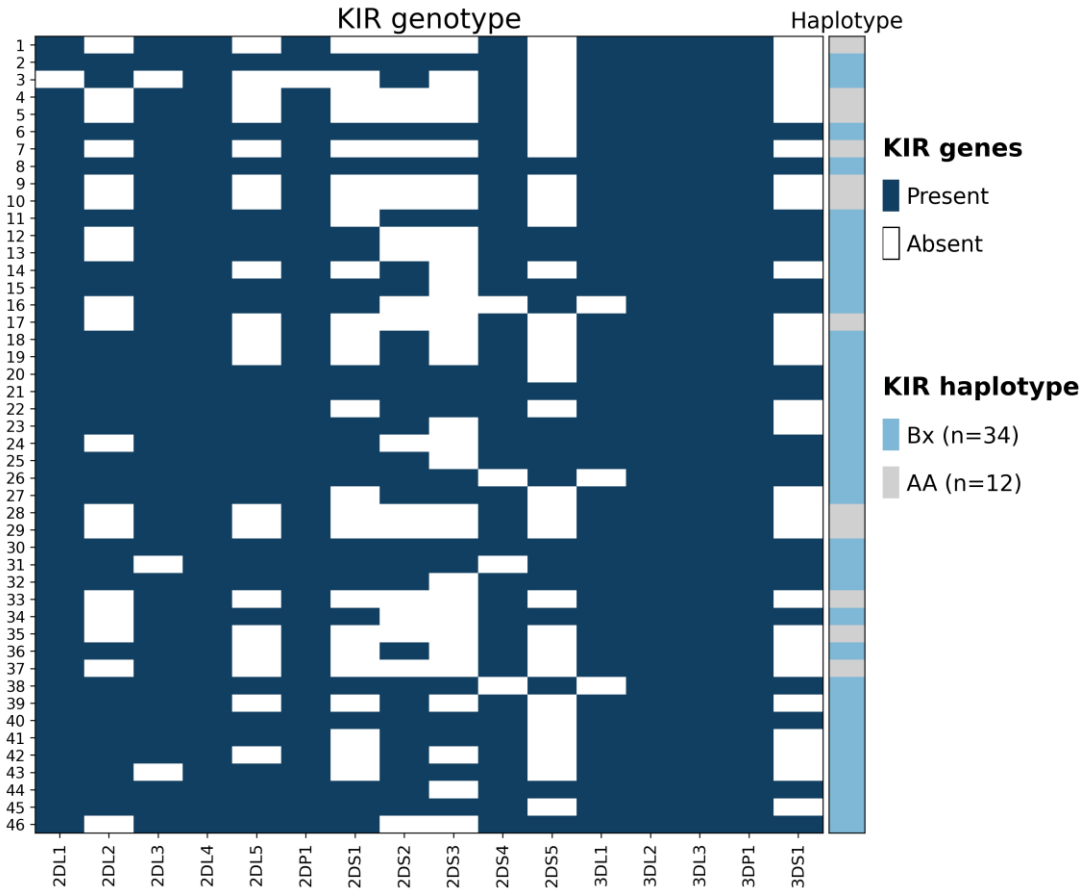
Ligand	ICUS median (IQR)	MDS median (IQR)	HD median (IQR)	p (ICUS vs MDS	p (ICUS vs HD)	p (MDS vs HD)
Pre–HLA	99.54 (98.00–99.93)	100.00 (96.53–100.00)	97.65 (93.04–99.47)	0.08	0.12	0.14
Pre–CD155	0.00 (0.00–0.01)	0.00 (0.00–0.00)	0.00 (0.00–0.02)	0.57	0.66	0.51
Pre–MICA/B	0.70 (0.00–7.54)	0.00 (0.00–0.00)	1.21 (0.54–4.83)	0.001	0.47	0.0006
Pre–CD274 (PD-L1)	0.32 (0.00–1.22)	0.00 (0.00–0.00)	0.74 (0.10–1.20)	0.04	0.54	0.04
Mon–HLA	99.28 (92.52–99.94)	99.97 (99.94–99.99)	97.11 (92.79–99.22)	0.008	0.36	0.01
Mon–CD155	0.01 (0.00–0.02)	0.00 (0.00–0.02)	0.03 (0.01–0.04)	0.41	0.18	0.11
Mon–MICA/B	0.78 (0.05–1.61)	0.00 (0.00–0.00)	0.88 (0.29–1.77)	0.002	0.59	0.004
Mon–CD274(PD-L1)	0.28 (0.04–0.93)	0.00 (0.00–0.00)	0.89 (0.35–1.27)	0.02	0.17	0.03
Gra–HLA	99.00 (92.06–99.67)	99.79 (98.78–99.96)	97.11 (95.16–99.68)	0.05	0.78	0.06
Gra–CD155	0.01 (0.00–0.03)	0.00 (0.00–0.00)	0.01 (0.01–0.03)	0.05	0.24	0.01

Gra–MICA/B	0.25 (0.02–0.66)	0.00 (0.00–0.00)	0.33 (0.14–1.08)	0.0005	0.49	0.0008
Gra–CD274 (PD-L1)	0.12 (0.00–0.47)	0.00 (0.00–0.00)	0.56 (0.08–0.97)	0.01	0.13	0.003

Comparison of the expression of NK cell ligands on hematopoietic precursors, monocytes, and granulocytes among patients with ICUS, MDS, and HD. Data are presented as median values with IQR. P values correspond to pairwise comparisons between groups.

ICUS, idiopathic cytopenia of undetermined significance; MDS, myelodysplastic syndromes; HD, healthy donors; IQR, interquartile range; HLA, human leukocyte antigen; MICA/B, MHC class I polypeptide-related sequence A and B; PD-L1, programmed death-ligand 1 (CD274).

Supplementary Table 5. Distribution of KIR genotypes in the study cohort.



Heatmap illustrating the presence or absence of killer-cell immunoglobulin-like receptor (KIR) genes across individual patients in the study cohort (n = 46). Rows correspond to individual patients, and columns represent specific KIR genes. Gene presence is indicated in dark blue, whereas absence is shown in white. The annotation bar on the right indicates KIR haplotype classification, distinguishing Bx haplotypes (blue; n = 34) from AA haplotypes (grey; n = 12).

KIR, killer-cell immunoglobulin-like receptor; AA, haplotype A homozygous genotype; Bx, haplotype B–containing genotype.

Supplementary Table 6. NK receptor expression according to IPSS-R 3.5 risk.

Parameter		LR-MDS (≤ 3.5)	HR-MDS (>3.5)	*p* value
NKG2A	Median IQR	75.60 (61.80–93.46)	69.28 (49.70–89.18)	0.41
TIGIT	Median IQR	24.46 (5.41–56.44)	56.02 (31.98–68.16)	0.07
PD-1	Median IQR	0.07 (0.00–0.42)	0.01 (0.00–1.70)	0.84
IRp60	Median IQR	95.10 (88.47–97.70)	95.72 (85.02–98.45)	0.68
KIR2DL1	Median IQR	8.41 (2.95–23.13)	20.70 (4.34–40.67)	0.12
KIR2DL2/KIR2DL3	Median IQR	18.49 (4.58–40.83)	32.51 (19.06–45.39)	0.31
KIR3DL1	Median IQR	2.82 (0.00–12.12)	3.69 (0.05–10.40)	0.62
NKp46	Median IQR	55.36 (14.27–71.94)	29.48 (0.00–75.46)	0.30
NKp30	Median IQR	47.58 (32.12–65.03)	35.36 (21.52–48.54)	0.18
NKp44	Median IQR	0.10 (0.00–0.42)	0.28 (0.10–0.44)	0.21
NKG2D	Median IQR	95.81 (90.66–97.03)	96.05 (91.79–98.64)	0.52
NKG2C	Median IQR	4.34 (1.29–17.04)	5.34 (3.82–17.19)	0.27
DNAM-1	Median IQR	95.46 (90.02–98.27)	96.19 (89.14–98.66)	0.78
KIR2DS1	Median IQR	0.00 (0.00–0.00)	0.00 (0.00–0.00)	0.47
KIR2DS2	Median IQR	2.21 (0.33–7.42)	13.22 (5.86–24.25)	0.0006
KIR2DS4	Median IQR	14.00 (0.00–89.41)	36.23 (10.66–82.26)	0.35

KIR3DS1	Median IQR	0.00 (0.00–0.07)	0.05 (0.00–7.10)	0.07
Perforin	Median IQR	47.50 (12.15–74.20)	29.88 (14.25–55.47)	0.60
Granzyme	Median IQR	35.10 (17.05–68.87)	37.44 (25.19–65.90)	0.87

Median expression (%) and IQR of NK receptors and cytotoxic molecules. P values indicate comparisons between LR-MDS (≤3.5) and HR-MDS (>3.5) using non-parametric statistical tests. NK, natural killer; MDS, myelodysplastic syndromes; LR-MDS, low-risk myelodysplastic syndromes; HR-MDS, high-risk myelodysplastic syndromes; IPSS-R, Revised International Prognostic Scoring System; IQR, interquartile range; NKp46, natural cytotoxicity receptor 1; NKp30, natural cytotoxicity receptor 3; NKp44, natural cytotoxicity receptor 2; NKG2A/C/D, natural killer group 2 members A, C, and D; DNAM-1, DNAX accessory molecule-1; TIGIT, T cell immunoreceptor with Ig and ITIM domains; PD-1, programmed cell death protein 1; KIR, killer cell immunoglobulin-like receptor.

Supplementary Table 7. Cytokine concentrations in LR-MDS and HR-MDS BM samples.

Cytokine	LR-MDS median (pg/mL)	LR-MDS IQR (25–75%)	HR-MDS median (pg/mL)	HR-MDS IQR (25–75%)	Δ median (HR–LR)	P value	FDR q value
EGF	0	0.00–28.91	0	0.00–28.91	0.00	0.99	1.00
FGF-2	0	0.00–2.73	0	0.00–2.73	0.00	0.79	0.99
GM-CSF	0	0.00–14.13	0	0.00–14.13	0.00	0.90	1.00
HGF	593.925	189.51–1158.29	399.465	215.85–671.63	-194.46	0.48	0.99
VEGF-A	491.23	361.36–721.12	459.2155268	196.75–945.12	-32.01	0.75	0.99
IFN-a	0	0.00–0.50	0	0.00–0.50	0.00	0.66	0.99
IFN-g	0	0.00–8.56	0	0.00–8.56	0.00	0.66	0.99
IL-1a	0.31	0.00–1.73	0.62	0.00–0.62	0.31	1.00	1.00
IL-1b	0.685	0.00–2.52	1.995	0.64–2.52	1.31	0.42	0.99
IL-6	6.445	0.00–9.21	6.85	0.00–9.21	0.41	0.87	1.00
TNF-a	0	0.00–6.30	0	0.00–6.30	0.00	0.66	0.99
IL-1RA	156.165	0.00–4694.91	139.94	9.10–1125.89	-16.23	0.69	0.99
IL-10	1.269659823	1.12–1.41	1.335	1.08–1.67	0.07	0.77	0.99
IL-2	0	0.00–7.61	0	0.00–7.61	0.00	0.74	0.99
IL-3	10.25	0.00–110.95	13.835	0.00–20.50	3.59	0.47	0.99
IL-4	0	0.00–10.76	0	0.00–10.76	0.00	0.56	0.99
IL-5	0	0.00–10.62	0	0.00–10.62	0.00	1.00	1.00
IL-7	0	0.00–1.00	0	0.00–0.93	0.00	0.71	0.99
IL-9	0	0.00–7.87	0	0.00–8.25	0.00	0.64	0.99
IL-12	0	0.00–9.00	1.89	0.00–9.00	1.89	0.39	0.99
IL-13	0.995	0.00–3.70	0	0.00–3.70	-1.00	0.81	0.99
IL-15	3.54	0.00–3.70	3.7	1.38–3.75	0.16	0.33	0.99

IL-17A(CTLA-8)	0	0.00–2.30	0	0.00–2.30	0.00	0.66	0.99
IL-22	0	0.00–21.14	15.55	0.00–21.14	15.55	0.81	0.99
Eotaxin(CCL11)	72.055	36.51–113.00	49.875	37.73–68.63	-22.18	0.21	0.99
IL-8	3.61	0.00–7.32	3.51	0.21–3.61	-0.10	0.80	0.99
IP-10(CXCL10)	39.985	20.57–66.29	53.66574504	33.11–90.77	13.68	0.20	0.99
MCP-1(CCL2)	77.975	29.45–111.55	73.33750408	14.27–118.87	-4.64	0.71	0.99
MIG(CXCL9)	34	1.19–106.75	23.48595534	11.31–42.00	-10.51	0.57	0.99
MIP-1a (CCL3)	10.425	4.68–13.63	9.26	3.70–16.46	-1.17	0.97	1.00
MIP-1b(CCL4)	11.6	0.00–55.61	11.6	4.82–55.20	0.00	0.57	0.99

Median cytokine concentrations (pg/mL) and IQR in BM supernatant samples from LR-MDS and HR-MDS MDS according to the IPSS-R 3.5 cut-off. Δ median represents the difference between HR-MDS and LR-MDS medians. P values were calculated using non-parametric tests and adjusted for multiple comparisons using the false discovery rate (FDR).

LR-MDS, low-risk myelodysplastic syndromes; HR-MDS, high-risk myelodysplastic syndromes; IQR, interquartile range; FDR, false discovery rate; IL, interleukin; IFN, interferon; TNF-α, tumor necrosis factor alpha; EGF, epidermal growth factor; FGF-2, fibroblast growth factor 2; GM-CSF, granulocyte-macrophage colony-stimulating factor; HGF, hepatocyte growth factor; VEGF-A, vascular endothelial growth factor A; Eotaxin (CCL11), eosinophil chemotactic protein; IP-10 (CXCL10), interferon gamma-induced protein 10; MCP-1 (CCL2), monocyte chemoattractant protein-1; MIG (CXCL9), monokine induced by interferon gamma; MIP-1α (CCL3), macrophage inflammatory protein-1 alpha; MIP-1β (CCL4), macrophage inflammatory protein-1 beta.

Supplementary Table 8. Immune cell subsets and soluble mediators according to mutational status in MDS patients.

Variable		Mut	NoMut	p	Variable		Mut	NoMut	p	Variable		Mut	NoMut	p
EGF	Median	0	0	0.13	**IL-9**	Median	0	0	0.09	**PD1^{+}CD4^{+} T cells**	Median	21.91	34.08	0.14
	IQR	(0 -	(0 -			IQR	(0 -	(0 - 0)			IQR	(16.12	(26.42	
Eotaxin	Median	59.73	43.03	0.56	**IP-10**	Median	53.66	21.28	0.08	**Naïve CD8^{+} T cells**	Median	2.49	9.65	0.01
	IQR	(36.52	(23.91			IQR	(22.42	11.08 -			IQR	(0.87–	(5.17–	
FGF	Median	0	0	0.28	**VEGF-A**	Median	462.6	586	0.37	**Memory CD8^{+} T cells**	Median	3.0	12.32	0.05
	IQR	(0 -	(0 -			IQR	(306.3	(309.9			IQR	1.54–	6.53–	
G-CSF	Median	0	0	0.99	**CD56^{dim}CD16^{bright}**	Median	13.86	85.48	0.003	**Effector Memory CD8^{+} T cells**	Median	5.5	16.57	0.004
	IQR	(0 - 0)	(0 - 0)			IQR	7.02–	82.26–			IQR	(4.19 -	(14.05	
HGF	Median	334.1	529.2	0.88	**CD56^{neg}CD16^{bright}**	Median	0.96	9.77	0.01	**Effector CD8^{+} T cells**	Median	15.46	42.5	0.01
	IQR	(163.6	(179.6			IQR	0.17–	6.29–			IQR	(6.98 -	(30.27	
IFN-α	Median	0	0	0.12	**CD56^{+}CD16^{neg}**	Median	1	2.69	0.66	**CD57^{+}CD8^{+} T cells**	Median	10.6	28.53	0.008
	IQR	(0 -	(0 - 0)			IQR	(0.33 -	(2.082			IQR	5.24–	22.86–	
IFN-γ	Median	0	0	0.12	**Naïve CD4^{+} T cells**	Median	18.55	26.08	0.28	**PD1^{+}CD8^{+} T cells**	Median	12.61	23.64	0.09
	IQR	(0 -	(0 - 0)			IQR	(10.97	(14.62			IQR	(7.4 -	(22.02	
TNF-α	Median	0	0	0.12	**Memory CD4^{+} T cells**	Median	22.35	55.9	0.002	**Tregs**	Median	3.36	2.785	0.29
	IQR	(0 -	(0 - 0)			IQR	(16.56	(51.96			IQR	(2.46 -	(1.86 -	
IL-1β	Median	2.445	0.685	0.87	**Effector Memory CD4^{+} T cells**	Median	7.72	13.67	0.10	**Th1**	Median	13.32	13.32	0.29
	IQR	(0 -	(0.16 -			IQR	(4.235	(11.1 -			IQR	(10.32	(11.86	
IL-10	Median	1.325	1.135	0.30	**Effector CD4^{+} T cells**	Median	0.64	0.415	0.24	**Th2**	Median	22.58	17.04	0.29
	IQR	(1.122	(1.028			IQR	(0.365	(0.19 -			IQR	(14.07-	(14.54-	
IL-8	Median	3.61	1.67	0.41	**CD57^{+}CD4^{+} T cells**	Median	2.98	3.28	0.67	**Th17**	Median	5.14	5.15	0.79
	IQR	(0 -	(0 -			IQR	(1.155	(2.052			IQR	(3.51-	(3.23-	

Comparison of circulating cytokines, chemokines, growth factors, and immune cell subsets between patients harboring at least one somatic mutation (Mut) and those without detectable mutations (NoMut). Data is presented as median values and IQR. Percentages represent the proportion of each immune subset within total lymphocytes, whereas cytokine and growth factor values correspond to measured circulating levels. P values were calculated using the Mann–Whitney U test.

MDS, myelodysplastic syndromes; Mut, patients with at least one somatic mutation (MDS ^{Mut}); NoMut, patients without detectable mutations (MDS ^{NoMut}); NK, natural killer; Tregs, regulatory T cells; IQR, interquartile range; EGF, epidermal growth factor; FGF, fibroblast growth factor; VEGF-A, vascular endothelial growth factor A; G-CSF, granulocyte colony-stimulating factor; HGF, hepatocyte growth factor; IFN-α, interferon alpha; IFN-γ, interferon gamma; TNF-α, tumor necrosis factor alpha; IL, interleukin; IP-10, interferon gamma-induced protein 10 (CXCL10); PD-1, programmed cell death protein 1.

Supplementary Table 9. Immune cell subsets, NK receptors, and circulating cytokines in MDS^{Mut} versus CCUS.

A. Immune cell subsets

Variable	MDS^{Mut} (n=44) Median	IQR	CCUS (n=7) Median	IQR	p value	FDR (BH)
Mature NK ($CD56^{dim}CD16^{bright}$)	11.57	(6.97–32.23)	70.88	(31.25–82.66)	0.19	0.48
Inhibitory NK ($CD56^{neg}CD16^{bright}$)	1.00	(0.19–2.04)	4.71	(1.30–19.82)	0.12	0.40
Immature NK ($CD56^{+}CD16^{neg}$)	0.83	(0.31–4.06)	4.21	(2.50–9.76)	0.02	0.23
$CD3^{+}CD4^{+}$ T cells	45.95	(33.25–52.19)	44.49	(36.42–53.50)	0.79	0.88
$CD3^{+}CD8^{+}$ T cells	22.23	(15.28–29.50)	22.01	(19.25–26.54)	0.85	0.91
$CD4^{+}$ naïve T cells	18.16	(9.71–23.40)	24.61	(13.89–26.24)	0.32	0.58
$CD4^{+}$ memory T cells	22.19	(16.81–36.33)	36.15	(22.28–44.89)	0.34	0.58
$CD4^{+}$ effector memory T cells	7.58	(5.74–10.46)	11.78	(6.38–16.48)	0.44	0.64
$CD4^{+}$ effector T cells	0.61	(0.30–1.42)	0.56	(0.53–6.22)	0.72	0.84
$CD4^{+}CD57^{+}$ T cells	2.58	(1.00–5.38)	4.83	(4.49–6.96)	0.20	0.48
$CD4^{+}PD1^{+}$ T cells	22.44	(15.44–33.11)	54.80	(51.61–57.91)	0.01	0.18
$CD8^{+}$ naïve T cells	2.67	(1.12–4.95)	3.78	(3.58–7.66)	0.30	0.57
$CD8^{+}$ memory T cells	3.05	(1.62–5.80)	7.43	(3.56–9.78)	0.27	0.56
$CD8^{+}$ effector memory T cells	5.41	(3.89–9.88)	5.50	(4.97–8.42)	0.60	0.75
$CD8^{+}$ effector T cells	14.29	(7.18–19.57)	46.58	(7.33–52.42)	0.40	0.61
$CD8^{+}CD57^{+}$ T cells	10.68	(5.25–17.86)	26.89	(7.07–30.52)	0.48	0.67
$CD8^{+}PD1^{+}$ T cells	12.34	(6.50–17.49)	31.20	(16.94–43.89)	0.06	0.31
Tregs	3.33	(2.26–4.41)	4.40	(4.18–4.58)	0.11	0.38
Th1	13.24	(10.30–15.22)	18.78	(15.06–19.41)	0.03	0.23
Th2	23.41	(14.24–33.24)	17.50	(11.37–21.26)	0.09	0.37

Th17	5.07	(3.23–6.63)	5.34	(4.46–6.70)	0.52	0.69
Th1-17	3.67	(1.78–5.84)	5.24	(5.00–6.06)	0.11	0.38
Gr-MDSCs	0.11	(0.01–0.66)	0.04	(0.02–0.15)	0.59	0.75
Mo-MDSCs	0.55	(0.12–1.11)	0.14	(0.09–0.18)	0.04	0.24

B. NK receptor expression

Variable	MDSMut Median (%)	IQR	CCUS Median (%)	IQR	p value	FDR
KIR2DL1	9.81	(2.83–26.22)	9.00	(4.58–36.38)	0.77	0.88
KIR2DL2/KIR2DL3	23.59	(4.26–45.00)	14.83	(12.63–28.32)	0.48	0.67
KIR3DL1	3.10	(0.01–11.03)	4.51	(0.00–18.44)	0.91	0.92
NKp46	48.86	(0.11–74.78)	20.44	(11.79–53.02)	0.63	0.75
NKp30	44.50	(23.86–60.56)	47.54	(29.32–58.98)	0.92	0.92
NKp44	0.19	(0.00–0.43)	0.00	(0.00–0.32)	0.28	0.56
NKG2D	95.81	(90.88–98.38)	90.64	(79.02–96.08)	0.09	0.37
NKG2C	5.22	(1.93–18.22)	7.37	(0.00–11.27)	0.55	0.71
DNAM-1	95.46	(88.97–98.67)	84.88	(63.85–89.76)	0.03	0.23
KIR2DS1	0	(0–0)	0	(0–0)	0.37	0.61
KIR2DS4	23.95	(0.30–85.72)	0	(0–14.88)	0.15	0.46
KIR3DS1	0	(0–0.33)	0	(0–0)	0.20	0.48
Perforin	38	(15.90–59.88)	42.65	(38.77–50.80)	0.42	0.63
Granzyme	35.10	(17.44–67.39)	37.82	(26.50–55.95)	0.61	0.75
CD94/NKG2A	70.74	(51.62–91.98)	79.08	(56.31–84.17)	0.84	0.91
TIGIT	47.72	(20.29–66.05)	35.97	(17.65–48.38)	0.45	0.65
PD-1	0.04	(0–0.48)	0	(0–0)	0.03	0.23

IRp60	95.53	(89.67–98.29)	86.85	(81.65–97.62)	0.62	0.75

C. Circulating cytokines and growth factor

Variable	MDSMut Median (pg/mL)	IQR	CCUS Median (pg/mL)	IQR	p value	FDR
EGF	0	(0–28.91)	14.46	(0–28.91)	0.626	0.674
Eotaxin	57.85	(34.2–98.05)	72.45	(48.82–85.41)	0.555	0.648
FGF	0	(0–2.73)	2.73	(0.68–2.73)	0.275	0.648
G-CSF	0	(0–0)	0	(0–0)	0.329	0.648
HGF	440.6	(189.9–949.4)	150	(85.32–211.4)	0.064	0.487
IFN-α	0	(0–0.5)	0.25	(0–0.5)	0.535	0.648
IFN-γ	0	(0–8.56)	4.28	(0–8.56)	0.535	0.648
TNF-α	0	(0–6.3)	3.15	(0–6.3)	0.535	0.648
IL-1β	1.06	(0–2.52)	2.52	(2.52–2.60)	0.185	0.648
IL-10	1.33	(1.14–1.43)	1.29	(1.07–1.40)	0.502	0.648
IL-8	3.61	(0–6.48)	2.92	(0.56–3.61)	0.499	0.648
IL-9	0	(0–8.25)	4.13	(0–8.25)	0.505	0.648
IP-10	52.08	(23.57–83.25)	61.36	(30.61–72.70)	0.886	0.886
VEGF-A	479.4	(339.4–773.6)	268	(127.6–472)	0.07	0.487

Comparisons between patients with MDS^{Mut} and CCUS. Data are presented as median values and IQR. Percentages represent the proportion of each immune subset within total lymphocytes. Cytokine and growth factor levels are expressed in pg/mL. P values were calculated using the Mann–Whitney U test. FDR correction was performed using the Benjamini–Hochberg method.

MDS, myelodysplastic syndromes; MDS^{Mut}, mutated MDS patients; CCUS, clonal cytopenia of undetermined significance; NK, natural killer; KIR, killer-cell immunoglobulin-like receptor; MDSC, myeloid-derived suppressor cell; Gr-MDSC, granulocytic myeloid-derived suppressor cell; Mo-MDSC, monocytic myeloid-derived suppressor cell; Treg, regulatory T cell; Th, T helper cell; IQR, interquartile range; FDR, false discovery rate; EGF, epidermal growth factor; FGF, fibroblast growth factor; VEGF-A, vascular endothelial growth factor A; G-CSF, granulocyte colony-stimulating factor; HGF, hepatocyte growth factor; IFN-α, interferon alpha; IFN-γ, interferon gamma; TNF-α, tumor necrosis factor alpha; IL, interleukin; IP-10, interferon gamma-induced protein 10 (CXCL10); DNAM-1, DNAX accessory molecule-1; PD-1, programmed cell death protein-1; TIGIT, T-cell immunoreceptor with Ig and ITIM domains.

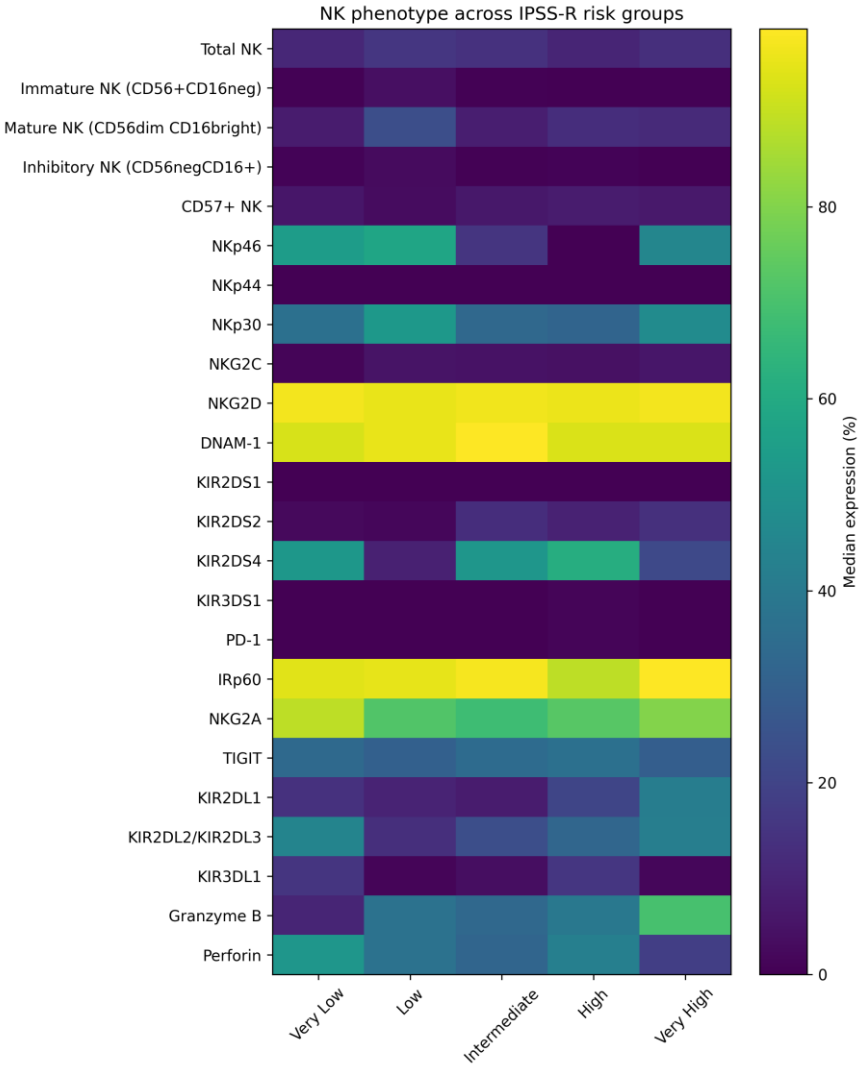
Supplementary Table 10. Hematologic parameters and immune cell populations at diagnosis and 1-year follow-up in MDS patients.

Variable	Diagnosis median (IQR 25–75) (N=13)	1y-FU median (IQR 25–75) (N=13)	*p-value*	Missing
Hb (g/dL)	10 (8.4–11.3)	10.4 (8.95–11.5)	0.56	0 (0%)
Leukocytes (×10⁹/L)	3.51 (2.09–5.84)	4.45 (3.87–6.14)	0.86	0 (0%)
Neutrophils (×10⁹/L)	2.4 (0.9–3.8)	2.85 (1.2–3.3)	0.95	0 (0%)
Lymphocytes (×10⁹/L)	1.2 (1–2.2)	1.35 (0.75–1.75)	0.94	1 (1.22%)
Platelets (×10⁹/L)	134 (84–176)	124 (89.75–176.2)	0.75	0 (0%)
T lymphocytes (%)	5.42 (2.74–7.65)	6.16 (4.77–12.01)	0.96	4 (4.88%)
TNK lymphocytes (%)	18.45 (11.73–19.44)	18.57 (11.89–25.83)	0.15	3 (3.66%)
Total NK (%)	34.92 (7.25–91.72)	20.52 (13.6–79.45)	0.55	4 (4.88%)
NK CD56dim CD16+	0.98 (0.39–1.96)	3.32 (0.48–8.00)	0.60	4 (4.88%)
Inhibitory NK (CD56negCD16+)	4.29 (1.86–17.49)	3.21 (1.55–8.44)	0.26	4 (4.88%)
Immature NK (CD56+CD16neg)	74.69 (64.16–91.01)	77.4 (59.62–88.49)	0.47	8 (9.76%)
NKG2A	35.16 (15.06–39.86)	33.53 (12.03–40.15)	0.19	7 (8.54%)
TIGIT	7.6 (1.20–17.82)	12.4 (5.06–24.55)	0.65	6 (7.32%)
IRp60	56.4 (29.03–85.67)	89.28 (82.19–92.24)	0.0007	6 (7.32%)
PD-1	89.67 (84.22–91.06)	24.3 (11.3–29.26)	0.0001	6 (7.32%)
NKp46	23.06 (0–84.91)	38.26 (0–86.55)	0.56	4 (4.88%)
NKp44	97.2 (90.82–99.22)	92.5 (83.65–99.1)	0.92	5 (6.1%)
NKp30	97 (96.3–98.7)	96.78 (91.86–98.45)	0.31	4 (4.88%)
NKG2C	0 (0–2.85)	0 (0–0)	0.60	5 (6.1%)
NKG2D	0 (0–0.175)	0.085 (0–0.29)	0.49	4 (4.88%)
DNAM-1	0.01 (0–1.12)	0 (0–0)	0.48	2 (2.44%)
Perforin	0 (0–0.27)	0.035 (0–1.235)	0.16	2 (2.44%)

Data is presented as median values with IQR, for patients with paired evaluable samples at both time points (N = 13). P values were calculated using the paired Wilcoxon signed-rank test. The column “Missing” indicates the number and percentage of non-evaluable samples for each parameter.

MDS, myelodysplastic syndromes; 1y-FU, 1-year follow-up; IQR, interquartile range; Hb, hemoglobin; NK, natural killer; TNK lymphocytes, T and natural killer lymphocytes; NKG2A, natural killer group 2 member A; NKG2C, natural killer group 2 member C; NKG2D, natural killer group 2 member D; TIGIT, T-cell immunoreceptor with Ig and ITIM domains; IRp60, inhibitory receptor protein 60 (NK receptor); PD-1, programmed cell death protein 1; NKp30, natural cytotoxicity receptor 3; NKp44, natural cytotoxicity receptor 2; NKp46, natural cytotoxicity receptor 1; DNAM-1, DNAX accessory molecule-1 (CD226).

Supplementary Figure 1. NK receptor expression according to IPSS-R risk stratification.



Data are presented as median expression values for each NK cell subset, activating and inhibitory receptors, and cytotoxic molecules stratified by IPSS-R risk category (Very Low, Low, Intermediate, High, Very High). Heatmap color intensity reflects median expression within each risk group.

NK, natural killer; IPSS-R, Revised International Prognostic Scoring System; NKp46, natural cytotoxicity receptor 1; NKp44, natural cytotoxicity receptor 2; NKp30, natural cytotoxicity receptor 3; NKG2C, natural killer group 2 member C; NKG2D, natural killer group 2 member D; NKG2A, natural killer group 2 member A; DNAM-1, DNAX accessory molecule-1; KIR, killer cell immunoglobulin-like receptor; PD-1, programmed cell death protein 1; IRp60, inhibitory receptor protein 60; TIGIT, T cell immunoreceptor with Ig and ITIM domains.